Daniel Kraus, BSc

Approach for a novel optical network design for future automotive applications

Master's Thesis

to achieve the university degree of

Diplom-Ingenieur

Master's degree programme: Information and Computer Engineering

submitted to

Graz University of Technology

Supervisor

Ao.Univ.-Prof. Dipl.-Ing. Dr.techn. Erich Leitgeb

Institute for Microwave and Photonic Engineering
Head: Univ.-Prof. Dipl.-Ing. Dr.techn. MBA Wolfgang Bösch

Graz, January 2019

Affidavit

I declare that I have authored this thesis independently, that I have not used other than the declared sources/resources, and that I have explicitly indicated all material which has been quoted either literally or by content from the sources used. The text document uploaded to TUGRAZonline is identical to the present master's thesis.

Date

Signature

Abstract

The automotive sector has been rigid over the last decades and only minor progress in terms of fuel consumption, assisted driving and alternative power- and drivetrain technologies has been achieved. Since any advancement in the automotive sector must be tested and approved, the design-to-product phase often requires several years and even then, certain technologies may never be widely distributed due to costs.

Still, vehicles are growing increasingly sophisticated. For example, Advanced Driver Assistance Systems (ADAS) such as Traffic Sign Recognition, Lane Keeping Assist System (LKAS), Collision Avoidance System, Automatic Parking and even Vehicular Communication Systems are already available in state-of-the-art vehicles. However, with greater sophistication comes greater complexity of those applications, systems, and networks. Regardless of the basic requirements, such as real-time, safety, security and so on, - certain conditions must be met. Otherwise, it is impossible to ensure the functionality of an application, the vehicle, and in a wider sense, the physical integrity of the passengers. Consequently, the goal is to optimize existing systems in terms of weight, cost, safety and functionality. A modern wiring harness, for example, can exceed the weight of several passengers and thus influences the driving behavior as well as fuel consumption. Additionally, every device and wire must be shielded against electromagnetic interferences. This setup is often quite expensive, and the complexity increases with every single addition to the network.

A way to reduce cost/weight is to optimize or use different technologies for existing bus systems and car networks. Therefore, such systems will be compared and analyzed in this MSc thesis. Based on this analysis, an approach for a novel optical network handling major issues with weight and interferences will be presented.

Kurzfassung

In den letzten Jahrzehnten hat sich im Automobilsektor wenig getan und es konnten nur geringfügige Fortschritte bezüglich Treibstoffverbrauch, unterstütztem/automatisiertem Fahren sowie alternativen Antriebstechnologien erreicht werden. Nachdem sämtliche technischen Neu- und Weiterentwicklungen über Jahre hinweg getestet werden müssen, um schlussendlich auch im Fahrzeug zugelassen zu werden, kann passieren, dass teure Technologien nie den Weg ins Fahrzeug finden werden.

Fahrerassistenzsysteme wie Verkehrszeichenerkennung, Spurhalteassistent, Notbremsassistent, automatisches Einparken und Kommunikationssysteme sind mittlerweile Teil moderner Fahrzeuge. Es wird immer schwieriger, diese Systeme in einem Netzwerk miteinander zu verknüpfen, da die Komplexität immer weiter zunimmt. Im Fahrzeug müssen gewisse Grenzwerte eingehalten werden, um den Anforderungen nach Echtzeit, Sicherheit, etc. gerecht zu werden. Ansonsten wird es nicht möglich sein, die hohen Sicherheitsstandards der Systeme einzuhalten und die Passagiere bestmöglich zu schützen. Ein moderner Kabelbaum übertrifft mit seinem Gewicht das einiger Insassen, da mittlerweile so viele elektronische Geräte und Bauteile verbaut sind. Es ist daher sinnvoll, die Systeme auf Sicherheit und Funktionalität zu optimieren und gleichzeitig Gewicht und Kosten zu senken. Die Elektronik im Fahrzeug muss gegenüber elektromagnetischen Störungen geschützt werden, damit diese Ziele erreicht werden können. Dies lässt sich aber nur selten einfach lösen, da jedes Gerät neue Störungen in den Kabelbaum bringen kann und das Abschirmen mit teuren Kabeln auf Dauer keine Lösung ist.

Um die Kosten und Gewicht zu verringern müssen andere Technologien für Bussysteme und Netzwerke im Fahrzeug in Betracht gezogen werden. Solche Systeme werden im Zuge dieser Masterarbeit verglichen und analysiert. Basierend auf der Analyse werden optische Systeme präsentiert, die die Probleme mit Gewicht und Interferenzen beseitigen könnten.

Contents

List of Figures

1 Introduction

1.1 Motivation & Problem Definition

Driving is the most dangerous mundane activity. Therefore, companies try to improve safety by adding a variety of Advanced Driver Assistance Systems (ADAS).

Over the past years, two different approaches have emerged to achieve autonomous driving. The first approach is mainly applied by well-established car manufacturers. They steadily increase the level of automation if the requirements of previous stages have been sufficiently satisfied. Current state-of-the-art vehicles are already able to drive autonomously in certain conditions (e.g. motorway). Still, a person must be able to take control of the vehicle at any point to fulfil valid regulations.
The second approach is promoted by start-ups and well-known companies with extensive budgets. Google, for example, claims that by improving existing systems, total automation of vehicles may never be achieved. Such start-ups often do not have any previous experience as car manufacturers. They develop autonomous vehicles from scratch and are trying to improve the functionality by analyzing huge amounts of data based on machine learning (Bloomberg, 2018).

The goal in both approaches remains the same: Individuals should be transported autonomously to a desired destination with just a few initial inputs. As good as that may sound, the technical effort to realize such a system with a minimal error margin is immense. Also, the amount of data required to achieve such an autonomous system is beyond current capability. The gap between vision and actual feasibility is often too far apart to comply with all the existing safety and reliability restrictions.

Due to several scandals in recent years, there has been a change of thinking in the automotive sector, which is generally very slow in adapting new technologies. Diesel engines might be banned in the next few decades, thus boosting the development of other technologies such as electric engines and the required batteries. The common perception of electrically actuated vehicles has improved by greater operating range and available infrastructure. The number of sensors, chips and cabling in vehicles has increased dramatically. Sensors measure rotation speed, pressure, temperatures, the steering angle and rotation of the vehicle, monitor the course of the road and register distances and obstacles in front or behind the vehicle. Modern optical sensors can measure the entire environment of a car and offer new opportunities for novel assistance systems required for autonomous driving. The communication between all sensors is handled within a huge network which are connected to various data buses. Those data buses must fulfil the standards and requirements of the vehicle (Hammerschmidt, 2014).

The sensors have a variety of tasks: For example, it is possible to influence the driving behavior of the vehicle by using control systems such as Electronic Stability Control (ESC). The system improves the stabilization of the vehicle on the road by measuring the traction, which correlates with the speed in curves and moment of force. Those parameters are detected with sensors, which transmit their recorded information to a main control unit, which processes the data and reacts accordingly. The system registers the steering motions of the driver with other additional sensors. For example, the data of the rotational speed sensors in the wheels will be evaluated within this process. The most important part is the yaw-sensor, also known as gyro platform, which measures the rotation of the vertical axis as well as other acceleration forces. To achieve the best measurement results it is essential to position this sensor as closely as possible at the center of mass of the vehicle, e.g. the propeller shaft tunnel (Hammerschmidt, 2014).

With all the components mentioned above – steering sensor, rotational speed sensors and yaw sensor – the ESC-computer can react accordingly to the transmitted data. Before the car even gets into a skidding motion, wheels can be decelerated to prevent the vehicle from leaving the driving surface. In modern ESC systems, the motor control unit is also included, which allows a regulation of the power intake from the engine. Other assistance systems can improve the driving experience differently. One example is the automatic vehicle interval control, better known as adaptive cruise control (ACC). This system measures the distance to the vehicle in front with a RADAR beam. If the distance becomes too small in a matter of safety, the vehicle is decelerated to increase the gap and prevent a possible rear-end collision. Another example is the lane departure warning system, which identifies the driving lanes by processing images of the road ahead. These images are made by a camera and measured optically. As soon as the lane is changed without using the indicator, the system will alert the driver or might even stay in the lane automatically. Parking assistance systems are also a standard in many upper-class vehicles. Those systems use ultrasonic sensors, which are positioned in the bumper bars of the vehicle. Modern parking assistance systems often use a camera as well, e.g. of the lane departure warning system, to calculate a virtual image of the environment. Based on this data and in combination with the sensors, the vehicle can park autonomously. The parking assistance system is just one example where one system could use components of another separate system to enhance the functionality and hence the performance. Therefore, it is required that all the control units, sensors etc. are connected to each other. In most cases, data busses are used to provide the communication between all those devices, which differ in bandwidth and functionality: The LIN bus (Local Interconnect Network) connects the control units of the vehicle's doors and windows, electric adjustable seats and other simple applications, where only a few bits are required to achieve the desired results. Most of those applications are not safety-critical and a malfunction is inconvenient but does not endanger the passenger. Since only a few bits are sufficient to communicate this data, the LIN bus is standardized with a data rate of 20 kbps. For more sophisticated systems like the ACC or ESC, this bus would not be acceptable. Many of those applications are in fact safety-critical and a malfunction could result in an accident (Hammerschmidt, 2014).

Currently, most systems in a vehicle use the CAN bus (Controller Area Network), which was introduced by Bosch 1983. This CAN bus reaches data rates of up to 1 Mbps for a maximum bus length of 1 kilometer. However, adding more elements to the bus decreases its functionality. Most of the sensors and actuators are part of a CAN bus system realized with copper cabling. Camera-based systems or other applications that require high bandwidths, cannot be incorporated into a CAN network. Thus, camera systems are often decoupled from bus systems and the data is merged at the device where all the calculations are performed. There are other bus systems, e.g. the Flexray bus, which provides higher data rates of up to 10 Mbps. However, such systems are much more expensive and do not really solve the problem of limited bandwidth. Another example would be the MOST bus (Media Oriented Systems Transport), which was designed mainly for multimedia applications within a vehicle. It can reach bandwidths of up to 150 Mbps; however, the system is not very reliable. Another problem in the automotive area is the incompatibility of standard computers and software. Intel-CPUs and operating systems such as Windows are not applicable in vehicles since they cannot comply with real-time and safety requirements. A failure of the brakes would be fatal in many cases. The software used in vehicles must meet all requirements and should be adapted accordingly. Even if a malfunction of one element occurs, the system must return into a safe state to prevent a brake failure. One of the most critical systems in a vehicle is the steering. If a failure of the vehicle dynamics management (VDM) occurs, it is of utmost importance that the mechanical steering is still working (Hammerschmidt, 2014).

Autonomous cars need a lot of data and use that data accordingly to function properly. Current bus systems must be substituted by other networks which can handle more data. One example for the growing complexity is the amount of wiring that increases with every single addition of an assistance system to the vehicle. Every sensor, actuator and camera must be connected to one or several central control units. A central control unit processes and distributes relevant data to other, simpler, control units. Based on the data, correct decisions must be made to maneuver the vehicle safely through all kinds of different situations. Eventually, the transport of one or several persons from one point to another should function without any faults. Those additions increase the weight of the vehicle, decrease the available space and bring more elements into the vehicle, which might cause unforeseen problems like e.g. interferences. Such interferences, mainly of an electromagnetic nature, are ubiquitous in a vehicle, where mostly electrical components are installed. This is not only true for automotive applications but also in airplanes and space-faring vehicles where any kind of interference can pose a serious threat to the functionality of the vehicle, and thus its passengers. Therefore, those influences must be taken into account, especially in the design phase (Kossel, 2014).

Currently, a test vehicle can be described as follows (Kossel, 2014): The standard equipment of a vehicle provides a few sensors for e.g. parking assistance. In addition to those sensors, at least another twelve sensors are required in the vehicle body. Furthermore, an automated vehicle requires GPS antennas to reliably estimate the position of the vehicle. The traffic in front of the vehicle is detected and observed by using a RADAR and LiDAR sensor. In contrast to RADAR, LiDAR works with laser beams. Based on the data gained, a 3D-model of the environment can be calculated. There are further LiDAR sensors in the front fenders as well as in the back of the vehicle. A camera positioned in the back behind the rear windshield captures the lane markings. Two ultra-sonic sensors on each side monitor the close area of the vehicle. The information gathered by all the sensors is computed by a computer which is positioned in the trunk. This information is used to generate images of the environment with useful information. It is displayed on a monitor at the dashboard. To ensure real-time there are two additional computers placed next to the main computing unit in the trunk. These computers are responsible to calculate the driving strategy as well as to control systems like steering, automatic transmission, motor or the brakes. In modern vehicles those systems are steered electronically, so no alterations are required. The major disadvantage is the enormous amount of cabling and the resulting weight (Kossel, 2014).

Within a vehicle there is confined space where a network can be positioned. Therefore, it is required to have a well-designed network which can function optimally in this available space. In addition, it is very important to use a network protocol with the desired properties. Based on all this information, it is obvious that future vehicle networks need to change in every aspect. While all requirements must still be met, the data rate, bandwidth etc. have to be increased by quite a margin to match the demands of current and future driver assistance systems. Problems and limitations of current systems will be discussed in detail in the following chapters and an adequate solution will be presented, which takes all those restraints into consideration. This includes all the various technologies that might be used for such a novel solution.

1.2 Structure of the Thesis

This section gives a short overview of the chapters in this thesis.

General Background and Definitions

In the first part of this work, the most important terms such as topologies, bus system etc. are explained to give a basic understanding of the problem.

Overview of various Bus Systems and Protocols

An overview of available bus systems and protocols is given. Based on this information, the area of application of these various systems should become clear. Following bus systems are discussed in this chapter:

- *Controller Area Network (CAN)*: High-speed protocol to allow adjustments of a control circuit based on sensor data in real-time. *Time-triggered CAN (TTCAN)* and *CAN with Flexible Data-Rate (CAN-FD)*.
- *Local Interconnect Network (LIN)*: Low-cost bus system with very low data rates for simple applications like motors of windows or heating of seats.
- *FlexRay*: Bus system with higher data rates (up to 10 Mbps), improved real-time capabilities and reliability for specific applications like drive-train, where CAN is not sufficient.
- *Media Oriented Systems Transport (MOST)*: Optical bus with a high bandwidth for transmission of multimedia applications like video or audio.
- *Byteflight*: Safety-critical protocol to support CAN to fulfil requirements of high-speed data communication. Uses optical transmission fibers to reduce EMI.
- *Ethernet/IP*: Potential alternative for future automotive applications.

Optical Technologies

Optical technologies have been explored in vehicles, but except for MOST and Byteflight, no proper protocol has been developed. Both designs do not fulfil the upcoming requirements, even though optical technologies can provide certain benefits, which are vital for future vehicle networks. The electromagnetic compatibility as well as a significant weight reduction are just a few of those advantages. In this section, the basic background to optical communication is given. Additionally, some existing technologies like LiDAR are elaborated.

Analysis

In this chapter, the properties of existing systems are analyzed. The network as a whole will be considered and the main challenges regarding the network are discussed. There are quite a lot of problems with current systems. Interferences, weight, and materials are just a few examples of those.
Furthermore, the major issues of CAN are discussed to show limitations in the context of automated and autonomous driving. The issues are then compared with challenges of future systems. Finally, there will be an analysis of control units to compare the real data with the assumptions made.

Solution and Implementation

In this chapter, the focus lies on designing a network architecture based on optical technologies, which decreases the complexity, reduces weight and offers sufficient bandwidth for fully autonomous vehicles. Two existing technologies are compared and adapted for autonomous application. Based on the information, a new design is presented, and a few calculations are done to estimate the potential data rates of the system. Furthermore, the protocol layer will be discussed.

In the end, the conclusion will give an overview of how the proposed design can handle issues of future autonomous networks.

2 General Background and Definitions

The first chapter deals with certain terms, which are ubiquitous in the automotive sector and thus vital to understand most of the discussed topics.

2.1 Definition of Elements and System Components in a Vehicle

The following terms are vital when considering communication systems for vehicles.

There are many elements in a vehicle that are connected to each other. Hillier (Hillier, 1991) defined following elements:

The *body shell*, which forms the skeleton of the vehicle.
The *engine* is the power unit of the vehicle.
Transmission system: aids in transferring the drive from the engine to the wheels. Its main components are the clutch, gearbox, final drive, and differential.
Suspension system: used to connect the wheels to the body or chassis frame.
Steering: wheels are connected with some kind of mechanism, which can exert a controlled motion
Brakes: components to decelerate a vehicle
Electric Equipment: various components which improve or automate certain processes

The definition is a bit outdated due to recent advancements, e.g. with electric engines, but the general classification still holds. Electrical equipment is growing almost exponentially in a vehicle, since all driver assistance systems fall under this category. Other utilizations such as steering, braking, the transmission etc. are supported by different electrical systems.

Some of them are quite simple and straightforward, while others are very sophisticated and hard to implement.

The **body shell** of a vehicle consists of different parts and materials. In recent years, new materials and production technologies were developed to improve the stability of the basic structure while decreasing the overall weight. As a result, passenger safety has been increased, and fuel consumption reduced. Naturally, the costs for developing such materials are high: however, when mass production is deployed, there is quite a fast degradation of the expenses. Steel, high-strength steel, aluminium, plastics and carbon fiber are used for the automotive body and chassis structure. The approximate weight reduction for the different materials can be declared as follows:

a) High-strength steel 10%
b) Aluminium 30-40%
c) Carbon fiber 50%

Modern versions of the body shell are often hybrids of ultra-high-strength steel, common steel and aluminium. Aluminium is used for the less safety relevant regions in the car, while the ultra-high-strength steel forms a secure cell, where the passenger cell is as much protected as possible in case of an accident. The body needs to fit all other parts like drivetrain or powertrain but also things like the wiring harness require some space which must be available when assembling everything in the last production stage. In the case of electric vehicles, the battery at the center, front or back has to be considered in the design phase and also for the final body shell. The battery itself is often built in as a large block located at a low center of gravity to influence the driving properties as little as possible. Additionally, it must be protected by some sturdy material to prevent any damage in a case of failure (e.g. battery fire) (Abele, 2017).

The internal combustion **engine** is still the most commonly used motor in an automobile. A fuel, normally diesel, petrol or gas, is mixed with an oxidizer and burned in the combustion chamber. As a result, the high-temperatures and high-pressure gases expand and apply pressure on mechanical components of the engine which leads to the vehicle's movement. Depending on the kind of fuel, different types of engines are used. The spark ignition gasoline engine uses gasoline (petrol) as a propellant. Air is mixed with the fuel and then inducted into the cylinder during the

intake process. Consequently, the mixture is compressed and ignited which results in the combustion. The pistons in the engine are then pushed by the power of these combustion gases. In the compression ignition diesel engine, the process is a little bit different. Here, the fuel and air are not mixed beforehand. Only air is present in the combustion chamber and compressed. The diesel is then sprayed into the hot compressed air and ignited (energy.gov, 2013).
Other engine types like the electric one have re-emerged during the past few decades. In the late 1880s, when the first automobiles emerged, steam-powered and electric engines were most commonly used. However, combustion engines soon replaced all other types and became the sole product on the market. The reason was rather simple: engineers could not solve the battery problem. Electric vehicles were only useful for short distances. In addition, the social aspect played quite an important role, since vehicles with electric engines did not produce the same level of sound as the ones with a combustion engine. Nowadays, the perception is changing, and due to increasing consciousness about global warming, depletability of resources, pollution and increasing fuel prices, electric engines are considered as the universal solution for these problems. Advances in the development of batteries now offer sufficient energy for the electric engine to cover longer distances (200 km up to 500 km). Another argument for electric engines is the considerably small efficiency of combustion engines compared to the electric ones. While gasoline engines effectively only use approximately 15% and diesel engines 20% of the fuel energy content, electric vehicles achieve over 90% (Shah, 2009).

The **transmission system**, also known as power-train, describes the cluster of components which are important for the transmission, and thus, the controlled application of the power generated by the engine. Such components are the clutch, gearbox, prop shaft, differential and final drive shafts.

There are numerous requirements which must be fulfilled by the employed transmission system (*Introduction to Transmission Systems* 2018):

- Vibrations and various shocks generated by the engine must not influence the components of the power-train.
- There should be means to allow bi-directional transmission of power.
- Control to allow power transmission at varying angles and lengths.
- Versatile linkage of engine and drive wheels.
- Control to reduce the speed between engine and drive wheels with a defined ration of 5:1.
- Diversion of power flow.
- Active wheel control (Differential) .
- Physical impacts of braking, acceleration etc. have to be compensated.

There are two types of transmission systems:

1) Hydraulic transmission
2) Mechanical transmission

The hydraulic transmission utilizes a liquid to transmit the rotating power of a mechanically driven wheel. This type of transmission is normally applied in automatic transmissions. In a mechanical transmission system, the driver of the vehicle can manually set the gears with a gear shift. A clutch allows to stop the transfer of torque of the engine to the transmission and wheels, thus a change of gears is possible without damaging the active components.

The **suspension** describes all parts that are required for a smooth and steerable motion of the vehicle on different surfaces. Those parts are tires, springs, shock absorbers and linkages between those components. The main tasks of a suspension are following (Collins, 2018a):

- Wheels should stay in contact with the road surface to allow control at all times.
- The suspension is an active protection for all other components since it absorbs most of the impacts of uneven surfaces.

To achieve a **steering** motion, the wheels are connected to several of the previously mentioned components such as linkages, rods, pivots or gears. Motions of a steering wheel are transferred to the mechanical parts and a correlating reaction is executed. The most important concept used in this context is the caster angle which makes steering self-centering, and thus improves the handling when going around corners. There are a few different types of steering which all yield similar results – in a corner, the inner wheel of a vehicle has a smaller turning angle than the wheel outside (Collins, 2018b).

In a modern vehicle, all **brakes** deployed are operated by a hydraulic system. The types of brakes can vary between disc and drum. While high-end vehicles or sport cars often only use expensive disc brakes, basic cars are often equipped with the considerably cheaper drum brakes. It is quite common that upper middle-class vehicles utilize both disc (front) and drum (back) brakes.
Hydraulic brakes consist of several cylinders which are referred to as master and slave. The slave cylinders are located at the wheels. There is a piston within the master cylinder which is pushing fluid in direction of the slave cylinder through a pipe. Further pistons in the slave cylinder are activated by the fluid and induce the brakes to exert pressure for the actual braking process. This system is designed in a way that the initial braking force is increased before it is applied at the brakes. Many modern vehicles are applied with twin hydraulic circuits to have at least one working braking system in case of a failure.
Power-assisted brakes support the driver by reducing the pressure that has to be applied on the braking pedal. When the engine is running, there is a vacuum in the servo unit. As soon as pressure is applied to the brake pedal, air is directed into the servo pushing a diaphragm which assists in the braking effort. Even if the engine is not running, the brakes will still work with this concept (*How the braking system works* 2018).

The **electric equipment** is basically covered by the wire harness and the various components (control units, sensors, actuators) connected to it. Information and power are supplied with such a harness and it forms the backbone of all the devices. In general, the wire fitting is done in the last stage of the production process (assembly stage). More information on the various devices will be given in the following chapters.

2.2 Topologies

A topology describes the structure of how network components and devices are connected to each other. In most cases, topologies are depicted as graphs, where devices are modelled as nodes and wires as links. Relevant topologies for the automotive sector are point-to-point, ring, bus and star which will be described in the following pages. There are several other topologies such as tree or mesh as well; however, those are barely used or not yet relevant for automotive networks and will not be mentioned in detail.

2.2.1 Point-to-Point

This topology, see Figure 2.1, is a simple connection between two nodes and offers the full bandwidth of the transmission medium. The communication is straight-forward, and no routing or other message handling is required (Bradley, 2001). When circuit- or packet-switching is used, it is possible to dynamically set up connections between various devices. An example for such a static point-to-point topology is a control unit and sensor connection. Color Video Blanking Signal (CVBS) cables and Low-Voltage Differential Signaling (LVDS) wires are often used for camera-based assistance system. Those devices are also connected with point-to-point links.

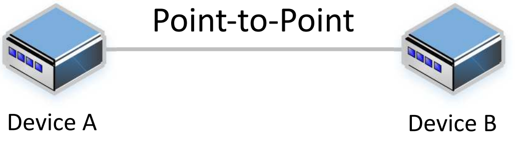

Figure 2.1: Point-to-point topology

2.2.2 Bus

All devices within the network are connected to the same transmission medium. There is no active component or device which handles the communication. This kind of topology, see Figure 2.2, is the cheapest solution for systems where a lot of wiring is required. By using a bus, the same line can be used by all nodes. However, a protocol is required to handle and prevent collisions that might occur. In general, data is only transmitted in one direction. One problem can be a failure of the bus wire, because then the whole network fails (Groth and Skandier, 2005, p. 10).. Therefore, it is often reasonable to have one or more redundant cables in a safety-critical environment.

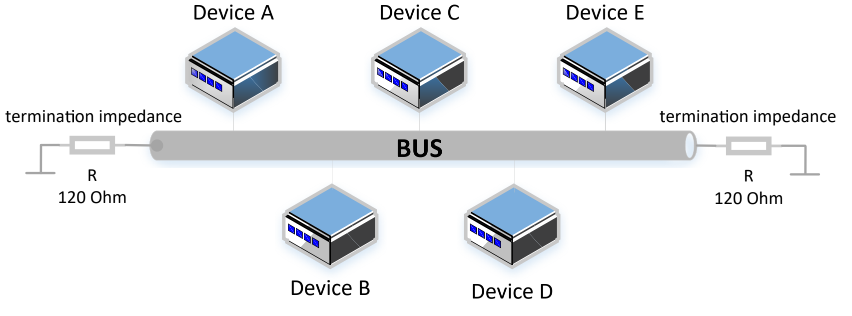

Figure 2.2: Bus topology (CAN) with 120 Ohm resistors as termination

2.2.3 Star

This kind of topology (see Figure 2.3) requires a central device to handle the distribution of the messages. Every single device in the network is connected to the switch/hub through a point-to-point link. The use of twisted pair, coaxial cable or even optical fiber is possible, if the star network is designed as such. This topology offers an easy setup as well as excellent failure safety. If one device fails, only the connection to this single device is interrupted and the rest of the network remains unaffected. The hub/switch is the heart of the network and a problem or failure of this device leads to a total breakdown. Furthermore, the cost of such a network is significantly higher than that of a bus or ring (Groth and Skandier, 2005, p. 11).

2.2.4 Ring

In this topology (see Figure 2.4) every device has two neighbors and the first device is connected to the last one.

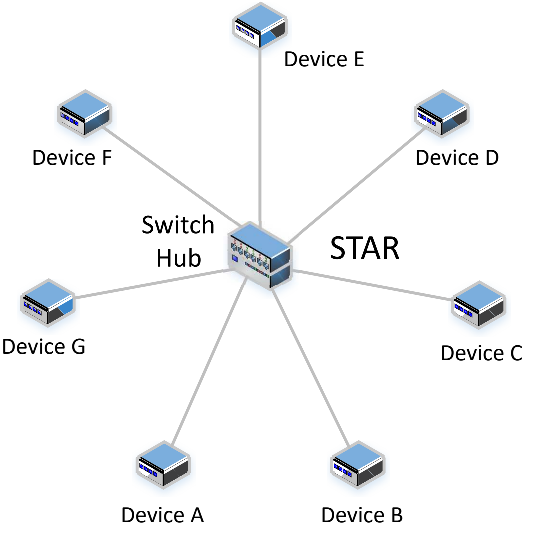

Figure 2.3: Star topology with a switch/hub

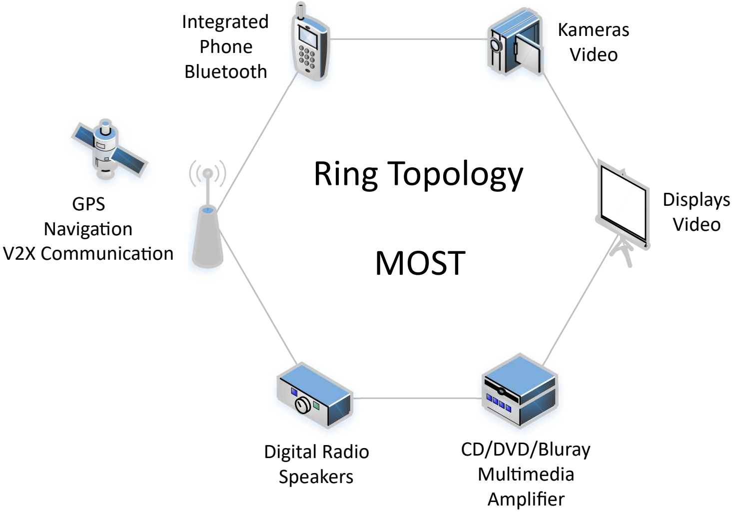

Figure 2.4: Ring topology

Communication is unidirectional by default but can be expanded (bidirectional) by adding another connection at the output of the devices. Then the topology is called Dual Ring Topology. This kind of topology increases the reliability of the network since the transport of messages is also possible in the opposite direction. The ring is quite cheap, easy to install and the achievable data transmission rates are higher than, e.g., in the bus. If one device fails, the whole network might collapse. Also adding and removing devices might lead to several problems (Groth and Skandier, 2005, p. 13). In an automobile, it is quite common that the ring topology is used for multimedia applications using optical fibers to increase the available bandwidth.

2.2.5 Tree

It is often the case that some topologies (bus or star) are combined to obtain most of the advantages. The so-called tree topology (or star bus, see Figure 2.5) is used for local area networks, where the bus acts as the backbone that connects several star networks. The resulting structure looks like a tree. If the bus fails, there is no means of communication between the tree branches anymore. However, the devices within one branch are still able to communicate with each other (Bradley, 2001). Thus, by adding redundant lines for the bus, this structure can remain reliable and flexible.

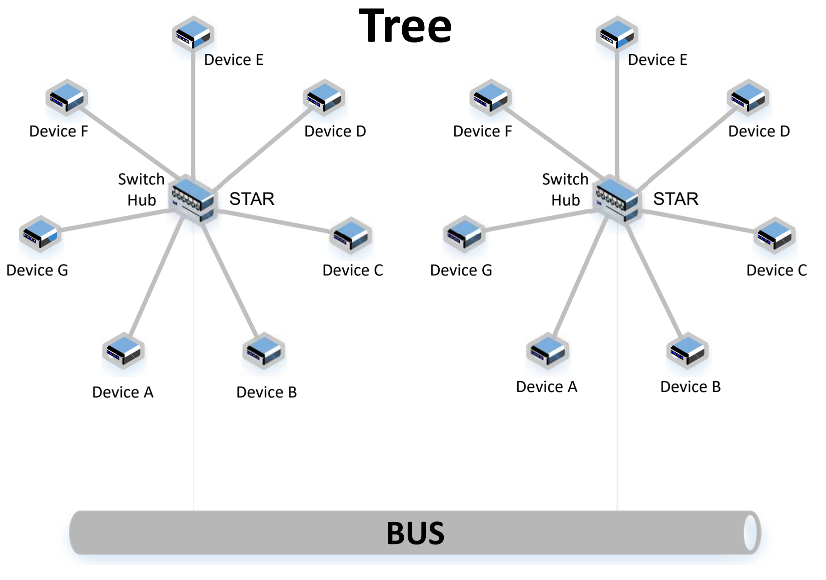

Figure 2.5: Tree topology

2.3 Bus System

A *bus* as a communication system was first introduced in computer architectures long before it became a standard in vehicles. The objective is to reduce the amount of wiring, weight and space requirements to a minimum (Reif, 2014, pp. 1–2).
This can be achieved by connecting all nodes of a network using a single wire. Since further electrification within a vehicle led to space and weight problems, this solution was considered as optimal in terms of cost and efficiency in the automotive area.
In the 1980s Bosch GmbH developed a bus for vehicles with a fitting protocol and called it *Controller Area Network*, short **CAN**. This protocol will be discussed in detail in 3.1.
A protocol is required to set the rules for clear communication within a network with at least two nodes. Without those rules, no valid communication would be possible. The bus is designed as an asynchronous serial system, meaning that it is not synchronized, neither by time nor a trigger. Nevertheless, time is quite important in every aspect of a safety-critical environment. Since messages cannot be sent and received instantaneously, there is a delay in the transmission. This delay time is also called *latency* and it should be at a minimum to increase the efficiency of a system. Consequently, real-time is the desired state for communication in a vehicle. There are three different types of possible communication when using a bus topology, see table 2.1. For one there is the classic *point-to-point* connection, where only two nodes – a sender and receiver – are in place. The second possible connection is *broadcast*, where one sender provides one message to several nodes in a network. The receivers see the message and can decide by means of the protocol, if the message is relevant or not. It is possible that none, only one, or several receivers will actually use the received information. The last kind of connection is *multicast*. In contrast to broadcast, the message will be processed further by all recipients (Reif, 2014, p. 2–3).

Often it is inevitable to combine and connect various bus systems. By doing so, several additional components such as a repeater, router or gateway are required to allow communication with other parts of the vehicular network. This is especially true for modern vehicles, where the network is highly sophisticated and various sensor data is required for several different

Communication type	Description
Point-to-Point	One sender, one receiver
Broadcast	One sender, many receivers possible
Multicast	One sender, many receiver

Table 2.1: Types of possible communication scenarios with bus topology (Reif, 2014, p. 3)

applications. There are various options to access a bus. The procedure is either *deterministic* or *non-deterministic*. If deterministic, the communication process is organized and pre-defined. Thus, no simultaneous access onto the bus is possible. The benefit of this method is the timing of the response of the various nodes within the network (Reif, 2014, p. 8).

For CAN, the non-deterministic approaches are instrumental, since all nodes should have the means to access the bus at any time to transport important and prioritized messages. This non-deterministic procedure on a bus is called *Carrier Sense Multiple Access* (CSMA). Unfortunately, the non-determinism increases the eventuality of collisions on the communication channel. Hence, there need to be different capabilities in place to handle them. Either collisions are ignored completely, or they are detected before and resolved afterwards. Those methods are called *CSMA/CD* (collision detection), *CSMA/CA* (collision avoidance) or as in the case of CAN, *CSMA/CR* (collision resolution). In general, the collisions are resolved by assigning priorities to the messages. The messages with the highest priority are always sent first (Vector Informatik GmbH, 2018). (CSMA/CR will be described in more detail in the next chapter.)

There is always the possibility that the physical transmission line is disturbed by interferences. Thus, mechanisms for detection and correction of errors are required. Data protection can be achieved by coding the message. When doing so, additional information is transmitted with the message to allow checking. Coding can also be used to optimize the data transmission. For this purpose, an encoder is added at the sender and a decoder at the receiver (see Figure 2.6). One option is to add bits, e.g. parity bits, to secure the data. There are more sophisticated checks with calculations like the *Cyclic Redundancy Check* (CRC). The quality of error detection can be described with the Hamming distance. Strings of same length will be checked for differences in the symbols. The minimum number of required substitutions of symbols to achieve the other string is the

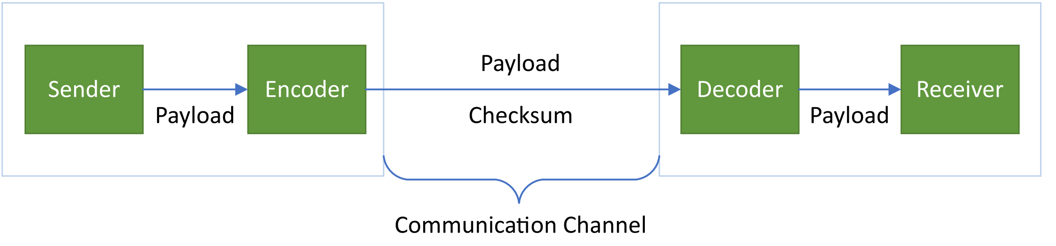

Figure 2.6: Basic principle of data protection by adding information. Adapted from (Reif, 2014, p. 11)

mentioned Hamming distance h. A number of e errors can be detected, if $h \geq e + 1$. However, correction is only possible if $h \geq 2e + 1$. This means for a minimum Hamming distance $h = 4$, then 3-bit errors can be detected, but only 1-bit errors can be corrected (Reif, 2014, pp. 11–12).

2.4 Real-Time

In most cases, current systems do not offer real-time capabilities. The requirements in the automotive context vary from system to system: The *Antilock Braking System* (ABS) must react within a few milliseconds and initiate counter measures to prevent locking of one or more wheels. In contrast to such a safety critical system, the actuation of window motors or seat heaters can be up to 100 milliseconds. Delays of less than 100 milliseconds cannot be registered by human beings anymore. Thus, real-time in the automotive context means that the required calculations are done within the defined time interval. If this is achieved in a time lower than the reaction time of humans, a system can be considered as real-time capable. Depending on the application, there are different requirements to real-time (Reif, 2011, p. 84):

a) **Soft deadline**: In most cases the predefined deadline will hold and if an exceedance occurs it often is not a problem due to the properties of the application.
b) **Hard deadline**: In contrast to the soft deadline the hard one must always be satisfied. As a result, all safety-critical systems (e.g. braking) use such hard deadlines. In the ABS example, a non-compliance of the deadline would lead to locking wheels. Other systems which

require a hard deadline are, e.g., engine actuators and powertrain components.

As a result, the real-time requirements differ from application to application. In systems such as ABS, ESP, etc. any kind of excessive delay poses a threat to the functionality and is equivalent to a total failure. Many functions of the engine management are also time critical to ensure smooth transitions in engine functionality or transmission. Missing those time-critical moments might lead to engine stutters or even failures. Consequently, for such systems a hard deadline must be applied. The more elements there are in a network, the harder it is to fulfil real-time requirements. Furthermore, it is quite difficult to achieve the deadline since it is often quite a complex task. With the introduction of Ethernet to vehicles, systems like *Advanced Driver Assistance Systems* (ADAS) also need real-time capabilities. This appears to be a challenge because of devices like cameras, RADAR or LiDAR, where image and data processing are required. All intermediate steps need a certain amount of time which adds up to a maximum latency. Additionally, Ethernet must be synchronized with other physical bus systems. The basic Ethernet version lacks real-time capabilities; however, there are some approaches to change this (see section 3.8).

Satisfying the deadlines is dependent on several factors, not only the electronic control unit (ECU) of the embedded system. All connected networks can have an impact on the overall system time. Since system failure due to a timing error might be possible, there must be a failsafe mechanism in place where the system is put in a safe state which does not influence other systems. The driver must be informed if such a failure occurs so that adequate measures can be taken. Additionally, there is redundancy for many critical systems and sensors to minimize the error rate. In the design phase of an automotive system, the priority often lies on optimizing the run-time. This can be achieved by using priority-based scheduling of the various tasks and messages. An overview of a design process is given in Figure 2.7 (Santos, 2017, p. 3).

In the design flow, each part of the application description is represented by a node of a graph. The connections between the nodes are equal to the data dependence. The overall time to get from the first node to the last is denoted as end-to-end latency. The architecture description represents

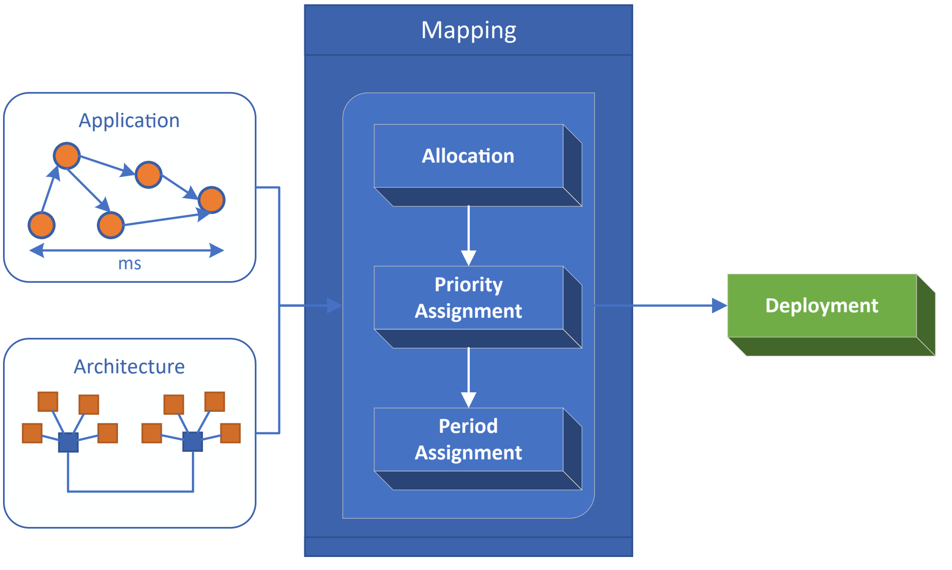

Figure 2.7: Design flow for a real-time system. Adapted from (Santos, 2017, p. 3)

the basic network topology that is used. In most cases this will be a bus or star-bus topology. The description of application and architecture are then mapped; tasks and messages are allocated; priorities and periods are assigned to the ECU tasks and bus messages before they will be deployed. With Activation Models - periodic activation model and data-driven actuation model - end-to-end latencies for real-time distributed automotive systems can be achieved (Santos, 2017, p. 2–3).

Periodic activation model
In this model, the most recent message activates the tasks. This results in a minimum release jitter of each component in the model. Hence, the worst-case latency is the sum of all worst-case response times and the component periods. The periods must be considered since each of the items is only activated periodically. Consequently, the worst-case time of both models can be calculated with equations 2.3 and 2.2: :

$$L_{i,j} = \sum_{o_k \in P_{i,j}} (T_k + r_k) \tag{2.1}$$

Data-driven activation model
The intermediate nodes are considered to calculate the worst-case latency. This means that the release jitter will be higher.

$$L_{i,j} = \sum_{o_k \in P_{i,j}} w_k \tag{2.2}$$

The major difference between the two approaches is that in the data-driven model the high-priority queues will exhibit low latencies, while low-priority message might be queued for a long time. In the periodic activation model, the situation is reversed. Low-priority messages will be scheduled in the best possible way, while high-priority messages might be delayed. Furthermore, each component of a periodic activation model is released instantly, as soon as the computation is done. In the data-driven model, this is not the case.
Real-time embedded systems face some major confinements in the automotive field of application: worst-case core execution time, frequency, precedence constraints, constraint exclusion, displacement time and jitter are just the most important ones (Santos, 2017, pp. 2–3).

For each of those tasks, either a soft- or a hard deadline will apply, as explained above. Scheduling is also quite important to optimize the overall latencies. If one task has to wait for another task to proceed or if tasks share data and resources, this might be far from optimal. Clearly, such tasks need to be synchronized, all restrictions must be adhered to, and several other parameters must be considered, to optimize scheduling.

In general, various tests are executed to determine the overall maximum latency. This can be achieved by doing a so-called *Timing Analysis*. This includes a static code analysis as well as running the code in a simulation. Furthermore, there will be a measurement of the actual runtime in a real system, a scheduling analysis and simulation (Santos, 2017, pp. 4–5).

To elaborate further, an example of (Santos, 2017, pp. 5–6) will be used, to emphasize the importance of real-time in automotive applications. For this purpose, a simplification of a brake system, see figure 2.8 will be considered. In this setup are 5 ECUs. One at each tire and another one, connecting all tire ECUs to the brake pedal. The four tire ECUs must be synchronized, to achieve the desired braking effect, if the braking pedal is actuated. There are additional parameters, e.g. the applied force with

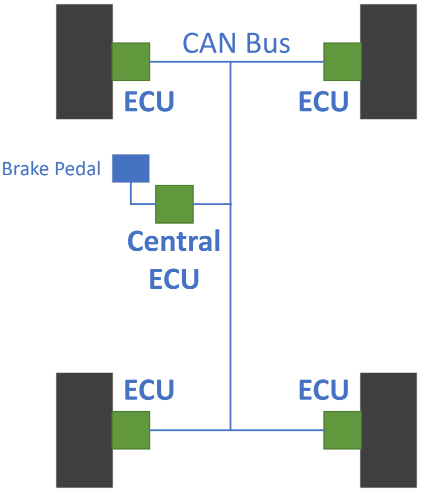

Figure 2.8: Brake system with 5 ECUs

which the pedal is pressed. Depending on the timing and the force, the according braking force will be executed – resulting in a controlled braking motion. If the braking would not be synchronized, there might be the risk of skidding, which would significantly increase the chance of an accident. Furthermore, the delay between pressing the pedal and the actual braking of the brakes needs to be a minimum. Considering the average reaction time of 250 ms of humans (Jain et al., 2015, p. 126), additional delay by the system would have grave consequences. Thus, the end-to-end latency of such a system must be a minimum. In most cases, there is a hard deadline which should be a maximum of 200 ms, but in most cases, it is distinctly lower.

2.5 Control Unit

The task of a control unit (CU) is, as the name suggests, to control certain functions and processes within the vehicle while it is being operated. Obviously, the requirements for a control unit are very high.

Such devices must endure (Reif, 2011, p. 198):

- Temperature range of −40°C up to +125°C
- Fast and severe changes in temperature
- Fuels and lubricants
- High humidity
- Mechanical impacts and vibrations

Thus, the electronic components must be shielded by a highly protective metal or synthetic encasing. A CU needs to be able to start up, even if the power supply is weak or if there are fluctuations with high peaks in the power supply network. Additionally, all EMC requirements (see section 2.6) must be fulfilled.

One of the most important Control units in the vehicle is the one responsible for engine control. The heart of the CU forms a microcontroller with a program memory (Flash-EPROM) or flash memory, where the executable code for all functions is stored. Inputs are delivered by sensors and actuators in real-time. Actuators convert the electric signals from the CU into mechanical parameters. Based on this input the CU makes calculations and comparisons. If there are deviations from the predetermined values, the CU must act and trigger countermeasures to regulate the system. Otherwise, a failure of the engine or other parts of the vehicle might occur, which is not permissible (Reif, 2011, p. 12).

Many systems influence each other; thus, it is important that all those conflicting systems are connected. E.g. In case of spinning wheels, the electronic stability program (ESP) becomes active. Then braking is initiated, but also engine management is signaled to reduce torque to counter the spinning of the wheels. Furthermore, the CU of the automatic transmission is sending a request to reduce torque during shifting operations. All those systems are connected to each other with a data bus like CAN (Reif, 2011, p. 12).

Modern CUs have up to 5 channels for CAN (or CAN-FD) busses and additional FlexRay and Ethernet interfaces. They can be used in both, common combustion engines, as well as electrically-powered vehicles. The data that has to be processed by a CU is either analog, digital, or pulse-shaped (Reif, 2011, p. 199): *Analog* measurements are, e.g. the voltage level of the power supply, the sucked-in airmass or boost pressure. Naturally, those analog values need to be converted in the CU into digital values for further processing. *Digital* signals are much easier to handle, since an additional conversion is not required. In most cases, such signals are coming from switches or digital sensor data (e.g. rotational frequency impulse) and can be directly processed. The third kind are *pulse-shaped* signals. Those signals are generated by inductive sensors with information about the rotational frequency. For those signals, a separate part in the electrical circuit is required, where any interferences are filtered out. Furthermore, the signal is converted into a digital square-wave signal.

In summary, the task of a CU is to handle the various signals of connected sensors and actuators, and do a conversion, if required. There has to be a protective circuit at the input, to shield the electronics from any power spikes. The signals are filtered, the voltage levels are matched and disturbances on the signal removed. Modern sensors can also do the required signal processing to speed up the communication.
As there are different input signals, naturally there is also a variety of output signals. The simplest ones are *switching* signals, where actuators are turned on/off. *Pulse-width modulated* signals are square-wave signals with a constant frequency. With this type of signals, actuators can assume certain operating positions (Reif, 2011, p. 200).
Further details on control units will be provided in section 5.5.1, where such a device is analysed.

2.6 Electromagnetic Compliance (EMC)

All electronic devices generate an electromagnetic field which can affect other devices in its environment. Each device has a different radiation which complicates the process of protecting devices against those emissions. Also, the generated radiation of every device must be as small as possible to allow nearby devices to still receive, e.g., radio signals. The vehicle itself has to be protected against any kind of radio transmissions and other external influences, which can interfere with the functionality of all devices within the vehicle. The on-board power supply provides power to all devices in a vehicle. It is common that a cluster of several devices in close proximity has the same physical power connection, which aggravates the protection against EMC radiation. The different lines are often part of the same wiring harness, meaning they are placed right next to each other. Feedback of systems can thus reach the in- and outputs of other systems rather easily. Such retroactive effects are, for example, impulse-shaped signals, which mostly occur at switch-on/off processes of components such as electric engines, valves or actuators. All those effects can propagate over the entire harness. If the propagation appears in a common conductor, the effect is called *galvanic coupling*. Galvanic coupling occurs, e.g., if a generated voltage influences the signal voltage of a nearby circuit. As a result, sensor signals might be disturbed or obtained sensor values could be corrupted. To counter this problem, it is sensible to use a separate return circuit for each branch (Reif, 2010, pp. 95–96).

Another issue can be *capacitive coupling*, when energy is transmitted from one conductor to another even without an actual connection. The strength of the coupling is directly dependent on the frequency and the distance of the circuit. The higher the frequency and the smaller the distance, the higher the coupled voltage. If this is the case, it is often required to isolate the circuits from each other, or using lower frequencies if possible (Reif, 2010, pp. 95–96).

The last influence, which plays a major role when talking of EMC, is *inductive coupling*. This coupling emerges if there are two or more current circuits located close to each other. Due to the electromagnetic induction, voltages can be created by the time-varying current of adjacent circuits. Voltages in the second circuit then also generate currents. This is the basic principle of a transformer. The frequency of alternating voltages, particularly signal rise- and fall-times, are the decisive factor for the over-coupling. Another factor is the mutual inductance, which is dependent on the position and size of loops. All those coefficients must be taken into account and countered accordingly (Reif, 2010, pp. 95–96).

Electromagnetic Compliance Testing

The testing process is often complicated since the number of devices from different manufacturers within a vehicle steadily increases. There are several measures that can be taken in the design phase to minimize potential problems with EMC. When working in an environment where magnetic fields are ubiquitous, any loop of conductive material can form an antenna. As mentioned, when coupling occurs, a current will flow

through the loop. Since the current is directly dependent on the size of the enclosed area of the loop, loops should be as small as possible or completely prevented. In many cases it is impossible to thwart the existence of loops, because a loop can basically form everywhere. To name a few examples: the differential lines of transmitter and receiver can form a loop or there also is a high chance, if subsystems share a circuit. Moreover, ground wires can form a massive loop with the ground plane (chassis) itself. Such loops are often impossible to avoid. Then, inductors or ferrite materials can be used to reduce the radio frequency emissions (Sauerwald, 2015).
CISPR 25 is one example for a standard where test methods and EMC thresholds are documented. This standard serves as a guideline to ensure that new components will not interfere with other existing systems or components in the car. To do such EMC tests, there are certain requirements that must be met. For CISPR 25 this includes the environment where the testing is to be done. In figure 2.9 (Paolo, 2018) the classification of CISPR 25 is shown.

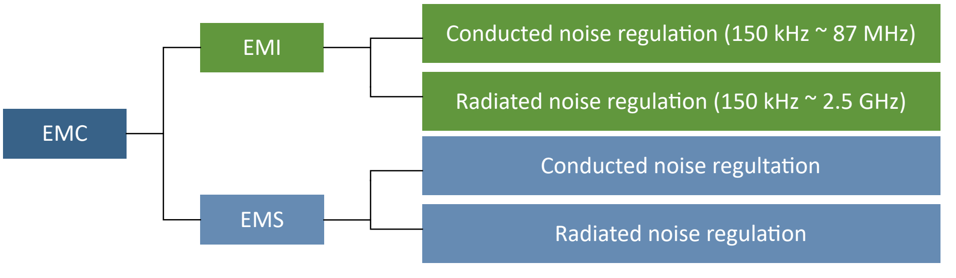

Figure 2.9: CISPR 25 EMC classification (Paolo, 2018)

The signal noise levels within an environment must be 6 dB lower than the lowest measured signal levels. This can often only be achieved in testing chambers, where the devices are shielded against ambient fields and noises. In general, CISPR 25 covers only the frequency range from 150 kHz up to 1 MHz. Thus, there are many other testing methods required. The ISO 11452-4 Bulk Current Injection (BCI) focuses on another type of testing. Here, interfering signals are directly guided into the wiring harness to check if the components can handle any irregularities coming from the wired connection itself (Sauerwald, 2015).

2.7 Impulses & Interferences

To cope with the impulses generated by elements in the on-board power supplies, the amplitudes of the noise sources must be limited. All types of noise sources within a vehicle are generally classified (e.g. DIN 40839), and thus it is possible to counter those by adapting the electronic components and improve the robustness against specific impulses.
The interfering amplitudes of noise sources have to be confined and the design of components should be constructed in a way so that they are not susceptible to certain disturbances. To simplify the process all commonly occurring impulses are encapsulated and classified (DIN 40839) (Reif, 2010, p. 97).

Another problem (within the vehicle) are high-frequency signals which can influence the reception of mobile signals and transmission of such signals in this frequency domain (450 MHz up to 5 GHz). Those high-frequency disturbances can occur when a high voltage ignition happens, at any switching operation, or a change in the direction of the current (commutation) in a DC motor. Also, the clock pulses of a control unit using microprocessors can influence the received signal quality of a wireless interface (2.4 GHz) or similar mobile devices close to those influences. In most cases, those signals appear periodically and can interfere with the receivers for mobile communication and make a signal reception impossible.

Signals arrive either as wide- or narrowband interferences. If the spectrum of the signals shows a continuous behaviour, it is called a wideband interferer. Most electric motors which are used for any control tasks are such wideband interferers. Narrowband interferers generate signal spikes and are usually microprocessors of control units. Devices with an antenna are in most cases directly disturbed at the antenna input, either through some coupling at the connected wires or by the electromagnetic field. The interferences can be easily measured with a spectrum analyser. As might be expected, the wiring harness can be the most problematic interfering element, if the wires indirectly operate as a transmitting antenna (Reif, 2010, p. 99).

Additionally, interferences are nowadays ubiquitous when driving in densely populated areas. Electronic devices, antennas etc. which might influence the electronics within a vehicle are everywhere. Conversely, the vehicle must also satisfy regulations and should not operate as an interferer to any broadcast signals such as TV or radio. In general, the body of the vehicle protects the electronic components pretty well, even if the car is driving through the near field of a strong sender. The electromagnetic field penetrates any openings in the body (e.g. at the doors). Testing the vehicles against such interferences is mostly done in antenna chambers. However, it is almost impossible to test all cases which will occur in a real environment. Thus, electronics might be disturbed by all kinds of external interferences and lead to undesired behavior in the vehicle (Reif, 2010, p. 102).

New wireless communication technologies that will be applied in vehicles in the future will create new challenges in terms of interferences. Those new technologies will operate at high frequencies to achieve high bitrates. Consequently, it will be quite difficult to achieve EMC for all systems without presumably higher costs and effort. Signal integrity is barely considered in future system designs and might have a major impact on the overall performance of a vehicular network. Manufacturing tolerances as well as variations cannot be neglected if electronics become smaller and smaller. If higher frequencies and speeds are used, certain effects such as reflections and crosstalk might cause interferences also for short distances, resulting in mismatches that lead to signal errors. According to (Paolo, 2018), there are two causes of losses:

- *"Dielectric absorption: high frequency signals excite the molecules in the insulation, reducing signal level. Dielectric absorption refers to the PCB material."*
- *"Skin effect: high frequency signal current tends to travel on the conductors with an increase in the self-inductance of the material. The effective reduction of the conductive material causes an increase in resistance and, therefore, the attenuation of the signal. The density of alternating current J in a conductor decreases exponentially from its value on the surface Js according to depth d from the surface" (Paolo, 2018):*

$$\delta = \sqrt{\frac{2\rho}{\omega\mu}}\sqrt{\sqrt{1+(\rho\omega\epsilon)^2}+\rho\omega\epsilon} \tag{2.3}$$

ρ ... resistivity of the conductor ω ... angular frequency
μ ... magnetic permeability ϵ ... permittivity of the material

One example where quite a lot of interferences might occur is the AM broadcasting band (526 kHz - 1.7 MHz). The frequencies of the switching circuits in the various control units is often in exactly the same frequency range. Thus, there might be interferences disturbing the AM radio reception in the vehicle during those switching processes. By using appropriate components for the switching circuits, the frequency of those processes can be moved in a higher band (2 MHz or above) (Paolo, 2018).

3 Overview of various Bus Systems and Protocols

The functionality and properties of various bus systems are discussed to show the advantages but also the problems which occur when thinking of future automotive systems. The most important protocol, the Controller Area Network (CAN) will be compared to other commonly used bus systems and some examples of current developments will be named.

3.1 Controller Area Network (CAN)

The *Controller Area Network* (CAN) is the most commonly used network within a vehicle. It was standardized in 1993 by BOSCH. Since the number of electronic elements rapidly increased within a vehicle, the amount of wiring had to be reduced. For this reason, the topology within a vehicle was adapted to a bus. All devices and control units have the same CAN interface and are equipped with a CAN controller chip, so no separate analogue or digital inputs are required which considerably simplifies the communication of the bus. This results in a weight- and cost reduction which has led to the triumph over other similar systems, and is the reason why CAN is still used in modern vehicles, despite its low data rates (National Instruments, 2014).

Each device in a vehicular network must be able to send and receive data. Therefore, CAN is designed as a Multi-Master-Bus, where every single device can become the Master and thus send data. To enable that functionality, each device within the network requires a CAN controller (chip), which undertakes the task of forwarding messages. There are no active components: a network protocol must be used, which is realized in hardware. Only one device at a time can send data over the transmission medium. The control is implemented with the use of a bus-arbiter. For instance, when using CAN, the CSMA/CR method is applied which transmits the message with the highest priority without delay. Further details on communication is available in section 3.1.3.

3.1.1 Properties of CAN

A depiction of a CAN bus can be found in section 2.2.2 in figure 2.2. The task of the 120 Ohm terminating resistors at the end of the transmission lines is to prevent reflections within the wire. When considering the shown bus structure, several advantages of bus systems compared to other network topologies become explicit (Dohmke, 2002):

1) Plug and Play – once a device is connected to the bus, the device can communicate with all the other devices on the bus.
2) One wire for the communication – weight, space and costs can be considerably reduced.
3) By using redundant wires, the reliability of a system can be increased.
4) Diagnostic components can be used to monitor the bus via broad-/multicast.

According to the official CAN specifications[1], only 32 nodes can be operated in a single bus. By dividing the bus into additional subnetworks, a higher number of nodes is possible. A protocol manages the communication on a bus and ensures that no collisions of messages occur. In the case of CAN, this process is handled by introducing sequences of priorities. If the bus is unoccupied, the message using the highest priority is forwarded onto the bus by the corresponding CAN controller. Since every peer of the network can listen to all messages (broadcast), it is possible to distinguish between the different priorities. In the CAN specifications (ISO 7498) the Physical Layer (signaling) and Data Link Layer (framing, addressing, bus access, data backup and protection) are covered. A CAN interface consists of the controller and a transceiver. The controller monitors the execution of the hardware protocol and intervenes if there are some issues. The transceiver physically couples the CAN controller with the CAN bus running in differential signal mode (Mayer, 2006, pp. 70–71).

The messages in a CAN network are assigned IDs. By doing so, the identity of the message itself is determined, and not only the destination node. Hence, information about all messages is available for all nodes in the CAN-network. By applying filters, the important or assigned messages for each node can be received. In CAN there are 11-bits assigned for the identifiers; thus, 2048 CAN messages can be specified with this amount. In

[1] ISO 11898-1:2015, 2015.

Specifications	Description
ISO 11898-1	Data link layer and physical signalling
ISO 11898-2	High-speed applications of 125 kbps up to 1 Mbps
ISO 11898-3	Low-speed applications 40 kbps up to 125 kbps
ISO 11898-4	Time-triggered communication (TTCAN)
ISO 11898-5	High-speed medium access unit with low-power mode (up to 1 Mbps)
ISO 11898-6	High-speed medium access unit with selective wake-up functionality (up to 1 Mbps)
SAE J2411	Single-wire specification for applications with low requirements regarding bit rate and bus length

Table 3.1: The most important CAN specifications

general, the data transmission is event-driven: messages are sent if something happens; however, there are often status messages in place, which are sent periodically. Each node in a CAN bus system is assigned the same privileges. Each node can access the bus if a message is intendent for the said node. As the message length is quite short the data transmission rate of up to 1 Mbps is in many cases sufficient to react to asynchronous events. However, the more complex a system the more messages will be transmitted, and the overall bus load will increase significantly. Consequently, the chance of collisions on the bus increases and it is impossible to comply with the hard deadline requirements of real-time (Mayer, 2006, p. 71).

The data rate of CAN lies somewhere in the range of 10 kbps up to 1 Mbps for a bus length of up to 1 kilometer. It is mainly dependent on the bus length and the speed of the transceivers. However, for increasing bus length the data rate decreases quickly. As an example, for a bus length > 1km, achievable data rates lower than 50 kbps are realistic. Another limiting factor is the physical condition of the wires used. Due to cheap wires, the maximum data rate is in most cases only 500 kbps. The basic CAN specifications (ISO 11898-1) of Bosch only cover the physical and data link layer. However, there are many extensions to the ISO 11898. In table 3.1, the most important ones are listed (Zimmermann and Schmidgall, 2014, p. 58).

High-Speed CAN

The ISO 11898-2,5,6 standards are designed for high-speed applications and achieve data rates of 125 kbps up to 1 Mbps. High-speed CAN is defined as a linear bus with 120 Ohm resistors as termination. Its main application is wherever event-triggered communication is required – this includes most parts of the powertrain (drivetrain) and gear. Nowadays, the data rate of high-speed CAN is not sufficient anymore. Instead, e.g., CAN with Flexible Data rate (CAN-FD), see section 3.3, acts as a replacement to fulfil the demands of modern vehicle networks. In following figure 3.1, the bus level of a high-speed CAN is depicted.

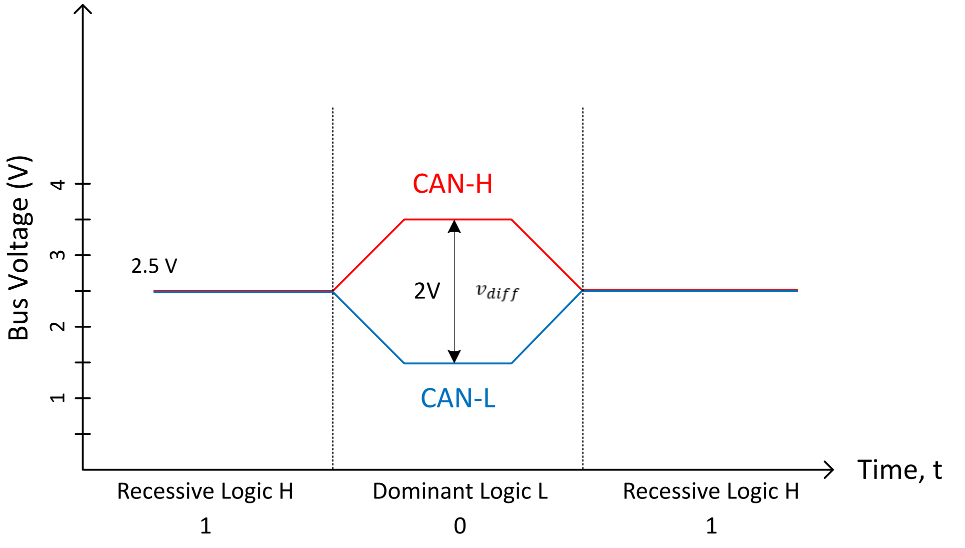

Figure 3.1: Typical bus level of a high-speed CAN. Adapted from (Blackman and Monroe, 2013, p. 3)

When transmitting a dominant bit (0), the CAN-H is driven towards 5 V, the CAN-L towards 0 V. The differential voltage v_{diff} for the dominant bit (0) is always 2 V. The mentioned 120 Ohm resistors reset the two wires to a nominal differential voltage of 0 V (Zimmermann and Schmidgall, 2014, p. 59).

Low-Speed/Fault-Tolerant CAN

The ISO 11898-3 standard is designed for low-speed applications with data rates of 40 kbps up to 125 kbps. Low-speed applications are, in most cases, comfort applications like the electric window lifter. The main goal is to further simplify the wire harness. Following figure 3.2 shows how the bus level for a low-speed CAN looks like.

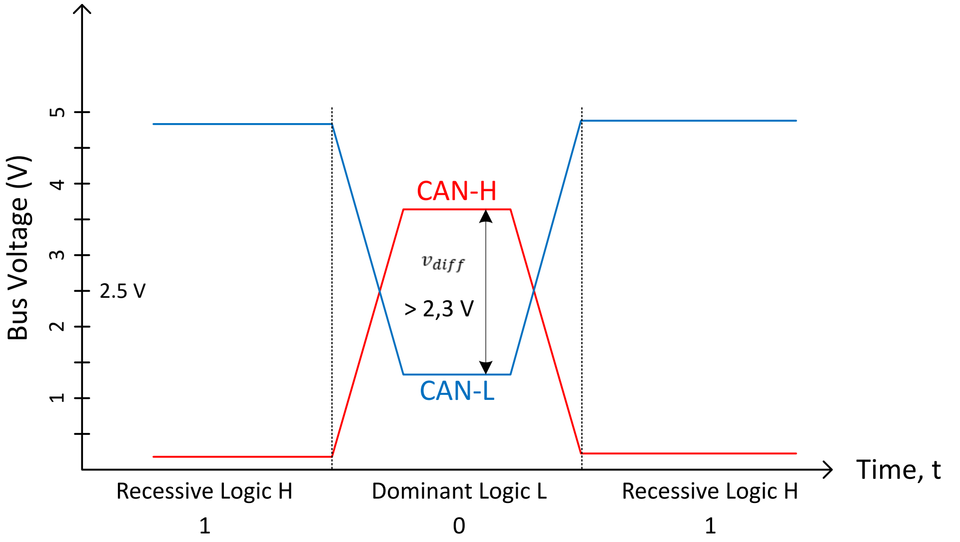

Figure 3.2: Typcial bus level of a low-speed CAN. Adapted from (Zimmermann and Schmidgall, 2014, p. 59)

In contrast to the high-speed CAN, an overall termination resistance of about 100 Ohm (but not below!) is sufficient. Instead of the linear bus topology, a star bus or tree topology can be used as well. Both low-speed and high-speed CAN use the same protocol and the same twisted pair cable. Low-speed CAN still works if one wire is damaged, while high-speed CAN requires both wires. Thus, it is quite important to install redundant cables for safety-critical High-Speed CAN applications. The main reason for using different CAN standards is that in certain applications, e.g. engine management, a higher data rate is required to match the fast processes in this domain. Furthermore, the distances are considerably higher compared to the comfort area (Zimmermann and Schmidgall, 2014, p. 2).

3.1.2 Transceiver, Network Topology and Bus Length

The common interface between a CAN controller and the transmission medium consists of a transmitting and receiving amplifier. In practice, this interface is often a two-wire differential bus. When the transceiver is operating as a transmitter, it converts and transmits the signal from the controller to the bus. As receiver, it provides the recessive level and shields the input comparator of the controller chip against voltage overloads from the bus. Due to this mechanism, failures of the bus, for example broken wires, short circuits, etc. can be detected. Furthermore, a galvanic insulation between CAN nodes and bus can be achieved (Di Natale et al., 2012, pp. 6).

There is a dependency of bit time and the signal propagation delay in form of the maximum achievable bitrate and the bus length. The bus length is directly dependent on the bit rate. The higher the bit rate the shorter the bus length. The following rule of thumb by (Zimmermann and Schmidgall, 2014, p. 58) gives an indication for a reasonable bus length.

$$bus\,length \leq 40\,...50\,m * \frac{1\,Mbps}{bit\,rate} \tag{3.1}$$

The maximum bus length can be easily estimated for the different bit rates. In theory this means that the actual bus length of a bus with 1 Mbps can be up to approx. 40 meters. This assumption is quite optimistic since a maximum distance of about 25 meters is more realistic for data rates up to 1 Mbps. However, for other bitrates e.g. 500 kbps this estimation holds quite well.

Components used within the network have different delay times and affect the overall signal propagation delay: CAN controller (50-62 ns), Optokoppler (40-140 ns), Transceiver (120-250 ns) and cable (5 ns/m) (Di Natale et al., 2012, p. 6). High bit rates affect the maximum bus length due to delay of the bus transceivers. All control units connected to the bus must be operated with the same bit rate (Zimmermann and Schmidgall, 2014, p. 58).

3.1.3 CAN Communication

CAN is a peer-to-peer network: there is no single master which controls the access of single nodes for reading or writing data onto the bus. If a CAN node is ready for data transmission, it checks if the bus is occupied. Then it writes a simple CAN frame onto the network. The CAN frames do not contain any addresses of the transmitting sender or receiving nodes. Instead, a unique arbitration ID tags the frame. All nodes in the CAN network receive the CAN frame and each of the nodes has to decide - depending on the arbitration ID - whether it accepts the frame or not. If several nodes try to transmit a message via the CAN bus simultaneously, the node with the highest priority (equals the lowest arbitration ID) receives access to the bus. Nodes with lower priority have to wait until the bus is available before they can initiate a new transmission. Consequently, this implementation of CAN networks guarantees the deterministic behavior for the communication of the CAN nodes (National Instruments, 2014).

Since there are only binary signals, all signals must be encoded accordingly. In CAN, *non-return to zero* (NRZ) encoding is used. This kind of encoding guarantees a minimal amount of transitions and a remarkable failure safety against external interferences. An example for NRZ is depicted in figure 3.3. Used states '0' and '1' are defined as recessive and dominant. The reason for this definition is that the dominant can always overwrite the recessive state; thus assigning priorities. This is also the case if several masters try to access the bus at the same time. Therefore, a safe communication for the signal with the highest priority can be ensured (Di Natale et al., 2012, pp. 2–3).

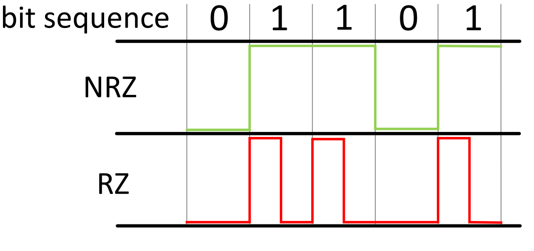

Figure 3.3: Comparison of non-return-to-zero (NRZ) and return-to-zero (RZ) binary codes

3.1.4 Frames

For data transmission CAN offers four different frame formats: **data frame**, **remote frame**, **error frame** and **overload frame**. The most important one is the data frame, where the actual data is sent. The data frame itself consists of several further fields like the arbitration-, control-, data-, CRC-, ACK-field and the seven recessive bits, which signal the end of the frame.
The remote frame is used to request data. A CAN node can obtain messages of other CAN nodes within a network. The structure of this frames is basically the same as a data frame with the difference that this frame does not carry any data. The data field is therefore 0 bytes long.
The error frame is responsible for signalling the CAN nodes in a case of an error. If an error occurs and is detected, all peers within the network know about it and can react accordingly.
The final frame is the overload frame. This frame can inform all peers in the case of a delay. When sending this overload frame the sending node is not able to receive any new messages until this issue is resolved. The error and overload frame can only be generated by the CAN controller itself. There is no possibility for a programmer to change these frames (Di Natale et al., 2012, pp. 13–14).
In following figure 3.4 the structure of a CAN package is displayed (CSS Electronics, 2018).

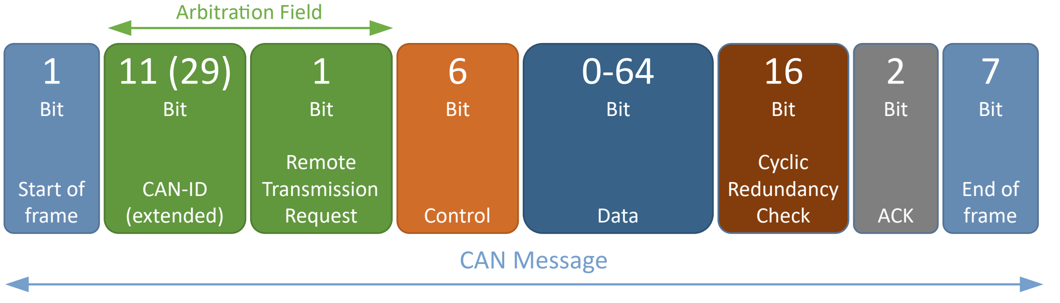

Figure 3.4: Structure of CAN message

CAN can be easily explained with the following example: in a network with 3 nodes, named A, B, and C, all three nodes try to write a message onto the bus at the same time. Now it has to be decided, which node is allowed to be the first one to send data. For this reason, we have the arbitration ID, which gives the messages a priority. In the beginning, all three nodes write the starting field of the frame onto the bus and check this by reading from the bus. Normally, the starting field is a dominant bit. In this case, all three writing processes should have been successful. In the next step, all nodes write their arbitration field bit by bit onto the bus. In this stage the nodes read/write from/onto the bus and compare the bits at the same time. If there is a difference between the written/read bit, the process of arbitration is terminated. This node then changes into the receiving state. In the end, only one node remains in the sending state. This node is the one with the lowest ID and therefore has the highest priority to send its data. All the other nodes which switch into the receiving state will stay in this state until the current transmitter has finished, and the next arbitration is started. The arbitration process is responsible that no bus capacity is lost. With this example, it is obvious that messages with a high priority can be transmitted almost without any delay (see Figure 3.5). However, if there is a lot of traffic on the bus, messages with a low priority often have to wait for a very long time to be processed (Dohmke, 2002).

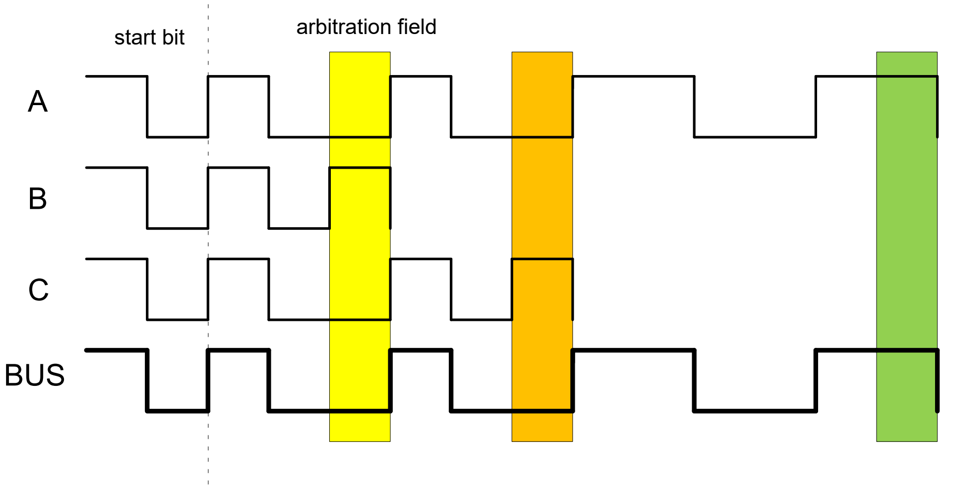

Figure 3.5: Priority assignment on a CAN bus (Dohmke, 2002)

Following section is based on (Zimmermann and Schmidgall, 2014, pp. 67–72): The length of a CAN frame can be calculated by considering all the different parts of the message.

$$T_{Frame} = n_{Frame} * T_{bit} = \\ = (n_{Header} + n_{Trailer} + n_{Idle} + n_{Data} + n_{Stuff}) * T_{bit} \tag{3.2}$$

The CAN ID can be either 11 bits or 29 bits (extended). $n_{Header} + n_{Trailer} + n_{Idle} = 47\,bits$ for 11 bits message IDs and respectively 67 bits for the extended version. The data length is variable in the range of 0 – 64 bits can be chosen in steps of 8 bits (8, 16, ...). The number of stuffing bits is directly dependent on the content of the message and can be calculated with the following formula 3.3:

$$n_{Stuff} = 0... \left\lfloor \frac{n_{Header} + n_{Trailer} + n_{Idle} + n_{Data} - 14\,bits}{4} \right\rfloor \tag{3.3}$$

For correct calculations, the value for n_{Stuff} must be adjusted downward to the first valid integer. As a result, formula 3.4 can be used as a reference when calculating the length of a CAN message:

$$T_{Frame} < 1.25 * (47\,bit(67\,bit) + n_{Data}) * T_{bit} \tag{3.4}$$

CAN		no stuffing		stuffing		
ID	n_{Data}	$n_{Frame,min}$	$T_{Frame,min}$	$n_{Frame,max}$	$T_{Frame,max}$	f_{Data}
11 bit	1 byte	55 bit	110 μs	65 bit	130 μs	7.5 kbps
	8 byte	111 bit	222 μs	135 bit	270 μs	28.9 kbps
29 bit	1 byte	75 bit	150 μs	90 bit	180 μs	5.4 kbps
	8 byte	131 bit	262 μs	160 bit	320 μs	24.4 kbps

Table 3.2: Message length and data rate for $f_{bit} = \frac{1}{T_{bit}} = 500\,kbps$ (Zimmermann and Schmidgall, 2014, p. 68)

A message in CAN can be sent if the according bit is set and if it is present in the buffer of the communication controller. Additionally, the bus must not be occupied for a successful transmission and no message with a higher priority should be in the waiting queue. Only then, the latency of the bus can be approximated with

$$T_{latency,min} = T_{Frame} \tag{3.5}$$

There is no upper threshold for a maximum waiting time. Thus, messages with a low priority might be stuck in a queue for an excessive amount of time. (Zimmermann and Schmidgall, 2014, p. 68) This is also the reason, why the CAN bus is non-deterministic and other bus systems e.g. FlexRay (section 3.5) were introduced for time critical applications such as the drivetrain.

3.1.5 Maximum Latency

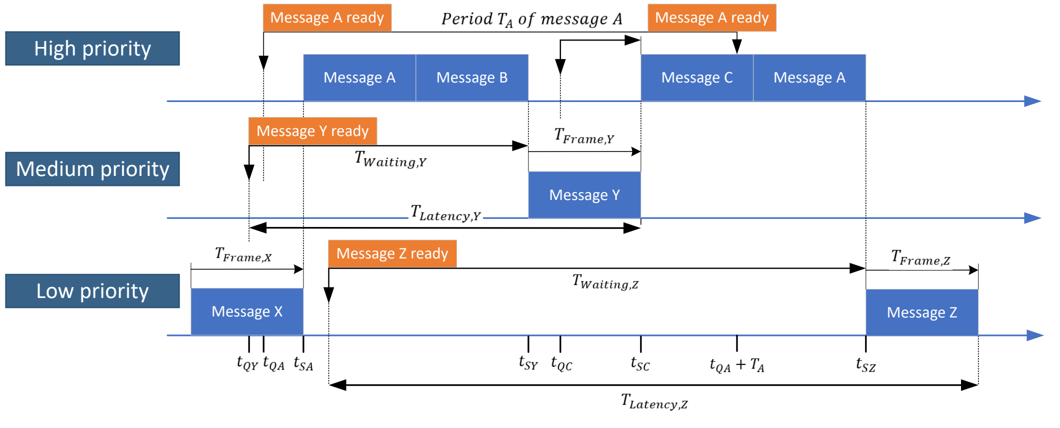

Figure 3.6: Worst-case latency for CAN communication. Adapted from (Zimmermann and Schmidgall, 2014, p. 68)

Figure 3.6 shows a typical scenario in CAN, where messages with high priority will always be handled first. Depending on the priority, a message will be transmitted if the bus is empty. It is possible that a message is already occupying the bus. Since CAN has no mechanism to disrupt a running transmission, the next message will only be sent as soon as the prior transfer has been completed. During the first possible transmission window the message with the highest priority is sent. If there are other messages with a lower priority in the meantime, they will all have to wait until all messages with a higher priority have been transmitted. There are some requirements to calculate the worst-case latency for a transmission in a CAN system (Zimmermann and Schmidgall, 2014, p. 69).

- The message identifier (ID) and all the priorities of the messages as well as their length $T_{Frame,k}$ must be known. The low priority messages can be classified with:
  - $lp(m)$ ... set of all messages which have a lower priority than the observed message m.
  - For the messages with a higher priority $hp(m)$ is defined.
- The sending period T_k must be known for all messages which are transmitted in a cyclic period. In all other cases T_k is assigned the minimum distance between two transmission attempts. This time is also known as *Interarrival Time*.
- All transmissions are made according to the priority of the messages.
- No transmission errors, and thus no automatic retransmissions are allowed.

If all those requirements are considered, the waiting time of an observed message m can be calculated with the following equation 3.6:

$$T_{Queue,m} = \max_{k \in lp(m)} (T_{Frame,k}) + \sum_{k \in hp(m)} \left\lceil \frac{T_{Queue,m}}{T_k} \right\rceil * T_{Frame,k} \qquad (3.6)$$

The first part describes the queuing time for the message with the highest length and the lowest priority. Consequently, the sum indicates the queuing time for the messages with a higher priority. The expression $\frac{T_{Queue,m}}{T_k}$ is rounded up to the next integer and it considers the factor that the waiting time of the message m could be longer than the periodic time of a message with a higher priority. Because the term T_{Queue} is appearing on both sides of the equation, the solution is an iterative one. In the first step, the second expression is presumed zero (Zimmermann and Schmidgall, 2014, p. 70). The iteration is converging, if the average bus load coincides with

$$busload = \sum_{allk} \frac{T_{Frame,k}}{T_k} < 100\% \qquad (3.7)$$

Only then, the maximum latency of the message m can be calculated using following formula 3.8:

$$T_{latency,m,max} = T_{Queue,m} + T_{Frame,m} < T_D < T_M \qquad (3.8)$$

This condition must be met so that no loss of message occurs. T_D is the upper limit latency for each message. This time is in general smaller than the periodic cycle T_M. It is obvious that the maximum latency emerges if all messages are ready for transmission at the same time. Then the messages with the lowest priority are queued and need to wait until all other messages have been transmitted. If other messages become ready for transmission in the meantime, the maximum latency for those low priority messages increases further (Zimmermann and Schmidgall, 2014, p. 70).

Message Priorities

As anticipated, the priority of the message is the major influence on the latency of a message if the bus is busy. Low priority messages have, in general, a higher latency than high priority messages. The priority of a message is high if the deadline (deadline monotonic priority) is short. This approach can be easily applied but is in no case optimal.

With the iterative method of Audsley, it is possible to verify if there is any constellation of priority with which all the requirements can be fulfilled. Each transmission error increases the latency, and an error frame with 31 bits is dispatched by the communication controller to signal this error. Following expression 3.9, (Zimmermann and Schmidgall, 2014, p. 71), shows the iteration process:

$$E(T_{Queue,m} + T_{Frame,m}) = \left[31T_{bit} + \max_{k \in hp(m) \cup m} (T_{Frame,k}) \right] * \left\lceil \frac{T_{Queue,m} + T_{Frame,m}}{T_{Error}} \right\rceil \tag{3.9}$$

The maximum latency emerges if all messages are ready for transmission at the exact same time. By choosing integer multiples of the message periods and fixed phase relations between the messages, this situation can be prevented. The problem in this regard is the Data Link Layer of CAN, which does not offer a network-wide synchronization. Thus, only local nodes can make those adaptations (Zimmermann and Schmidgall, 2014, p. 72).

3.1.6 Error Detection

Another important part during the transmissions is error detection. If some error occurrs during a transmission, there must be some mechanism to check why the process is not successful. In the most ordinary case the incorrect bit has to be retransmitted, so that there is no loss of information. The CAN protocol possesses several mechanisms with which errors can be detected and distinguished (Di Natale et al., 2012, pp. 13–17):

- *Frame-Check*: The frame will be compared to the initial specifications of the length and structure. If those do not match with the standard, the frame has to be retransmitted.
- *Cyclic redundancy check (CRC)*: A checksum is added to the frames. At the receiver this checksum is recalculated and compared with the one of the received packet. Is there mismatch of this checksum, the frame has to be retransmitted.
- *Acknowledge (ACK) error*: A single acknowledgement is sufficient to signal the bus that at least one peer successfully received the message. During this process, the recessive bit is overwritten by the dominant bits of the receivers. If no acknowledgement is detected at the sender, this could mean that the ACK-field is corrupted or was not transmitted at all.
- *Bit stuffing*: A bit is added to a transmission sequence of five or more similar bits. This bit is called *stuff bit*. This stuff bit basically gets the complementary value of the other bits, meaning that in a sequence of five high-bits (five '1' in a row), a low-bit (0) will follow. Since those stuff bits are only added at the transmitter and removed at the receiver, the structure of the frame is not compromised. Bit stuffing offers synchronisation in cases of long bit sequences without bit transitions.
- *Monitoring*: Another mechanism is monitoring, where all nodes within a CAN network observe the bus level. Are there any differences in the bits, these bits have to be retransmitted.

Bit stuffing

Considering the stuffing bits, the overall transmission time of a CAN message will increase. Then, the maximum transmission time T_{max} of a message m will be is given by equation 3.10:

$$T_{max} = \left(n_{ID} + 8\, n_{Data} + 13 + \left\lfloor \frac{n_{ID} + 8\, n_{Data} - 1}{4} \right\rfloor \right) \quad (3.10)$$

where:

n_{ID}	34 (11-bit identifier) or 54 (extended 29-bit identifier)
n_{Data}	denotes the data bytes

(Davis et al., 2007, pp. 248) show that the formula can be further simplified for 11-bits in equation 3.11 and 29-bit in equation 3.12, respectively, to:

$$T_{max} = (55 + 10 n_{Data}) * T_{bit} \quad (3.11)$$

$$T_{max} = (80 + 10 n_{Data}) * T_{bit} \quad (3.12)$$

The CAN bus is event-triggered, meaning there is no real-time behavior. However, with the priorities, certain messages can be transmitted almost without any delay. There are several improvements to the CAN protocol. One is the Time-Triggered CAN (TTCAN) protocol (see section 3.2), which offers real-time behavior. Also, the event-triggered behavior remains in this approach.

3.1.7 Bit Arbitration (CSMA/CR)

In the case of CAN it is vital that no collisions occur. For this reason, the Carrier Sense Multiple Access/Collision Resolution (CSMA/CR) is applied. This procedure counters collisions invoked by bit arbitration. Arbitration in this context means equal distribution of the resources to the different devices. This should counter multi-access to the bus. Still, there is the necessity of distinguishing between the different signal levels. Two are used in this matter, namely the dominant, and the recessive signal level. The dominant level prevails over the recessive. Mathematically, this corresponds to an AND conjunction. If a collision occurs, the message with the higher priority will then be transmitted without any problems, while the one with a lower priority must stop the transmission (Lawrenz, 1997, pp. 31–32).

3.1.8 Bus Termination

When using electrical transmission lines as a bus, there will be reflections at each end of the wire. Such reflections occur as soon as a signal is transmitted over optical or electrical transmission media. A part of the signal power will be reflected to the origin of the signal, and therefore affect the overall signal. Deficiencies within the wire trigger an impedance mismatch or a non-linear alteration of the characteristics. Signal reflections have to be avoided to ensure matching, if a node is requesting the electrical state of the bus. To achieve safe transmissions within an automotive bus network, terminating resistors with a value of 120 Ohms are required. These resistors are positioned at each end of the wire to compensate those reflections. Another action can be taken by avoiding long stubs lines (Di Natale et al., 2012, p. 8).

Most important properties of CAN

The functionality of the CAN protocol is as follows: At the end of each phase of arbitration only the peer with the highest priority can allocate the network bus. This means that a node in a CAN network can either send or receive. However, only one node can send at a time, all the other nodes have to be in a receiving state during this time frame. Additional to the priority, each message has an identifier (ID) by which the receivers can distinguish if a message has been received or not. Collisions in this context do not lead to a delay at every single peer. Therefore, the message with the highest priority can be sent almost in real-time.

The key advantages of CAN according to (Di Natale et al., 2012, pp. 1–2) are

- Low cost
- Easy protocol management
- Deterministic resolution of a conflict
- Embedded features for error detection
- Retransmission

CAN and its problems will be further analyzed in section 5.3. Some improvements of CAN have been achieved by adding timing (see section 3.2) and flexible data rate (see section 3.3).

3.2 Time Triggered CAN (TTCAN)

As previously discussed, only the message with the highest priority will obtain the best possible latency. Other messages with a lower priority will often be queued, and thus the latency will be much worse. For those messages, no real-time can be guaranteed and it is not even certain that the message will be delivered to a busy bus at all. Additionally, if the control units accessing the bus are not synchronized in any kind, peak loads could occur when all CUs try do so at the same time. In contrast to CAN, the bus access of the peers must be synchronized for TTCAN in a pre-defined time window as it is the case in *Time Division Multiple Access* (TDMA). Consequently, a time master is introduced, which initiates a cyclic communication employing reference messages. All control units are synchronized as soon as they receive the first reference message (Reif, 2014, p. 16).

If a specific message should be transmitted frequently, a control unit can obtain several time frames in a cycle, not only one. A control unit requires only knowledge of the time slots in which it can transmit messages and when the transmitted messages should have been received. There are three different kinds of time frames (Zimmermann and Schmidgall, 2014, p. 74):

- In a *reserved time slot*, only a single control unit can transmit messages. No collisions can occur when using this technique.
- *Arbitrating time slots* allow the bus access to several control units. A collision detection/correction algorithm is required to prevent such incidents. The CSMA/CR procedure is applied. The communication is then event-triggered. It is similar to the standard CAN communication, except that each device has to check if their message can be transmitted and received completely before the end of the allocated time frame.
- The third type of time slot are *without any restrictions* and can be chosen freely. They are envisaged for further extensions to allow additional messages without changing the overall communication scheme.

Not all messages have to be transmitted in every single cycle. Instead, it is possible to combine multiple cycles into one system cycle. Messages will then be transmitted again only if the system cycle restarts. A system can possess up to eight time-masters to retain the reliability of the system in case of a total failure of one master (Zimmermann and Schmidgall, 2014, pp. 72–74).

In comparison to the standard CAN protocol, the major difference lies in the deterministic transmission by introducing the TDMA-like approach; bit and data rates of TTCAN are the same. However, a new problem arises in the increased latency for event-triggered messages with high priority. Due to the time frames, such messages require a longer time to be transmitted. Also, the existing problem with limited bandwidth is not solved by this approach. As a result, TTCAN is only feasible for certain applications, like controlling and measuring tasks which are done periodically all over again. This is also the reason, why TTCAN is not widely spread in automotive applications (Zimmermann and Schmidgall, 2014, p. 75).

3.3 CAN-FD

As discussed in section 3.1.2, the CAN protocol is limited in terms of data rate and bandwidth. Since other protocols such as FlexRay (section 3.5) do not really offer a solution to the bottlenecks of CAN, and a vehicle-wide implementation is too costly, Bosch decided to enhance the existing CAN protocol. This improvement was presented in 2012 and permits CAN to use a flexible data rate. Hence, the data transmission rates are higher and the payload can be increased from 8 to 64 bytes. Both improvements can be used dynamically. If higher data rates are not possible due to a long length of the transmission medium, the payload can be elevated to up to 64 bytes to increase the data throughput. This revision of the CAN protocol is called *Controller Area Network with Flexible Data-Rate*, short CAN-FD (Zimmermann and Schmidgall, 2014, p. 76–77). CAN-FD is envisaged to be a solution for the growing data traffic which will occur with the incorporation of ADAS. The message structure of CAN-FD is depicted in Figure 3.7.

The difference between a normal CAN and a CAN-FD message lies in the addition of three additional bits. All three bits are part of the control field. One is added in the header, which is called *Extended Data Length* (EDL). By using this additional bit, the bit rate can be increased by quite a margin

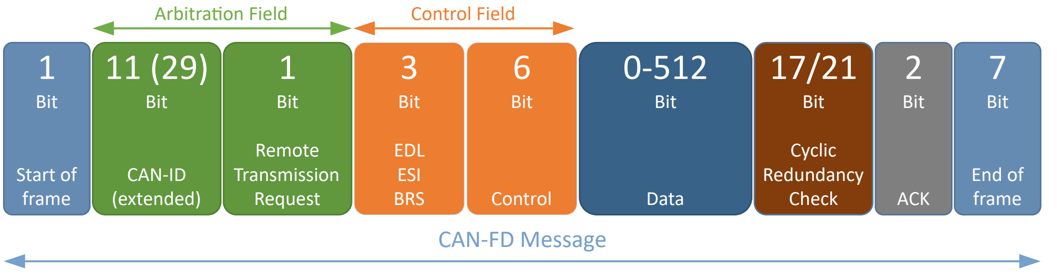

Figure 3.7: CAN-FD message structure

(up to 4 Mbps). The actual switching between the bit rates can be done with the *Bit Rate Switch* (BRS). The final bit is called *Error State Indicator* (ESI). The ESI is used to identify the state in case of an error of one of the network nodes. These modifications lead to an increment of the CAN-FD message by the size of the inserted bits (Zimmermann and Schmidgall, 2014, p. 77–78).

The required adjustments for calculating the duration of a CAN-FD message can be seen in formula 3.11, (Zimmermann and Schmidgall, 2014, p. 78).

$$T_{Frame} < 1.25 * \left[29\,bit(49\,bit) * \frac{1}{f_{bit,N}} + (26\,bit + n_{Data}) * \frac{1}{f_{bit,H}} \right] \quad (3.13)$$

where

n_{Data}	number of data bits
$f_{Data} = \frac{n_{data}}{T_{Frame}}$	payload
1.25	bit stuffing in the worst case
$f_{bit,N}$	normal bit rate
$f_{bit,H}$	increased bit rate after switching

The estimated improvement of the payload is visible in table 3.3. By altering the header, the CRC checksum must be adapted as well. However, it is still required to separate network subsets in several bus lines to minimize the bus load, and thus, bottlenecks. The benefit of using CAN-FD is not only the higher data rate but also the resulting improved real-time capabilities. At the same time, almost 4-8 times the amount of data can be transmitted. Thus, the maximum latency for high priority messages decreases.

n_{Data}	CAN 2.0 f_{bit} = 500 kbps	CAN FD $f_{bit,N} = f_{bit,H}$ = 500 kbps	CAN FD (switching) $f_{bit,N}$ = 500 kbps $f_{bit,H}$ = 4 Mbps
8 byte	not possible	29 kB/s	79 kB/s
16 byte		35 kB/s	131 kB/s
32 byte		40 kB/s	195 kB/s
64 byte		44 kB/s	260 kB/s

Table 3.3: Payload rate estimation for CAN and CAN-FD (Zimmermann and Schmidgall, 2014, p. 78)

The Cyclic Redundancy Check (CRC) for CAN-FD has been adapted to resolve some existing issues of the standard CAN. There are three algorithms which can be used for verification. The verification keys are now longer; more bits are required for the CRC (17/21 bits instead of 16). Furthermore, a stuffing bit is used at the beginning of the CRC and after each fifth bit. With this adjustment, the overall data integrity is improved and known issues with CAN are resolved (Mutter, 2015).

3.4 Local Interconnect Network (LIN)

LIN was introduced 1998 as a cheap alternative for connecting noncritical components to each other. The reason for the low cost lies in the physical layer because (ISO 9141)[2] allows the usage of single-wire lines. The bus level can be directly derived from the electrical system and is analog to CAN (recessive, dominant) (Reif, 2014, p. 22).

As visible in figure 3.8, mostly applications such as heating, seat controls, demister, and display information are connected to a LIN bus. Those control systems require a minimal data rate since only a few bits and bytes must be transmitted to achieve the desired adjustment. The designated bit rate covers the range of 1 - 20 kbps. There are 3 different fixed bit rates which are commonly used: 2,4 kbps, 9,6 kbps and 19,2 kbps (Zimmermann and Schmidgall, 2014, p. 80).

[2] ISO TC 22/SC 3, 1998.

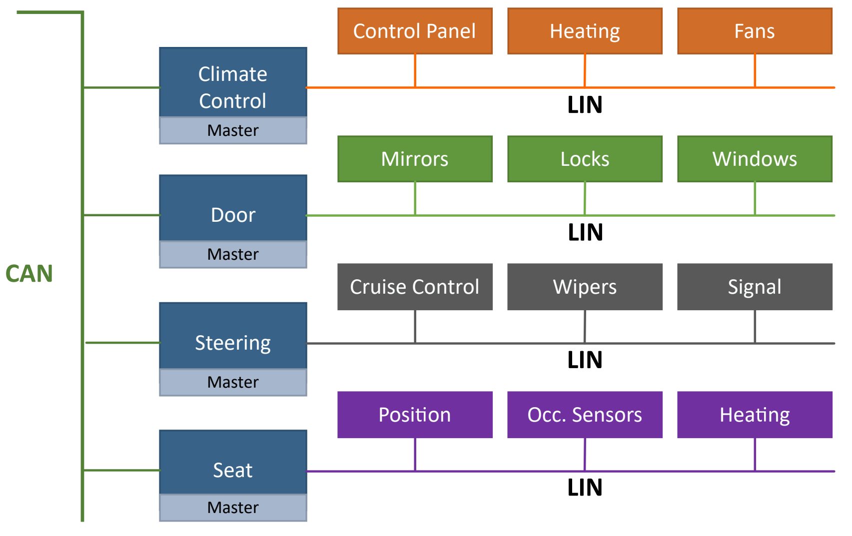

Figure 3.8: Example of typical LIN applications

Like CAN, it is a message-oriented protocol. However, there is only a single master node in the LIN bus system, which controls one or more slaves. This one master node often acts as the gateway node to a higher-level bus network, which is mostly a CAN network. The slaves are in most cases sensors, actuators or some simple switches. The communication works with tasks and is time-controlled with a scheduling table by the master. Nodes can have three different types of communication: point-to-point, multicast or broadcast – the same as in CAN. In general, there is a maximum of 16 nodes in a LIN subnet. In reality, LIN clusters often consist of only 4 nodes. By adding a slave task to the master node, the master cannot only receive messages but also declare relations for the communication between nodes. The LIN bus is an unshielded single wire connection. Once again, there are a dominant and recessive levels for signaling. While the dominant level '0' equals the voltage of about 0V, the recessive level '1' equals the battery voltage. To set the recessive level at the master node, a $1\,k\Omega$ pull-up resistor is required. For the slave nodes, $30\,k\Omega$ pull-up resistors are used to adjust to the battery voltage (Reif, 2011, pp. 107).

It could be difficult when using different wiring to distinguish between the different signal levels. Also, the transmission must be robust against interferences and radiation. Thus, certain tolerances are required for the sending and receiving domain to still allow a valid and stable data transmission. The tolerance bands at the receiver can be often up to 40% of the signal level for the recessive and dominant level, as depicted in Figure 3.9. Those tolerances are required to guarantee reliabilty (Specks and Rajnäk, 2003).

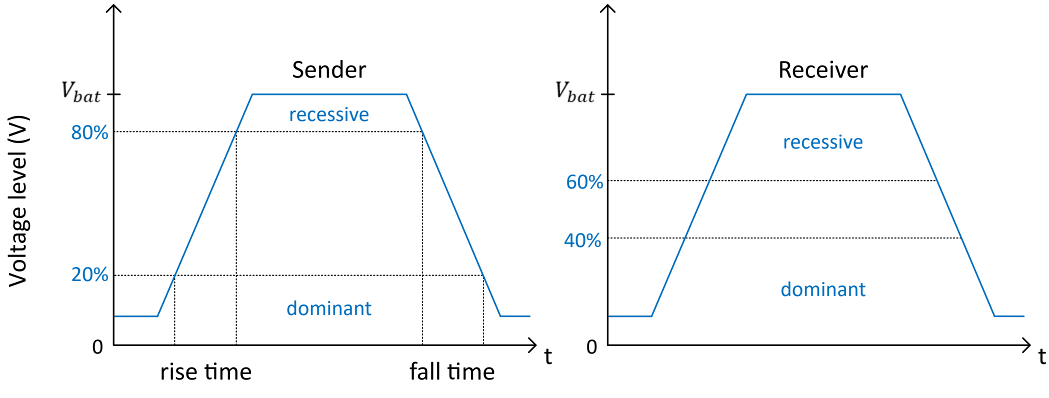

Figure 3.9: Tolerance bands at the LIN receiver. Adapted from (Borgeest, 2010, p. 100)

The LIN frame is quite simple. It only consists of a header and data field. While the header gives reference for synchronization, including the Identifier (ID), the data field includes the actual information. In a LIN description file all the information and specifications of all nodes in the LIN network are recorded.

For a reliable communication between master and slave, synchronization between the nodes is of utmost importance. At each beginning of the frame, such a synchronization is initiated. Included in the header of the frame is a synchronization break, which simplifies the procedure to detect the beginning of a new synchronization request. A so-called *SynchBreak* consists of at least 13 consecutive dominant bits and a recessive level. Then, the *SynchField* is transmitted to start the synchronization between the nodes. The bit string used for synchronization is '01010101'. In the header of the frame is also an Identifier (ID). Based on the ID, it is possible to know what kind of message it is and for which nodes it could be important. As a result, nodes in the network know if they should receive the message or ignore it. The ID consists of 8 bits. 6 of that 8 bits are used for 64 ID characters. Each of those 64 IDs defines a unique event. ID = 60 is, e.g., the master request for commandos and diagnose. The two remaining bits are used for the checksum to counter problems during transmission. If the header has been received successfully and the checksum is correct, the actual data transmission will begin. Slave nodes will know by the Identifier if they are meant to receive the data. When a slave node is receiving data, it has to respond with an acknowledgement so that the sender is informed that the data has been successfully transmitted (Reif, 2011, pp. 108–110).

There is also a mechanism to save energy by putting nodes into sleep mode. The master can issue such a goto-sleep command with the mentioned ID 60. Then, the slave nodes will transfer into that state if there is no active data transmission for a short period of time. Both, slaves and master can wake the network up if it is in a sleeping state (Reif, 2011, pp. 108–110).

The following LIN bus example is described in (Reif, 2011, p. 110) and rephrased:
Climate control is the best example when talking about a LIN bus. The control/display unit is the master in this system and is responsible for regulating the rotation speed of the fresh air fan. It is quite a simple control loop where the actual temperature within the car is compared to the desired one. To obtain the temperature, a sensor which measures the temperature regularly is required. The control unit can calculate from the temperature difference, which rotation speed of the fan has to be achieved to diminish the temperature mismatch. It will transmit a message onto the bus with the according identifier to change the rotation speed of the responsible slave. The corresponding slave will use the information and adapt to the demanded rotation speed and give an acknowledgement to the master, if the process is successfully realized.

There are some basic prerequisites for the system to work. E.g. there must be a functional connection to an overlying CAN network, which delivers important information such as the rotation speed of the engine. This information is required for the fail-safe mechanism of the fresh air fan. If the rotation speed of the fan is under the idle threshold, the high load might lead to an engine stall. Thus, the fresh air fan must be deactivated based on the rotation speed of the engine to prevent such a failure.

Error detection and correction is handled by the master, who controls his slaves with a status bit. The correction can vary since there is no clear definition for error handling in the official specifications (Reif, 2014, pp. 20–

21). Thus, no arbitration or collision management is required since the master handles the entire bus access.

3.5 FlexRay

FlexRay is a multi-master bus system and supports the star, bus and line-topology. The protocol guarantees certain properties of the transmission, as well as high transmission rates and a fault-tolerant design. The field of application of FlexRay is mainly the powertrain and drivetrain system, as well as active safety systems like X-by-wire (X for brake, steer etc.) (Reif, 2011, p. 132).
There is the possibility to transmit messages redundantly (2-channel system) to increase the reliability. The line connection used is either a shielded and/or a twisted 2-wire-line with a characteristic impedance of 80 to 110 Ohms (Zimmermann and Schmidgall, 2014, p. 98).

One specific application, for example, is the secure and reliable data transmission of a central control unit to each of the control units positioned at the four dampers of the wheels. Such a system requires higher data rates for the transmission since the number of control and status signals compared to CAN is much higher and ever increasing. The signals must be transmitted with absolute reliability and as quickly as possible (real-time) to ensure the functionality of those systems.
In the official FlexRay specifications[3], a maximum distance of 24-meters between the different nodes is defined. For FlexRay, the most commonly used network topology is a star due to higher obtainable bit rates. When using an active star coupler, it is possible to increase this distance between the control units to a maximum distance of 72-meter cable length. In an active star coupler network, it is most likely to achieve the maximum bit rate of 10 Mbps. This is quite a difference to a passive coupling system, where only 1 Mbps are realistic. When using a 2-channel system and the second channel also for additional transmission and not as redundancy, higher bit rates up to 20 Mbps are theoretically possible. Each of the channels uses a twisted-pair cable. In common bus topologies, such bit rates are not likely since the number of nodes (4 to 22) and the wire length are more critical. In newer versions of the protocol, 2,5 Mbps and 5 Mbps are

[3]BMW AG, Daimler AG, 2010.

also permissible to allow simpler implementations. Each node of a FlexRay system consists of a host processor, communication controller, a bus driver and an optional bus guardian (Zimmermann and Schmidgall, 2014, p. 98) (Reif, 2011, pp. 133–134). The structure of a FlexRay system is shown in Figure 3.10.

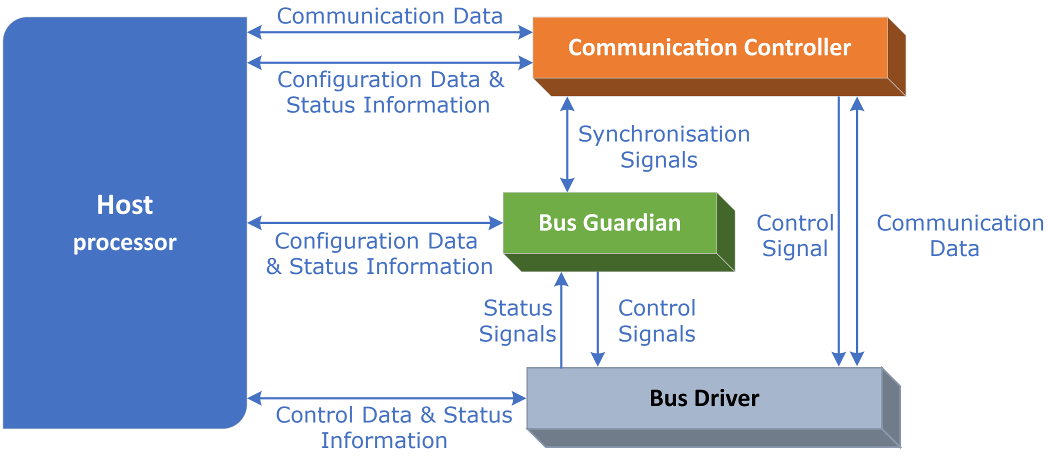

Figure 3.10: Structure of FlexRay. Adapted from (Reif, 2014, p. 24)

The host processor acquires all the necessary sensor data and forwards this information to the communication controller. In the communication controller, the received sensor data are processed and transmitted to the associated actuators. The controller also provides scheduling, synchronization, and control of the bus access. The bus driver converts the information into physical voltage signals and vice versa. It is also responsible for protecting the whole FlexRay controller against electrostatic charges. Finally, with the bus guardian, FlexRay has a mechanism to detect communication and synchronization errors and start appropriate counter-measures to correct those problems (Zimmermann and Schmidgall, 2014, p. 98) (Reif, 2011, pp. 133–134).

The precondition for a deterministic data transmission is a global time reference. To provide real-time to the system, the whole communication process is divided into a static and dynamic segment. For the static segment, each message is transmitted at a fixed time slot, also known as *Time Division Multiple Access* (TDMA) method. As a result, the communication process is deterministic. The minimum length of a static segment is two TDMA windows to ensure that the sync frames are also transmitted. The dynamic segment uses the *Flexible Time Division Multiple Access* (FTDMA) method. For the dynamic communication, the message IDs are prioritized and transmitted if required. Thus, the latency requirements are not as high as for the static segment. With this type of segment, an event-triggered communication like CAN is possible. However, this means that messages with a high Frame ID might be queued for a long time (Reif, 2014, p. 26).

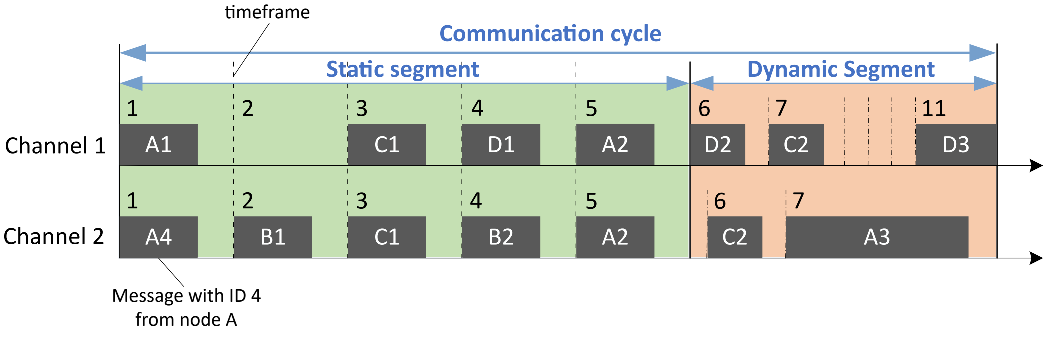

Figure 3.11: Communication cycle of FlexRay. Adapted from (Heinecke et al., 2002)

The FlexRay protocol is divided into five layers (Reif, 2011, p. 136):

- Coding / Decoding
- Media Access Control (MAC)
- Frame & Symbol processing
- Clock synchronization
- Monitoring of schedule by bus guardian

Since there are interfaces among all core mechanisms, a process is required which coordinates, observes and synchronizes all changes. This process is called Protocol-Operation-Control (POC) (Reif, 2011, p. 137). The frame of FlexRay consists of a Header with the Frame ID, the Payload with the actual data (max. 254 byte) and the Trailer with CRC bits to enable data protection. FlexRay can be also used with optical transmission media, but in most cases a similar implementation to High-Speed CAN – a differential voltage interface on a two-wire line – is used. Unfortunately, FlexRay is very inefficient for short messages and the resulting bandwidth is smaller than anticipated (nowhere near the 10 Mbps). Furthermore, the TDMA concept does not provide a dynamic behavior for the communication procedure and substituting the software when switching from event-triggered to a time-triggered operation is quite expensive in terms of effort (Zimmermann and Schmidgall, 2014, p. 77).

3.6 Media Oriented Systems Transport (MOST)

The MOST bus uses optical fibers as a transmission medium. The protocol was first established in 1998 by BMW in cooperation with Daimler AG. However, the operational area is only convenient for multimedia applications such as audio, video, navigation or other telecommunication systems, which require a high bandwidth. Real-time is not the essential purpose of this protocol, even though the high bandwidths could allow such a realization (Schmid, 2006).

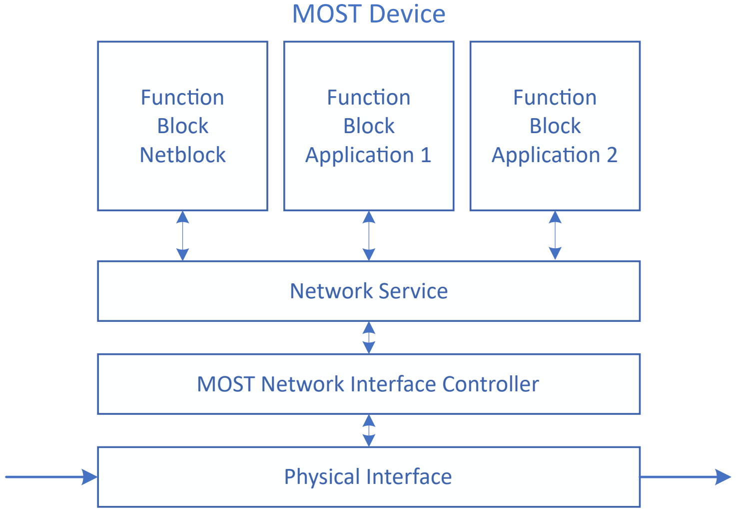

Figure 3.12: Structure of a MOST device (MOST Cooperation, 2010)

MOST supports Plug & Play for up to 64 nodes. It is possible to add devices simply by adding or removing them at the designated interfaces. For automotive application, the bus is usually arranged in a ring topology (see section 2.2.4). Other supported topologies can be star or chain. In a MOST network, one device will be determined as the master. The master is then responsible for regulating and synchronizing the network – all other devices act only as slaves. In contrast to CAN, MOST covers all seven layers of the ISO/OSI model and is thus attractive due to the existing and therefore relatively cheap bus controllers and transceivers. Also, the transmission protocol of MOST works independently of the physical transmission lines. In the first release, the bandwidths were limited to 25 Mbps - synchronous up to 24,8 Mbps, asynchronous 14,4 Mbps. Newer versions of the protocol, like the MOST150 standard, can reach up to 150 Mbps (Schmid, 2006).

MOST possesses an asynchronous control channel with a data rate up to 700 kbps. This channel is only used for transmitting simple control commands to signal states of devices. The clock frequency for this control channel is, in most cases, 44.1 kHz.
The actual data is transmitted by use of an optical fiber, which consists in many cases of a polymer (Polymer optical fiber POF). The main advantage of this POF and other materials used for optical fibers, is the insensitivity to electromagnetic interferences. Thus, they do not generate any additional electromagnetic waves which could influence another device or system. In addition, the weight is considerably lower and due to the electromagnetic insensitivity, the positioning of cables is much more flexible (Reif, 2011, p. 115).

The structure of communication is rather simple and basically a unidirectional point-to-point connection between the various elements (control units) of this ring network. The optical signal is regenerated in every single device and sent further until the message reaches its designated target. As a result, each control unit requires exactly one input and output for this kind of topology and communication. For communication, a master will be designated who controls, times and generates the messages. All other devices in the network must synchronize to the same bit and frame clock of the master and retain either an active or an inactive state. In an active state, the control units can modify and add/extract data from the incoming data stream before sending it along the path. If a device is in an inactive state, the information is just bypassed without changing its own state. For each device the stream passes, there is a delay of $45\,\mu s$ (MOST 25) or $1\,\mu s$ (MOST 50, 150) respectively. Since every message goes around in a full circle (ring topology) the delay when using MOST 25 can amount to a maximum of 2,88 ms solely for passing by. For MOST 50 or 150, the delay is considerably lower. Also, the length of the lines, message length of several μs etc. have to be considered – resulting in a considerable delay in a network with the maximum number of nodes (Zimmermann and Schmidgall, 2014, p. 121).

In general, data is modulated into the optic range and Manchester-coded, enabling a bit clock synchronization on the receiver side. The received optical signal is then converted back into the electric domain at the control unit for further processing. There is also an electrical wire solution for MOST, where a twisted two-wire line is applied. For higher bandwidths ($>$ 100 Mbps), however, this twisted two-wire solution is not feasible anymore (Zimmermann and Schmidgall, 2014, p. 121).
In Figure 3.13, the structure of a typical MOST controller is displayed.

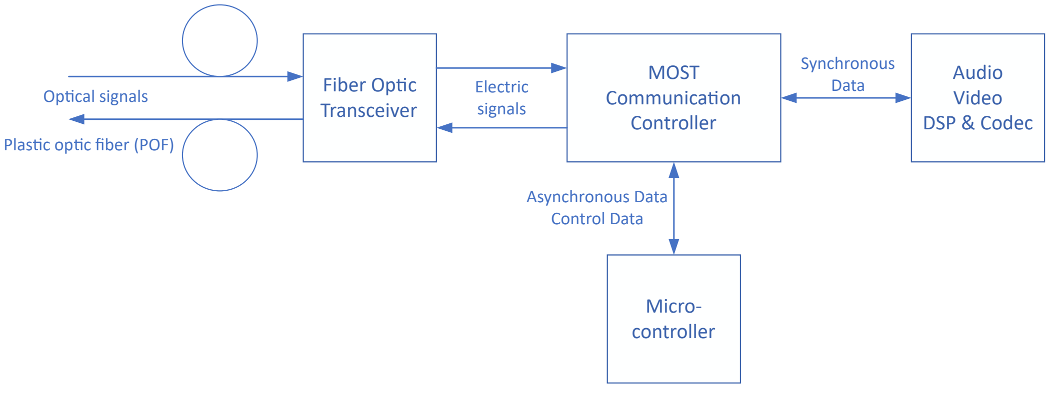

Figure 3.13: Structure of a MOST controller (MOST Cooperation, 2010)

There are two communication modes in MOST, which can be activated / deactivated by control messages: The *synchronous* part of the MOST network is mainly used for real-time transmissions of audio/video or sensor data. Access to the data is regulated by time multiplexing, in specific *Time Division Multiplexing* (TDM) (see chapter 4.5.4). Physical channels can only be occupied for a certain amount of time, e.g. if an audio file is played. It is possible to vary the bandwidth by assigning an arbitrary number of bytes to a logical channel. By assistance of a routing protocol, the synchronous data can be delivered to the desired destination. The maximum number of synchronous data bytes allowed in a frame is limited to 60 bytes (Schmid, 2006, p. 30).

The *asynchronous* part is handled differently. If asynchronous data is transmitted, a so-called boundary descriptor must be set to guarantee the exact start of the asynchronous data. Asynchronous data transmissions are mainly used when a high bandwidth is required, or large data chunks are sent. The number of asynchronous data bytes on an asynchronous channel is limited to 48 bytes, if a 48-byte data link layer is appropriated. If an alternative data link layer is used, the maximal packet length amounts to 1014 byte for MOST25/50 and 1506 bytes for MOST150 (Zimmermann and Schmidgall, 2014, p. 126).
MOST requires control data for the communication between the different nodes connected to the bus. Data access is achieved by using the CSMA (Carrier Sense Multiple Access) procedure, which offers fixed and predictable response times. Even though a control message is 32 bytes long, only two bytes can be transmitted in a frame simultaneously. As a result, a chunk with 16 frames is required to transmit a control message (Schmid, 2006).

Frames in MOST are created by the Timing-Master. The frame size is dependent on the MOST version. For MOST25, the data frame is 512 bits, while for MOST150 it is 3072 bits (= 384 bytes). The higher the data rate, hence bandwidth, the higher the number of allocable bits. A MOST150 frame is visible in Figure 3.14.

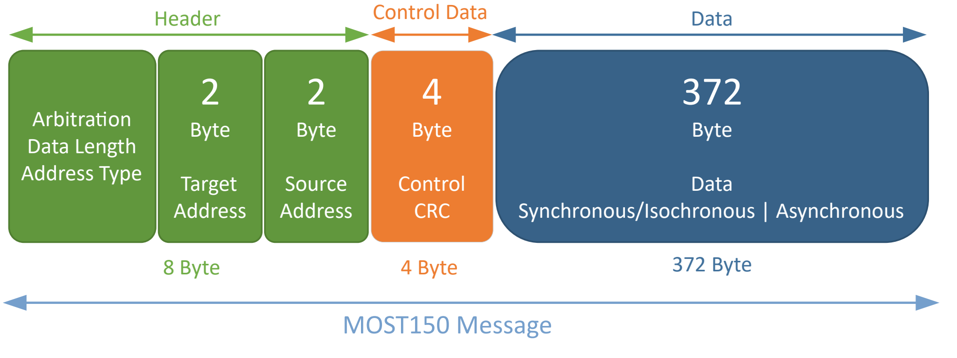

Figure 3.14: MOST150 message structure

Next to fiber, several other components exist in the MOST control unit for optical communication. To receive and transmit signals, specific components such as a Fiber Optical Transceiver (FOT) are required. Both, a

photodiode as well as a light-emitting diode, are part of this transceiver. The task of the photodiode is to convert the incoming optical signal into an electrical signal (voltage). Details on the functionality of optical receivers and transmitters is available in sections 4.4 and 4.3. In contrast to an optical receiver, the optical transmitter converts the incoming electrical signals from the MOST transceiver into light signals for transportation on the optic fiber bus. It is possible to use a variety of different wavelengths for optical communication. In the first release of MOST, a wavelength of 650 nm (Infrared) was used. Nowadays, 850 nm, 1300 nm and 1550 nm are typical values for wavelengths, due to the lower attenuation in those areas in the spectrum (Audi AG, 2002, pp. 17–43).
Since Ethernet/IP is growing to be a potential threat to the existence of MOST, there are several inputs to counter this development. A bandwidth higher than 150 Mbps and the concept of MOST as a physical layer for Ethernet packets are just two examples of current considerations (Zimmermann and Schmidgall, 2014, p. 120).

When taking all this into account, it is obvious that this kind of topology and structure is not at all optimal for real-time applications. One major disadvantage of MOST is the default rate, since the protocol is simplistic, without proper instruments to counter safety and reliability issues. To improve the reliability, it is possible to use a double-ring topology.

3.7 Byteflight

The Byteflight protocol was introduced by BMW and is the first time-controlled bus system for safety-critical applications. It is designed to support CAN in its function and improve the overall system in terms of safety, reliability and transmission speed. Furthermore, similar properties such as fault-tolerance and determinism are required, as well as an interface and enough bandwidth to use diagnostic methods. Byteflight uses optical fibers as a transmission medium and applies the star topology with bidirectional, half-duplex communication. Thus, the lines are immune to electromagnetic interferences. Nodes in a star network can be decoupled from the network when using a star coupler module. Inside the star coupler is an optical transceiver module for each connection. Using

On-Off keying (OOK), permanent blocking by optical transmitters can be prevented (Berwanger, Peller, and Griessbach, 2000).

To achieve the high data rates of 10 Mbps, an optical polymer fiber is used for the physical layer. Under full bus load, the data rates are still over 5 Mbps and thus considerably higher compared to CAN. Byteflight uses the *Flexible Time Division Multiple Access* (FTDMA) procedure to realize a deterministic and solely time-controlled behavior. Incoming and outgoing signals are always similar making the entire process reproducible (Borgeest, 2010, p. 102).
Figure 3.15 shows the topology, defined by (Berwanger, Peller, and Griessbach, 2000, p. 5). There, a star net coupler is used, to connect several fiber optic transceivers (FOT) to a central node with an embedded Byteflight controller. All other nodes (ECUs) are connected with this central node. The connection is established with a fiber optic cable.

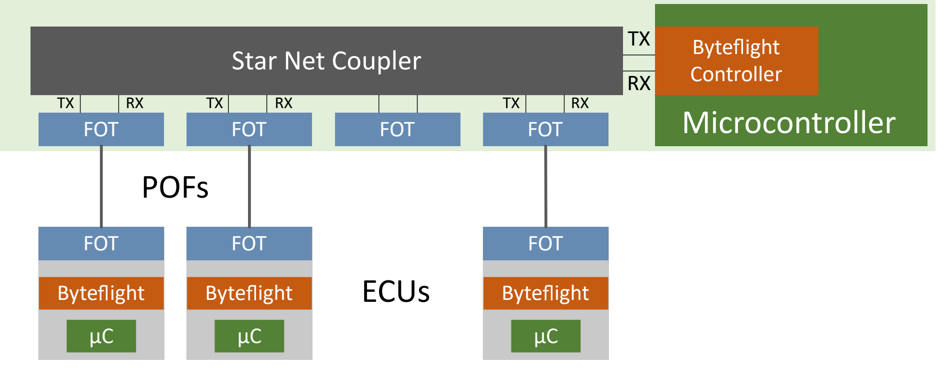

Figure 3.15: Byteflight topology, Adapted from (Berwanger, Peller, and Griessbach, 2000, p. 5)

The protocol is far more flexible than CAN in terms of bandwidth. Communication is initiated by a synchronization pulse providing all devices in the network with the same time-base. Every device can become the time master and supply this pulse. One cycle is set to 250 μs for a data rate of 10 Mbps. In between those pulses it is possible to transmit messages. All messages have a unique identifier and can only be sent once per cycle - resulting in a collision-free communication. A slot counter is started which increases up to a certain maximum. As soon as the counter equals an identifier (ID) value with a valid transmission request, the counter is halted and the transmission for the message with the corresponding identifier is initiated. During that period, no other communication will be continued. Within one communication cycle several high-priority messages can be transmitted. After successful transmission, the counter continues, and the procedure repeats itself. Hence, the latency times for messages are deterministic.

ByteFlight offers a protocol-/hardware steered minimum latency for which high-priority messages can be sent. It combines the best aspects of synchronous and asynchronous communication methods to offer low-priority messages more flexibility. Another characteristic of Byteflight is the capability of changing the synchronization pulse type to indicate, e.g., an alarm. With this mechanism, various safety functions can be enabled. The synchronization pulse can be detected by logical implementations on the components of the optical transceiver module. The structure of a Byteflight message is visible in Figure 3.16.

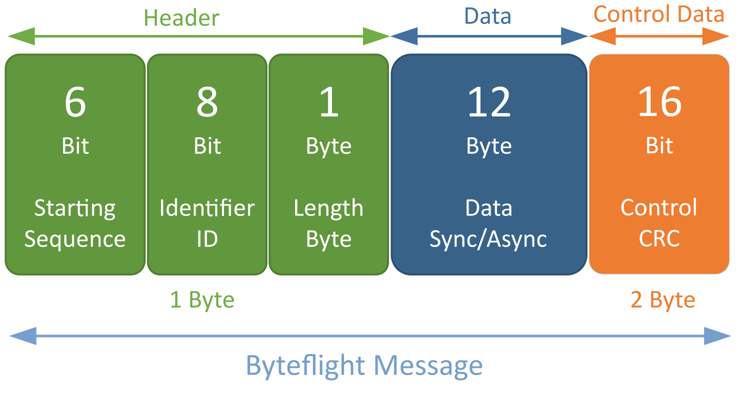

Figure 3.16: Byteflight message structure

The waiting period between messages can be estimated with following formula 3.14 from (Berwanger, Peller, and Griessbach, 2000, p. 2):

$$t_{wait} = t_0 + t_d * (ID - ID_{t-1}) \tag{3.14}$$

where:

t_0	minimum waiting period (1100ns)
$ID - ID_{t-1}$	Substraction of IDs to obtain intermediate waiting period

In general, there is no retransmission mechanism in place in case of transfer errors. Synchronization errors and message format errors, however, can be detected and handled accordingly. Cyclic Redundancy Check (CRC) is used to check for the wrong formats, while Synchronization errors are detected by validating the SYNC pulse (Berwanger, Peller, and Griessbach, 2000, pp. 2). Since redundancy is often a critical requirement for such applications, there are different approaches, how this can be achieved with this concept. The proposed concept by (Berwanger, Peller, and Griessbach, 2000, pp. 6) is to use more gateways and connect the various ECU to at least 2 different gateways.

3.8 Ethernet

Ethernet, also known under the IEEE 802.3 abbreviation, has not been regarded as a solution for vehicular networks for quite a long time, because the protocols are extensive and hard to scale down to a level which is required for automotive applications. In its original form, Ethernet was quite similar to the structure of CAN - a bus system with CSMA/CD method. The physical layer of Ethernet allows transmissions up to 100 Mbps in full duplex. However, for quite a long period, Ethernet did not comply with the OEM EMI/RFI requirements due to the RF noise produced. It is also not properly protected against any interferences from the environment, which is quite expensive to realize. The achievable latency using Ethernet lies in the microsecond range but is, in most cases, too high to replace communications to time-critical sensors or control units. Furthermore, there is no tool to set or allocate bandwidth in a controlled manner to allow multiple sources to transmit data. Another issue is that the impact of mechanical forces and the wide operational temperature range cannot be handled by a standard Ethernet/IP network (Schaal, 2012).

Therefore, Ethernet is usually used only for diagnostics and firmware updates. However, there are many benefits when using Ethernet/IP. The protocol itself is well-tested and established. It is applied for camera-based assistance systems, which require a higher bandwidth than available with CAN, FlexRay, and other protocols. Ethernet provides developers with a high and scalable bandwidth with substantial flexibility.

Initially, no interfaces and no suitable wiring technologies were available. Optical fibers could have been used, but instead, another technology was contemplated. For camera applications mentioned above, a technology called Low-Voltage-Differential-Signaling (LVDS) is used. Due to the low voltage levels (350 mV), the LVDS signals are very sensitive to electromagnetic interferences. Thus, LVDS requires quite expensive shielded cables to guarantee sufficient reliability. Additionally, placing the cable within the vehicle becomes rather difficult (Bogenberger, 2011, p. 36) (Schaal, 2012).

Figure 3.17 shows the message structure of Ethernet according to IEEE 802.3.

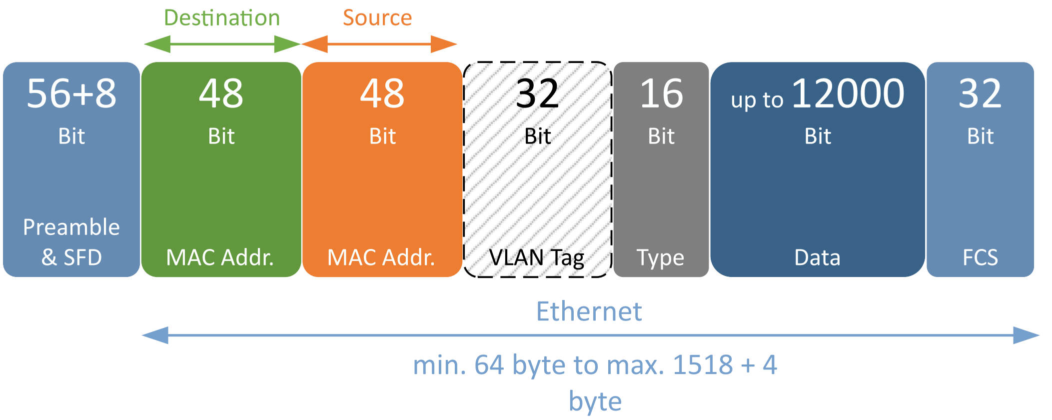

Figure 3.17: Ethernet message structure. Adapted from (Zimmermann and Schmidgall, 2014, p. 140)

SFD stands for *Start Frame Delimiter*. This SFD is often required to synchronize the clock in the beginning for some phyiscal layers. The *Medium Access Control (MAC)* addresses are unique and are designated to the communication controllers of Ethernet. There is also one optional part, the so-called VLAN tag. This tag can be used for virtual subnetworks. The *Frame Check Sequence (FCS)* at the end of the message is quite similar to the CRC. It is a check sum to verify the integrity of the message (Zimmermann and Schmidgall, 2014, pp. 139–140).

Ethernet uses the star topology, where a switch transfers the messages to exactly one designated receiving node within the network. Each device in the network is connected to the switch with a pair of two-wire-lines (point-to-point). The switch identifies all nodes by their unique ethernet addresses. Sometimes the receiver is unidentified, or several devices require the same message. Then the switch conveys the message to all nodes within the network.

In contrast to CAN, the system works without any collisions. However, there can be a bottleneck at the switch, if several messages arrive simultaneously to be transmitted to the same receiver. Only the first message is immediately delivered, while the other messages are buffered. Those messages are transmitted one by one with some time delay. Messages can be dropped, if the cache of the switch is undersized. If the network is large, several switches can be used. The star topology then extends to a hierarchical tree structure (Zimmermann and Schmidgall, 2014, p. 139).
The described basic properties of Ethernet are not convenient for a vehicle application. There is no proper protection against electromagnetic interferences, extreme temperatures, moisture, and vibrations. Therefore, a specific physical layer was developed named BroadR-Reach. The potential bit rate can reach up to 100 Mbps in full-duplex-operation. A single pair can be used for transmission in both directions (Zimmermann and Schmidgall, 2014, p. 139). The requirements are the same as for FlexRay. The delay in a switch due to the buffering when transmitting messages to the same receiver shows that Ethernet in its basic form is not suitable for real-time applications. By adapting protocols to real-time capabilities, the data rate decreases in most cases.
In section 2.4, it has already been mentioned that there are problems with the real-time capabilities of Ethernet. Thus, certain methods based on AUTOSAR 4.2.2 and IEEE 802.1AS (802.1AS-ref) were used to add timing and synchronization for video and audio applications. In AUTOSAR, a Global Time Master (GTM) was introduced. The GTM is the reference for all sub-networks and devices like gateways, where time correction is necessary to keep synchronization. When using CAN and Ethernet, the time slaves have to do this correction by comparing the transmitter time stamp with the local received time stamp. For FlexRay, due to determinism, the reference time is already provided by the standard clock. The approach in IEEE 802.1AS is somewhat similar. Naturally, the synchronized time must be distributed to the whole system. The message run-time (between ports) and Best Master Clock Algorithm (BMCA) are two additional procedures

to keep synchronization – which is started by an initial sync- and follow-up message (Jesse, 2016).

The message run-time is the indicator for ECUs if they are in a synchronized network. With the BMCA, the ECU with the best system time becomes the overall master in a dynamic system. In a vehicle, however, many predefinitions are required to optimize communication. This concerns BMCA, as well as the time stamp itself. If the global time master fails, there need to be certain mechanisms in place to keep the synchronization alive. For example, it is possible to use a backup timer which continues to run in case of a failure. However, the BMCA structure is too sluggish and even with a backup master, the whole synchronization is predestined to fail in certain scenarios. Another obstacle remains the inability of switch drivers to forward their port number. Meaning that, e.g., the message run-time mechanism does not work for the switches (Jesse, 2016). This problem, however, seems to has been solved by newer versions of AUTOSAR (> v4.3).
In automotive applications several different time domains for GPS time, UTC time or sensor data evaluation is required. Even though both AUTOSAR and IEEE 802.1AS-ref included options for additional time domains, this might still be an area where improvement are required for future automotive systems. This is also true for all the other restricting properties of the protocols. Even though, there are steady advancements, more complex systems including LiDAR etc. might hit a brick wall at some point. Thus, other approaches and concepts are necessary in this case.

In figure 3.18, some systems are depicted for which Ethernet can be applied. All applications where a higher bandwidth is required due to sensors and actuators like cameras, would be fitting use cases (Jesse, 2016, p. 2).

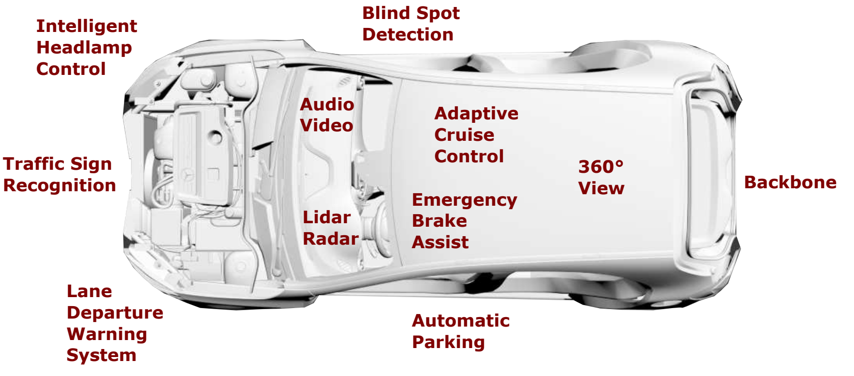

Figure 3.18: Examples for potential Ethernet use cases

3.8.1 Time-Sensitive Networking

Another approach is *Time-Sensitive Networking* (TSN), where data can be transmitted over Ethernet in real-time with a maximum latency of 100 μs over five hops. This standard was introduced in 2015 and allows deterministic real-time communication over Ethernet. As usual, a global time and a schedule are required for message paths across multiple network components. Consequently, a maximum latency for scheduled traffic can be achieved for such networks, and time-critical messages can be delivered reliably.

TSN extends the functionality of Ethernet with following properties (TT-Tech Computertechnik AG, 2018):

- Message latency is guaranteed through switched networks.
- Critical and non-critical traffic can be converged in one network without risk of impact on the delivery of critical traffic by collisions with non-critical traffic.
- Higher layer protocols can share the network infrastructure with real-time control traffic.
- Components can be added to real-time control systems without network or equipment alterations.
- Network faults can be diagnosed and repaired faster because of more precise information on their source.

The standards of TSN use a time-aware shaper (TAS). The messages are queued, and the schedule allows a deterministic transmission through switched networks.

On top of Ethernet, TCP/IP or similar network protocols can be used for the actual packet transmission. At the start of an ethernet message, a fixed bit string is sent. In this message is information about the frame preamble and the start frame delimiter (SFD) for clock synchronization. Each device in a network is identified using the so-called Medium Access Control (MAC) addresses.
Following calculations are done by applying the formulas in (Zimmermann and Schmidgall, 2014, p. 142). An ethernet message can be mathematically described with the following equation :

$$T_{Frame} \approx (n_{Header+Trailer} + n_{Data}) * T_{bit} \tag{3.15}$$

where:

$n_{Header+Trailer}$ describes the overhad of the message

The maximum size is 30 Byte (= 240 bit).
The maximal bandwidth of an ethernet connection can be calculated with the following equation:

$$f_{Data} = \frac{n_{Data}}{T_{Frame} + 96 * T_{bit}} \tag{3.16}$$

The reason for those additional 96 bits is to have a guard window between the messages. As a result, a 100 Mbps network achieves a bandwidth of 6 up to 12 MB/s, where the data length is between 52 and 1500 Byte. To calculate the total latency during the transmission, all active switches have to be considered. Consequently, the latency can be expressed with the following statement (Zimmermann and Schmidgall, 2014, p. 142):

$$T_{latency} = T_{Frame} + \sum T_{switch} \tag{3.17}$$

T_{switch} is dependent on various parameters. Firstly, the latency of a switch is up to the internal mode of operation. The message must be delayed until the device obtains the destination address of the control unit. It is possible to estimate this time with $T_{switch,min} = 112 * T_{bit} = 1,2\,\mu s$. This minimal time cannot be achieved in the field and a latency in the range of 5 μs seems more realistic.

Sometimes, switches do have a different mode of operation and wait until they received and stored the whole message. Only then, they forward the message to the receiver. With this kind of operation, they can verify the checksum of the message and will forward it, if it is correct. Otherwise, faulty messages can be discarded, and the path of retransmission is considerably shorter. However, the delay of such switches is higher and amounts to $T_{switch} = T_{Frame}$ (Zimmermann and Schmidgall, 2014, p. 142–143).

3.8.2 1000BASE-H

Another interesting standard for Automotive Ethernet is the IEEE 802.3bv, also known as 1000BASE-H. The full official name is *Standard for Ethernet Amendment 9: Physical Layer Specifications and Management Parameters for 1000 Mb/s Operation Over Plastic Optical Fiber*.
Figure 3.19 from (*IEEE Std 802.3bv-2017* 2017, p. 38) shows the used topology. PMD stands for Physical Medium Dependent Component. Full duplex operation is only supported, if two unidirectional fibers are used for the communication.

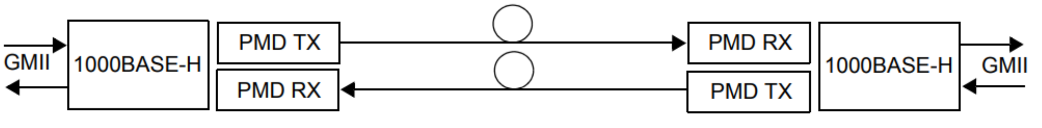

Figure 3.19: 1000Base-RHx topology (*IEEE Std 802.3bv-2017* 2017, p. 39)

This Ethernet standard is optimized for short link environments as is the case in automotive, industrial, and home networking applications. This standard adds 1000 Mb/s Physical Layer specifications for operation on duplex plastic optical fiber (POF) of point-to-point connections. This standard can deliver a solution for applications with high bandwidth requirements. It is realized with a very cheap step-index POF with a wavelength of 650 nm and a 1 mm diameter. More information on this topic, especially optical fibers, will be provided in the following chapter. The operation mode is full duplex and supports a bit error rate (BER) of 10^{-12}. Furthermore, there is a communication side-channel for PHY management (*IEEE Std 802.3bv-2017* 2017, p. 38).

4 Optical Technologies

In this chapter, general information about optical components, currently available optical technologies and their possible applications within a vehicle will be discussed. There is a common misconception that optical technologies are only suitable for transmitting data with minor losses over large distances. Even if the statement is generally true, there are many advantages which qualify this technology for other applications as well.

4.1 Overview

In the past decades, the significantly higher costs of fiber often posed an insurmountable obstacle, especially in the automotive sector where every cent is considered. Nevertheless, to realize complex autonomous and automated systems within vehicles, an investment in this technology seems inescapable. However, the main obstacle seems that there is a lack of understanding optical technologies and thus, the possible potential for solutions these technologies offer is simply ignored.

For an optical communication channel, the same basic components as for other communication systems are required: A sender, a transmission medium, and a receiver. It is in principle the same as a microwave system, only the frequency range differs. Typical values for the optical carrier frequencies are about 200 Terahertz (THz). Electrical signals are converted into optical signals at the sender, transmitted over a channel (fiber or free-space) and converted back to an electrical signal to allow further processing of the information. Instead of electrons, photons are the decisive particles carrying the data. A schematic representation of an optical transmission system is depicted in figure 4.1.

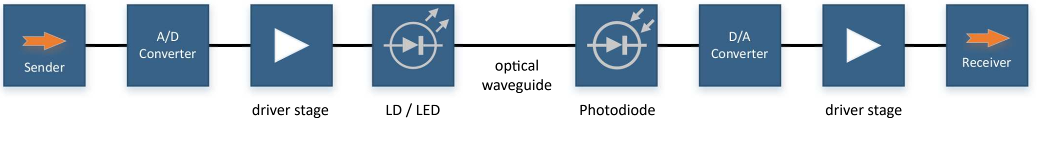

Figure 4.1: Structure of an optical transmission system. Adapted from (elektronik-kompendium.de, 2013)

By converting the signals from the electrical into the infrared domain, high bandwidths are possible. In laboratory setups, bandwidths of over 70 THz can be achieved using a single optical fiber, and in theory, even higher bandwidths are attainable. However, the conversion of electrical to optical signals limits the potential transmission speeds beyond 70-80 Terabit/s. New technologies and more precise components push these limits, but only small advances are achieved. Since such technologies are very expensive, they will not be feasible for common use in the next few years (elektronik-kompendium.de, 2013).
There are certain wavelengths, where the signal attenuation is significantly lower. Those wavelength bands are used more frequently due to a higher variety and lower costs of available components. Those so-called *optical windows* or *transmission windows* are situated at following wavelengths: 850 nm, 1300 nm and 1550 nm (figure 4.2). The latter ones do have quite good attenuation properties with less than 5% losses per kilometer. When using 1550 nm, the attenuation can be as low as 0.2 dB/km. The advantage of the 850 nm band compared to the others is that laser and electronics can be manufactured out of the same material (Gallium arsenide). All three bands are about 25000 – 30000 GHz wide (Tanenbaum and Wetherall, 2010, p. 102).

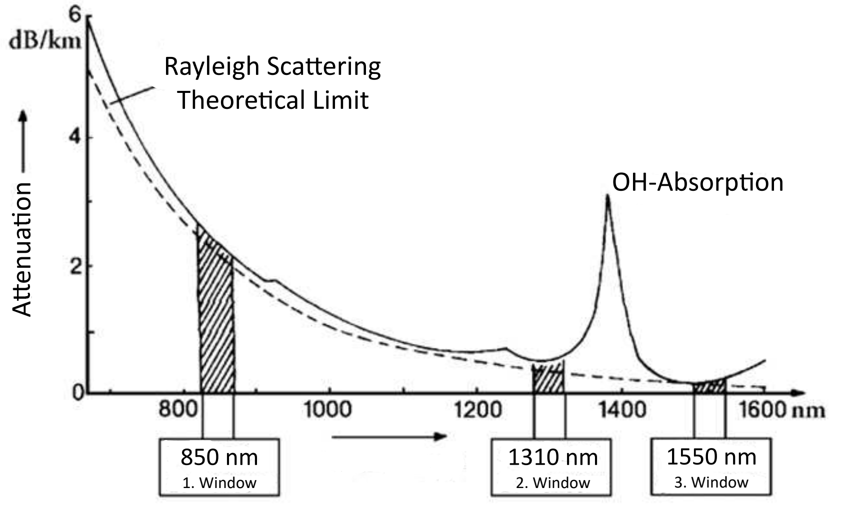

Figure 4.2: Optical Windows - Attenuation of light through fibers. Imagesource: (ksi.at, 2013)

The are two general types of optical communication systems: *guided* and *unguided*.
Guided optical communication is also known as fiber-optic communication, where the optical beam is enclosed by an optical transmission medium, in most cases a silica. Unguided optical communication is the transmission over a free-space. The free-space can be the atmosphere of the earth or a vacuum like space. Other than normal wave propagation, the optical beam is far more directed (forward direction), and thus not feasible for broadcasting applications. The problem in atmospheric transmission is that the optical beam is influenced and attenuated by many different effects, and consequently it is quite difficult to achieve a high-quality connection over longer distances (Agrawal, 2012, pp. 16–17).
In this context, only fiber-optic communication systems will be considered.

Attenuation is, arguably, the most important factor when considering optical communication. As mentioned, attenuation depends on the wavelength of light, as well as the physical properties of the material used. When using cheap fiber, the attenuation is far higher than that of a pure silica fiber. The attenuation in decibel can be described with the following formula 4.1:

$$Attenuation = 10\, log_{10} \frac{transmitted\ power}{received\ power} \tag{4.1}$$

Attenuation limits the overall transmission range of the system. Power and α can be estimated with the equations 4.2 and 4.3 in (Zubia and Arrue, 2001, p. 111). The power decreases exponentially with the distance d:

$$P(d) = P(0) * 10^{\frac{-\alpha * d}{10}} \tag{4.2}$$

α stands for the attenuation coefficient and expresses the value of attenuation as a function of the fiber length. It can be estimated with

$$\alpha = -\frac{1}{d}\, 10\, log \frac{P(d)}{P(0)}\, dB/km \tag{4.3}$$

A standard optical communication channel with one transmitter and receiver is unidirectional: data transmission is possible in only one direction. To clarify, an optical sender can only send but not receive data. The same is true for the receiver - only signal reception is possible. As a result, certain

arrangements are necessary to achieve bidirectional communication. For one, the easiest solution would be to use one fiber for the forward channel and using a separate one for the back channel. There is also a component which combines this functionality in one device: A *fiber optic transceiver* (FOT), which can both transmit and receive optical data. More elegant solutions are multiplex techniques, where multiple signals are combined and sent over the optical channel in e.g. a single time frame or different wavelengths.
A signal can have two levels: *recessive* and *dominant*. The recessive level (the '0' bit) is often also described as 'dark', while the dominant level (the '1' bit) is also called 'bright', representing the state of the signal. One interesting and quite useful property of the optical signal is that it does not need to be terminated like an electrical signal. Components like a termination impedance (see section 3.1.1) are obsolete and not even an isolation of the line is required (Fasser P., 2007).

The electrical signal has to be converted into an optical signal. This can be achieved by applying modulation resulting in an optical bit stream with either a return-to-zero (RZ) or nonreturn-to-zero (NRZ) format. NRZ and RZ are binary codes and indicate e.g. a positive ('1') or negative ('0') voltage.

- *Return-to-zero*: In RZ, the amplitude returns to zero between each pulse, so before the bit duration is over. This means that there is an on-off pattern for this format which also influences the required bandwidth. The bandwidth for RZ signals is higher compared to the NRZ format, however, in certain situations where chromatic dispersion and fiber nonlinearities are present, the RZ can perform better.
- *Nonreturn-to-zero*: Compared to RZ, the required bandwidth is almost half for NRZ. There are no frequent pulse drops and the pulse width is directly dependent on the bit pattern. As a result, the NRZ pulses have more energy than the RZ ones. However, the pulse width has to be controlled and pulse spreading during transmission might cause problems (Agrawal, 2012, pp. 13–14). The difference between NRZ and RZ is depicted in Figure 4.3.

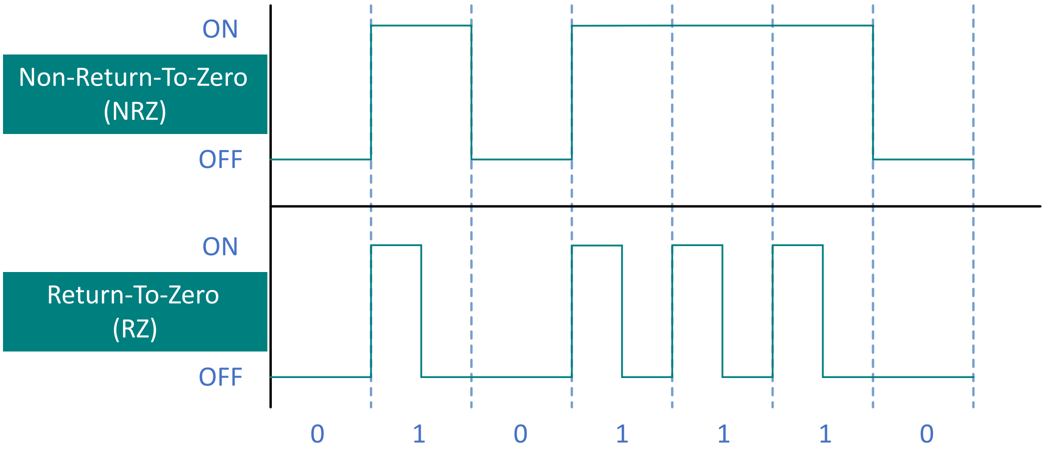

Figure 4.3: Comparision between Non-Return-To-Zero (NRZ) and Return-To-Zero (RZ)

4.2 Wave Propagation

The propagating optical waves comply with *Maxwell's equations*. In the optical domain, where nonconducting media without free charges are used, the form differs a bit and reads as follows (Diament, 1990):

$$\text{Faraday's Law} \qquad \nabla \times \vec{E} = -\frac{\partial \vec{B}}{\partial t} \tag{4.4a}$$

$$\text{Ampere's Law} \qquad \nabla \times \vec{H} = \frac{\partial \vec{D}}{\partial t} \tag{4.4b}$$

$$\text{Gauss' Law} \qquad \nabla \cdot \vec{D} = 0 \tag{4.4c}$$

$$\text{Gauss' Law } (\vec{B} \text{ Fields}) \qquad \nabla \cdot \vec{B} = 0 \tag{4.4d}$$

$\vec{E}$ ... electric field vector	$\vec{H}$ ... magnetic field vector
$\vec{B}$ ... magnetic induction	$\vec{D}$ ... dieelectric displacement

$\vec{D}$ and $\vec{B}$ are also known as the flux densities and can be put in relation to $\vec{E}$ and $\vec{H}$:

$$\vec{D} = \epsilon_0 \vec{E} + \vec{P} \tag{4.5a}$$

$$\vec{B} = \mu_0 \vec{H} + \vec{M} \tag{4.5b}$$

$\vec{P}$ ... electric polarization	ϵ_0 ... vacuum permittivity
$\vec{M}$ ... magnetic polarization	μ_0 ... vacuum permeability

$\vec{M} = 0$ in optical fibers, because of the non-magnetic nature of silica glass (Agrawal, 2012, pp. 29–30).
In the optical domain simplifications of the Maxwell equations are noticable. Certain effects, e.g. attenuation, are far weaker and can be ignored in most cases when using high-quality glass fibers. Glass has non-conductive properties and no charge carries exist (Strobel, 2016, p. 24). The propagation or phase velocity v of an electromagnetic wave in an optical medium is described by:

$$v = \frac{1}{\sqrt{\mu\epsilon}} = \frac{1}{\sqrt{\mu_0\epsilon_0\epsilon_r}} = \frac{c}{n} = \frac{\omega}{k_0 n} \tag{4.6}$$

c ... speed of light (vaccum)	ω ... angular frequency
n ... refraction index	k_0 ... free-space wave vector $\vec{k_0}$ (vaccum)

The optical carrier wave (unmodulated) can be derived from the simplified Maxwell equations and is described by the following formula 4.7 in (Agrawal, 2012, p. 14):

$$\vec{E}(t) = \hat{e}Acos(\omega_0 t - \phi) = \hat{e}\,Re[a\,exp(i\phi - i\omega_0 t) \tag{4.7}$$

$\vec{E}$ ... electric field vector	A ... amplitude	ϕ ... phase
$\hat{e}$ ... refraction index	ω_0 ... carrier frequency	

Depending on the type of modulation, either analog or digital, different techniques are used. It is possible to either modulate the amplitude (A), frequency (ω_0) or phase (ϕ). Hence, the analog modulation schemes: *amplitude modulation* (AM), *frequency modulation* (FM) and *phase modulation* (PM). In the digital domain they are also known as *amplitude-shift keying* (ASK), *frequency-shift keying* (FSK) and *phase-shift keying* (PSK) (Agrawal, 2012, pp. 14–16).

Analog modulation types	Digital modulation types
amplitude modulation (AM)	amplitude-shift keying (ASK)
frequency modulation (FM)	frequency-shift keying (FSK)
phase modulation (PM)	phase-shift keying (PSK)

Table 4.1: Analog and digital modulation techniques

The most widely used technique is on-off keying (OOK), where the signal power is switched between two levels. It is a very simple form of ASK modulation and indicates if there is a carrier wave or not. OOK is often combined with *pulse-code modulation* (PCM).

4.3 Optical Transmitter

The electrical signal must be converted into an optical signal. Only then can the signal be coupled into an optical fiber for transmission. This can be achieved by using an optical transmitter. Mainly semiconductor components are used since they offer several advantages and are considerably cheap in production.
The following requirements must be met by the optical transmitter to work as a reliable light source for communication (Hochmuth, n.d., p. 9):

- Emission of light in the designated transmission window of the optical waveguide.
- Small spectral width of the light $\Delta\lambda$.
- High efficiency of the converter using simple electrical circuits.
- High degree of coupling the light into the optical waveguide.
- Modulation capability of the light flux with very high frequencies.
- High lifetime and reliability at room temperature.

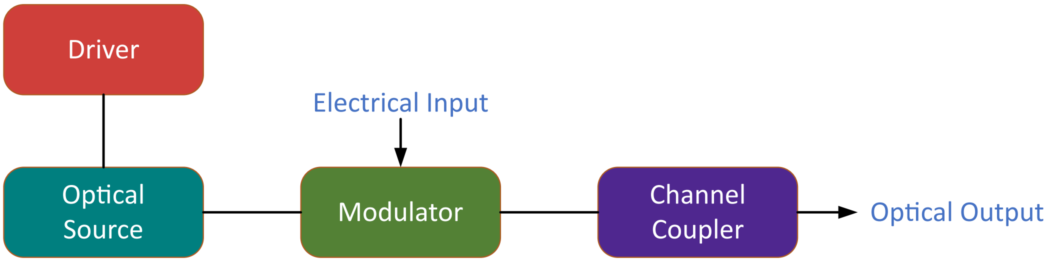

Figure 4.4: Optical transmitter structure (Agrawal, 2012, p. 19)

In the following table 4.3 the components of such an optical transmitter (see figure 4.4) are listed and described (Agrawal, 2012).

Component	Task
Driver	Supplies the optical source with a constant current to guarantee the operation for the specific application of the diode
Optical source	Mostly semiconductor lasers such as light-emitting diodes (LEDs) or laser diodes (LDs) are used for this purpose, since modulation is easier to implement with this technology. Laser setup is also possible, but very expensive and a waste of limited space. Advantages: *"compact size, high efficiency, good reliability, optimal wavelength range, small emissive area compatible with fiber-core dimension, direct modulation at high frequencies"* (Agrawal, 2012, p. 77).
Modulator	To generate an optical signal, the optical carrier wave must be modulated.
Channel coupler	Task of the coupler is to focus the optical signal with a lens *"onto the entrance plane of an optical fiber with the maximum possible efficiency"* (Agrawal, 2012, p. 18). If the channel is the free-space, then this coupler is also a lens which focuses the beam to achieve a maximum distance.

Table 4.2: Components of an optical transmitter and their tasks

In this context the *launched power* must be mentioned, which is an important design parameter for optical transmitters. As the name implies, the launched power describes how much energy is actually inserted into the fiber and received. The optical power is only dependent on the radiance of the optical source.

$$Launched\ power = 10\,log_{10}\left(\frac{power}{1mW}\right) \tag{4.8}$$

1 mW is a typical value, and thus chosen as the reference value in this equation (Agrawal, 2012, p. 579).
As mentioned in table 4.3, there are primarily two types of semiconductor light sources: Light-emitting diodes (LEDs) and laser diodes (LDs).
LEDs are designed for lower data rates. A characteristic value for the maximum data rate of affordable LEDs is around 200 Mbps. Any application with less than 200 Mbps can be easily implemented by using LEDs. For higher data rates, a laser diode (LD) is required. Most semiconductor diodes are silicon- or germanium-based diodes with p-n transition. p and n denote the doping of the different layers. While p is an indication for positive charge (holes are the majority carrier), n indicates negative charge (electrons are the majority carrier). When used as a light source, the semiconductor diodes are operated in the forward direction. By doing so, a recombination of charge carriers is achieved and thus photons are emerging. Conversely, when the diodes are operated in the opposite direction, an absorption of photons will occur, and the charge carriers are separated (Strobel, 2016, p. 160).
The conductance depends on the polarity of the operating voltage at anode and cathode. The voltage-current characteristic of such semiconductor sources can be estimated with:

$$I \sim e^{\frac{eU}{kT}} - 1 \tag{4.9}$$

I	Current in forward direction
U	Voltage between anode and cathode
k	Boltzmann's constant ($= 1.381 * 10^{-23} J/K$)
T	Temperature
e	Unit charge ($= 1.602 * 10^{-19} As$)

The resulting energy of the photons equals the distance of the active energy levels. To paraphrase, an electron absorbs energy as soon as a voltage is applied and moves into the conduction band. After some time, the electron will fall back into a hole in the valence band and during this process, the electron will emit energy in form of a photon. Following equation 4.15 shows this correlation (Fasser P., 2007, p. 98):

$$\Delta E = E_2 - E_1 = h * f = \frac{h * c_0}{\lambda} \tag{4.10}$$

λ ... wavelength	c_0 ... speed of light in vaccum
f ... frequency	h ... Planck's constant ($= 6.626 * 10^{-34}$ Js)

Figure 4.5 is a simple illustration of an energy band of a semiconductor.

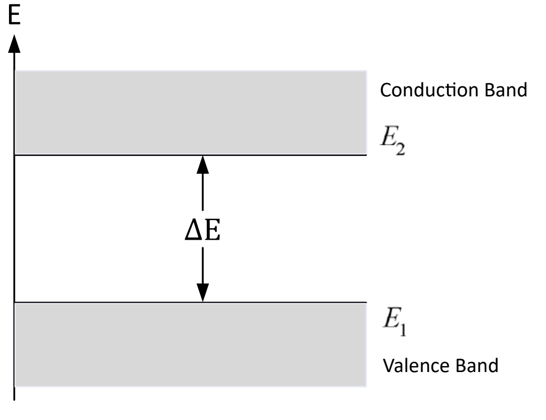

Figure 4.5: Energy band of a semiconductor

During the transition from the conduction band E_2 to the valence band E_1, it is likely that a photon is emitted. There is another effect during the process - a photon can induce a transition of an electron in the other direction $(E_1 \textit{ to } E_2)$. A photon can experience three different effects: *absorption*, *spontaneous emission* and *stimulated emission*.
Absorption occurs if an electron is excited to move into a higher energy level. When an electron drops spontaneously back from a higher energy level, it can lead to a spontaneous emission of a photon. Spontaneous emission is a random process and cannot be induced. However, a photon can be specifically used to create a similar effect. As a result, a transition

of an electron from a higher band to a lower might occur. Thus, another photon might be emitted. This type of emission is called *stimulated* or *induced* emission. A requirement that stimulated emission can emerge is the presence of a so-called *population inversion* (Fasser P., 2007). An illustration of those processes is depicted in figure 4.6.

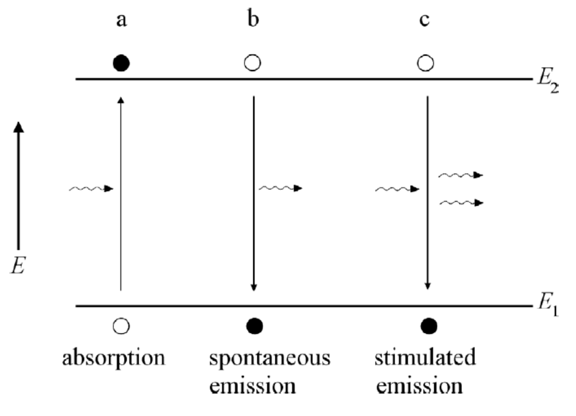

Figure 4.6: Emission types of photons (Strobel, 2016, p. 159)

All processes, even absorption and induced emission, are statistically dependent. There is always a certain probability that the one or the other effect will occur. Following variables are statistically connected to each other when considering absorption (Strobel, 2016, pp. 150–151).

The transition probability of an electron from E_1 to E_2 is proportional to:

- number of existing electrons
- population number N_1
- lower energy level E_1

For stimulated emission, the dependencies are reversed. In case of stimulated emission, additional energy must be applied to achieve population inversion. This method of supplying energy is called *pumping*. There are three different types of pumping: thermal (supplying heat), light (optical pumping) or injection of a current (electrical pumping). As a result, the stimulated photon is the same in terms of wavelength and phase as the photon used for stimulation. The process of stimulated emission is common in laser sources, while in other light sources such as LEDs, only the spontaneous emission will appear (Strobel, 2016, pp. 159–160).

4.3.1 Light-Emitting Diodes (LEDs)

A LED is quite a simple structure consisting of a n- and p-doped layer. By applying a certain voltage (cut-off voltage) a recombination in the depletion layer is initiated, where electrons will move from one band to another. This effect is the spontaneous emission, which has been described in section 4.3 above. Energy is produced by this process, which is emitted as light (photons) (Dossin J., 2007, p. 6).
The beam of the emitted light is very wide in terms of angle and spectral width (30-60 nm), meaning that the emitted light of a LED can only be coupled into fibers with a large diameter. Otherwise, there might occur high losses if most of the light is not coupled into the fiber.
The launched power in 4.8 can be estimated for typical indicator LEDs. The actual received power is then rather low and the launched power is somewhere in the range of -10 dBm for a LED. In figure 4.7, the principle of a semiconductor LED is illustrated.

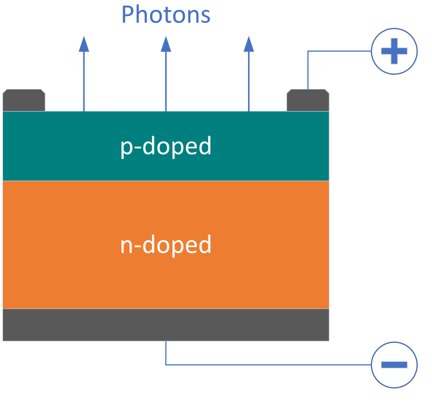

Figure 4.7: Semiconductor LED with different doped layers

Due to the specific properties and the low rise and fall times, as well as the comparably low output, the operation of a LED is restricted to short transmission distances. However, when certain properties, such as high

linearity are required, the LED proves to be very useful.
The optical power and the forward current of a diode can be encapsulated in the P-I characteristic curves, see figure 4.11. With increasing temperatures, there is a higher chance of a non-radiant recombination. At some point, however, saturation will be reached. The higher the current, the higher the dissipation power, and thus the temperature of a diode. This heating process should be limited to guarantee a controllable environment. Hence, the heat sink of a diode is placed as closely as possible to the recombination zone (Strobel, 2016, p. 166).
There can be various radiation patterns of a LED, depending on the surface where the light is emitted. Illustration 4.8 shows a few different far-field emission patterns of different types of LEDs (planar, hemispherical, parabolic). Each type has certain advantages, which can be used for specific applications.

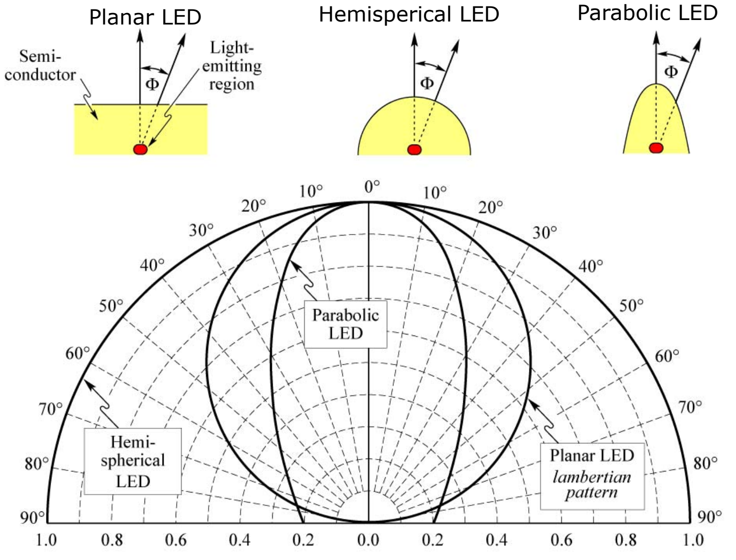

Figure 4.8: LED Far-Field emission pattern (Schubert, 2006)

Other types of LEDs, like organic LEDs (OLED), are most commonly used for display technologies. They are optimized for such applications and not useful for other use cases.

4.3.2 Laser Diodes (LDs)

Like LEDs, Laser Diodes are also semiconductor components and consist of a p-n transition. The diverse emission forms the major difference between those two kinds of semiconductors. Instead of a spontaneous emission, the emission for the LD is stimulated. To achieve this type of emission, a strongly stimulated medium is required: the number of the stimulated atoms in the conduction band is greater than the number of unstimulated atoms in the valence band. As already described in section 4.3, the situation is normally reversed (= population inversion). To achieve an induced state, the laser material must be stimulated (= pumping). If a light beam is induced into the medium, the electrons in the material emit their excess energy in the form of photons. As a result, the emission of a photon is stimulated by another photon. Those photons possess the same level of energy, direction and polarization. The induced photon can then trigger the emission of another new photon resulting in an amplification of the original light beam. This effect only works if the wave length of the induced light beam is equal to the energy level difference of the atoms in the laser material (Dossin J., 2007, p. 9). This principle can be seen in figure 4.9.

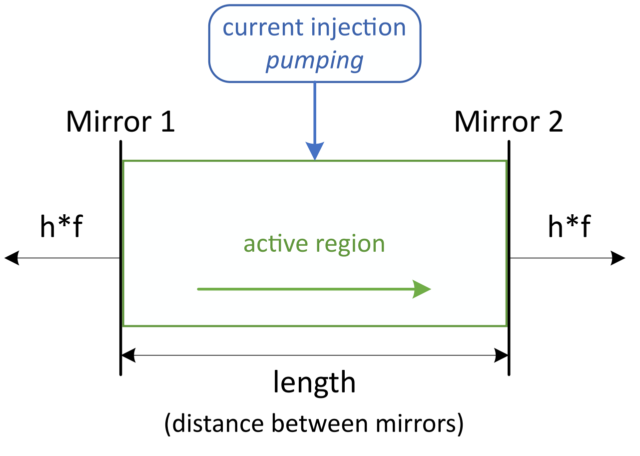

Figure 4.9: Principle of a laser, used in LDs. Adapted from (Brückner, 2011, p. 70)

When using a semiconductor, the energy for the pumping is basically a current. The main advantage of the semiconductor material is that light with the desired wavelength (LED and LD) can be created. If a current is dispatched through the pn-transition, the stimulated emission causes an amplification of the spontaneously emitted photons. The spontaneous emission occurs only randomly, and the intensity is quite low. Thus, an induced or stimulated emission is preferable to achieve a proper signal amplification. Following criteria by (Fasser P., 2007, pp. 57–59) must be fulfilled to attain an induced emission:

- Population inversion - there must be more electrons in the upper level than in the lower
- The electrons stay a long period in the upper level. During this time, no spontaneous emission should emerge
- Photons with a fitting wavelength $\lambda = \frac{h*c_0}{h*f}$ exist

To increase an efficient amplification, a feedback using mirrors is required. The mirrors have to be positioned in a certain distance to each other. Such a constellation is depicted in figure 4.10.

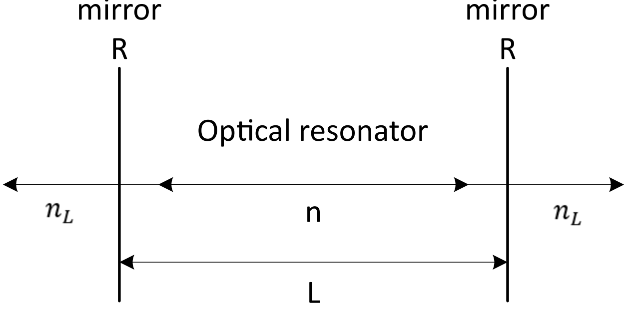

Figure 4.10: Optical resonator structure used for LDs

Only then, the mirrors form a resonator and stationary waves can spread out. If a beam enters this construct, a part will be reflected while the rest will leave through the mirror and be considered as loss. The reflected part will stay in the active medium and will be amplified through induced emission. A resonator round trip equals two times the length of the distance between the mirrors. To achieve the best possible amplification effect, the losses in the resonator, medium and at the mirrors must be minimized. Also, the energy of the pumping must be sufficiently high to attain a gain. Thus, the optical amplification needs to be higher than the optical losses (Brückner, 2011, pp. 70–71).

When the current is injected (pumping), electrons will move from the valence band to the conduction band. The laser's power can be estimated with the following approximation:

$$P \sim e^{g\zeta - \alpha\zeta} \tag{4.11}$$

g	gain exponent
α	resonator loss
ζ	spatial coordinate in propagation direction

The resonator losses are due to mirror losses and scattering in the laser. However, when exceeding a certain threshold current, the amplification can compensate any resonator losses. Mathematically, this means that $g = \alpha$; – thus, the laser oscillation condition is fulfilled (Strobel, 2016, pp. 170). Figure 4.11 shows what a PI characteristic for LED (left) and LD (right) could look like. The depiction is generic and does not reflect a certain type of LED/LD.

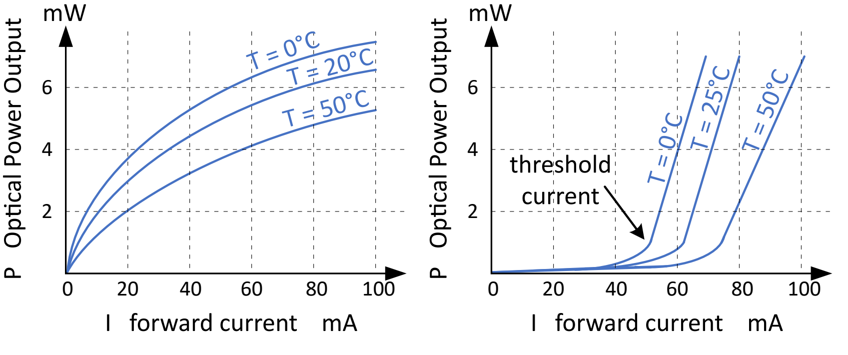

Figure 4.11: PI characteristic of a LED (left) and a LD (right)

It has to be clarified that the output power of a LD will reach a point, where thermal destruction might occur, if too much current is applied. With following equation, the temperature can be put into correlation with the threshold current:

$$I_{th}(T) \sim e^{\frac{T}{T_0}} \tag{4.12}$$

where T_0 is the characteristic temperature

Apparently, T_0 has quite an impact on the overall influence of temperature. If T_0 can be maximized, the nominal temperature can be significantly higher as well. Thus, GaAs-laser diodes can be used to achieve values for T_0 of 150-250K. Still, at some point the P-I characteristic will reach a level where non-linearity will attune. Another important effect is aging of the laser. Over time, non-radiant recombination is increasing and the overall performance decreases the higher the injection current. To counter aging, the threshold current should be constant and cooling elements, e.g. Pelletier elements, can be applied to decrease the rate of this aging process. The modulation of semiconductor lasers is mainly digital, because there are non-linearities, bends etc. which would lead to harmonics in the analog domain. Thus, by using digital modulation, a lot of potential disturbances can be eliminated. Furthermore, the waves need to be guided properly to achieve an effective and efficient optical radiation. This can be achieved by restricting the light wave and recombination region to a narrow range (Strobel, 2016, pp. 172–177).

The radiation pattern (far-field) of a laser diode (Fabry-Perot semiconductor laser) is visible in figure 4.12. When comparing the pattern with the one of a LED (figure 4.8), it is obvious that the radiation is much narrower in figure 4.12.

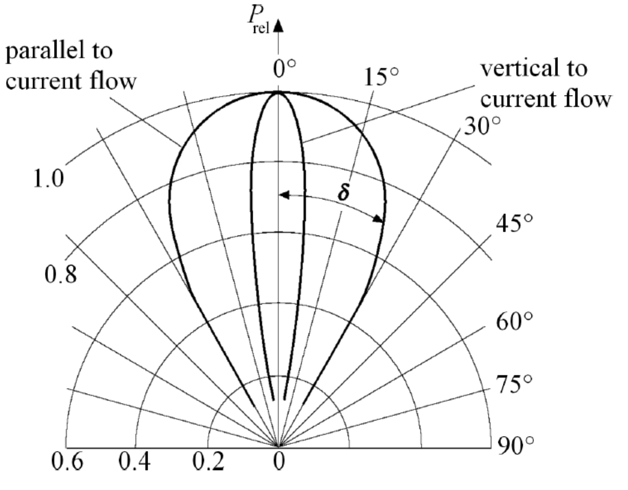

Figure 4.12: LD Far-Field emission pattern (Strobel, 2016, p. 171).
P_{rel} . . . optical output power related to the optical output power for perpendicular radiation.

Depending on the type of fiber, different types of lasers are reasonable. For single-mode fibers, clearly a single-mode laser makes sense. The same is true for multi-mode fibers, where a multi-mode laser is required.
In a semiconductor laser, both transversal modes, as well as longitudinal modes exist. When considering figure 4.10, standing waves will appear in the resonator. Hence, nodes at the mirrors are required. Then, the length of the resonator can be easily calculated, if wavelength λ, integer μ and the reflection index n is known:

$$L = \frac{\mu\lambda}{2n} \tag{4.13}$$

When using a GaAs laser with following specifications: $\lambda = 850\,nm$; refraction index 3.5; length $300\,\mu m$ – approximately 3000 nodes can be obtained (Strobel, 2016, pp. 183). The distance between the various modes can also be calculated with following equation:

$$\Delta\lambda = \frac{\lambda^2}{2nL} \tag{4.14}$$

For the GaAs laser, the mode distance $\Delta\lambda$ equals approximately $0.3\,nm$. In general, there is a classification of two different types of lasers: *gain-guided lasers* and *index-guided lasers*. The index-guided laser is more suitable for single-mode lasers, and thus single-mode fibers, while the gain-guided laser exhibits multi-mode behavior. The basic differences between those types of lasers can be seen in figure 4.13.

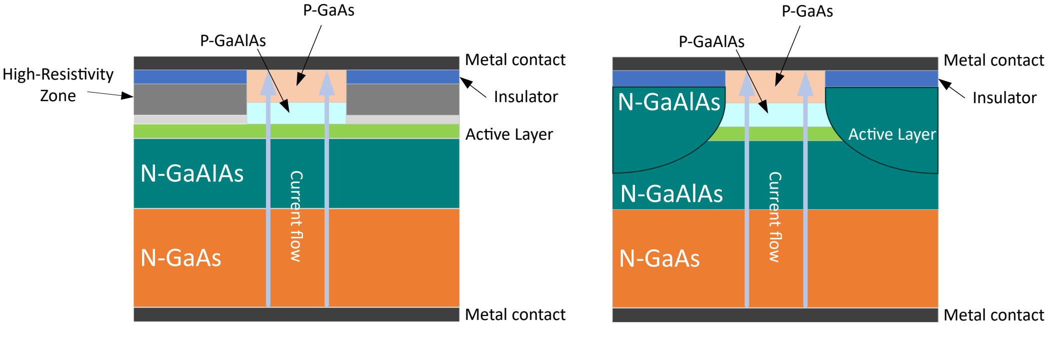

Figure 4.13: Difference between gain-guided (left) and index-guided (right) laser semiconductors. Adapted from (Hecht, 2011, p. 287)

The gain-guided laser exhibits a narrow stripe where the current will flow. The rest of the path is blocked by high-resistivity zones, which prevents any current flux in these regions. The path length matches the chip dimensions. Only the narrow region displays gain - recombination of current carriers and the desired population inversion will occur.

For the index-guided laser structure, the narrow stripe width is not achieved by simply blocking the rest of the area with insulating regions. Here, physical properties of different materials are used to adapt the refractive index. The material of the stripe in the active layer exhibits a lower refractive index, therefore the light will stay in this area. The shape shown in figure 4.13 (on the right) can be attained by etching the required regions in the fabrication process. At the top, once again an insulator layer is required to prevent any undesired current flows. At both ends of the semiconductor structures, metal contacts are used.

Index-guided lasers are more commonly used than gain-guided lasers due to better light confinement and increased beam quality. Gain-guided lasers, however, are much simpler to make and feature better results for multi-mode fibers, even if the injection current is high (Hecht, 2011, pp. 287–288). The major differences between single-mode and multi-mode will be explained in the next section fiber layout.

4.4 Optical Receiver

An optical receiver converts the optical signal from a fiber back to the original electrical signal. An electric pulse is generated as soon as photons hit the detector. There are several properties an optical detector should have (Fasser P., 2007, p. 203) (Brückner, 2011, p. 106):

- Absorption of the light should be in the same wavelength domain.
- Susceptibility should be at a maximum. This parameter is coupled to the bit-error-rate. The lower the requirements regarding bit errors, the higher the susceptibility of the optical receiver.
- Swiftness of detector. The photocurrent should be able to follow a quick modulation of the luminous power. Transmission bandwidth is directly connected to the swiftness.
- Inherent noise and dark current should be a minimum.

- Detectors and optical components should consist of the same materials to simplify an integration of various elements.

The components of a receiver are the following and visible in figure 4.14:

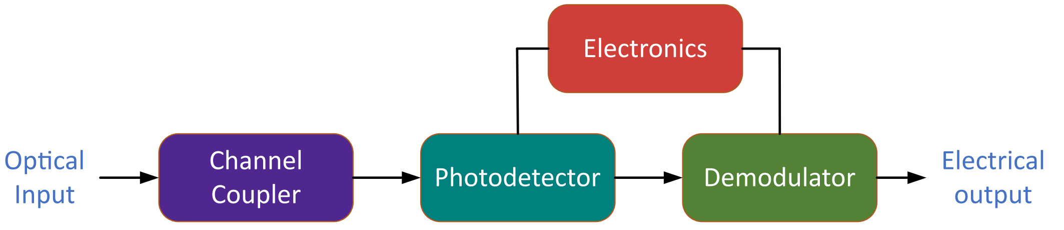

Figure 4.14: Components of an optical receiver (Agrawal, 2012, p. 20)

Component	Task
Channel Coupler	The incoming optical signal beams are focused onto the photodetector. This can be achieved e.g. by a lens.
Optical source	The actual conversion of the optical signal into electrical form is done by the photodetector, which is typically a semiconductor. The properties and requirements are basically the same as for the optical source and are best met by semiconductor components: high sensitivity, fast response, low noise, low cost and high reliability (Agrawal, 2012, p. 128)
Demodulator	The type of demodulator used in an optical receiver design is dependent on the modulation scheme used. Intensity modulation with direct detection (IM DD) is the most commonly used demodulation scheme - a decision circuit identifies bits as 1 or 0. The Signal-to-Noise ratio (SNR) at the output of the photodetector determines the accuracy of the decision circuit.

Table 4.3: Components of an optical receiver and their task

The photoelectric effect is the foundation for every semi-conductive optical receiver. Light of a certain wavelength λ or frequency f will be transported from the valence- into the conduction band. If light hits a semiconductor, it is only absorbed if the quantum energy of the photons is higher than the bandgap energy. This is only true, if following mathematical statement is fulfilled:

$$h * f \geq E_g \tag{4.15}$$

Because of the absorption, an electron-hole pair will be formed. An electron is elevated from the valence- to the conduction band. Incident photons may generate an electron-hole pair. The likelihood of such an event depends on the absorption length of the photons. With following equations, the absorption length l and the reduced power P at a certain depth ζ, can be determined. At this depth, the number of photons is reduced to $\frac{1}{e}$. α denotes the absorption coefficient (Fasser P., 2007, pp. 203–204) (Strobel, 2016, p. 186):

$$P = P_0 e^{\alpha\zeta} \tag{4.16}$$

$$l = \frac{1}{\alpha} \tag{4.17}$$

Both, absorption length and coefficient depend on wavelength and semiconductor material. In figure 4.15, various material dependencies of semiconductors are shown. α and l are displayed as a function of the wavelength λ (Strobel, 2016, p. 186).

During the conversion process of photons to electrical current, it may happen that photons are lost or do not lead to a generation of electron-hole pairs due to various reasons, e.g. reflection. The actual amount of usable charge carriers is also denoted as *quantum efficiency* η. Photocurrent I_p and responsivity R are important parameters for calculating quantum efficiency. They can be put into correlation, since the current flow is proportional to the incident optical power P_{in}.

$$I_P = RP_{in} \tag{4.18}$$

With the following equation, the number of usable generated electron-hole pairs and incident photons, hence the quantum efficiency, can be estimated (Agrawal, 2012, p. 129):

$$\eta = \frac{electron\,generation\,rate}{photon\,incidence\,rate} = \frac{\frac{I_p}{q}}{\frac{P_{in}}{h\nu}} = \frac{h\nu}{q}R \tag{4.19}$$

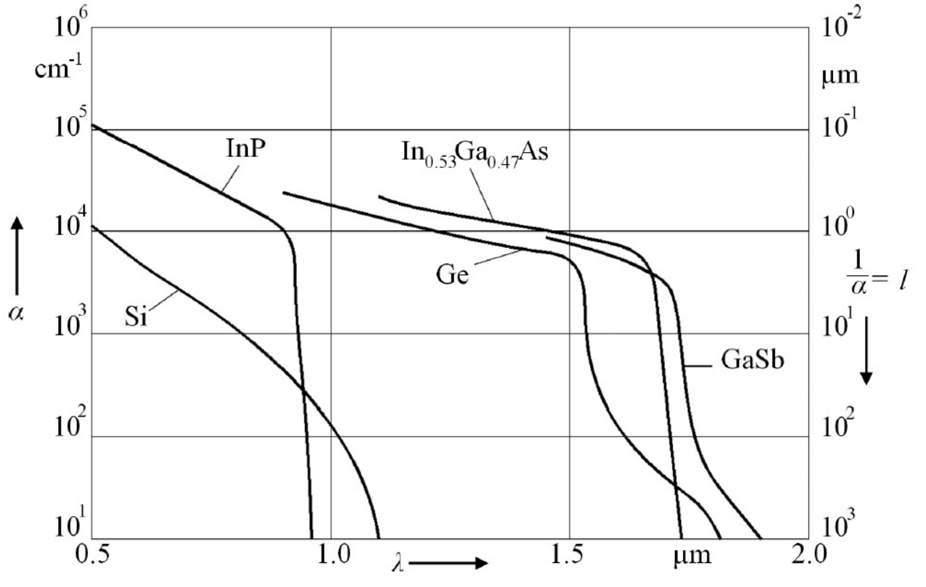

Figure 4.15: Material dependencies in a semiconductor optical receiver (Strobel, 2016, p. 187)

The responsivity R can be calculated with the following formula:

$$R = \frac{\eta q}{h\eta} \approx \frac{\eta\lambda(\mu m)}{1.23985(\mu m * \frac{W}{A})} \quad (4.20)$$

The responsivity represents the input-output gain of a detector system and is directly dependent on the wavelength. Consequently, the higher the wavelength, the more photons are present (Agrawal, 2012, p. 129).
To achieve the highest possible quantum efficiency, either the thickness of the absorption layer has to be a maximum or the Fresnel reflection coefficient a minimum. Then it is possible to attain efficiencies of almost 0.8. Formula 4.20 yields a convenient solution since only the wavelength in μm is required to obtain the responsivity. In the following table, a few typical responsivity values for different diodes are listed (Strobel, 2016, p. 196):

Diodes	**Wavelength** λ	**Responsivity** $R(\frac{A}{W})$
Silicon	0.85 μm	0.5 A/W
Germanium	0.85 μm	0.7 A/W
Germanium	1.5 μm	0.8-0.9 A/W
InGaAs	1.5 μm	0.9 A/W

Table 4.4: Responsivity values for different diodes

When considering semiconductor photodetectors, there is a trade-off between responsivity and bandwidth. The bandwidth is limited by elements in the circuit, which lead to, e.g., electric parasitics.

$$\Delta f = [2\pi(\tau_{tr} + \tau_{RC}]^{-1} \tag{4.21}$$

τ_{tr} ... gain exponent $\quad \tau_{RC}$ ... resonator loss

The rise time of a photodetector depends on both transit time τ_{tr} and the RC time constant τ_{RC}. Consequently, both transit time as well as the RC time constant should be a minimum, if high bit rates are required. As an example: $\tau_{tr} + \tau_{RC}$ should be less than 10 ps, if the system should achieve bit rates of about 10 Gb/s (Agrawal, 2012, p. 131).

4.4.1 PN Photodetector

To prevent a recombination of electrons and holes, which might happen when using undoped semiconductor material, doping is necessary. As already discussed in the previous sections, a PN junction is the most established structure. Thus, the simplest photodetector is a PN-diode (see figure 4.16, left).

At the junction between the p- and n-doped layers, the electrical field will be a maximum. Charge carriers drift from this region either to anode or cathode, leaving the depletion zone rather empty. The task of the depletion region of the PN photodetector is to provide a sufficiently large zone, where the conversion of photons to electrons can take place. At the PIN

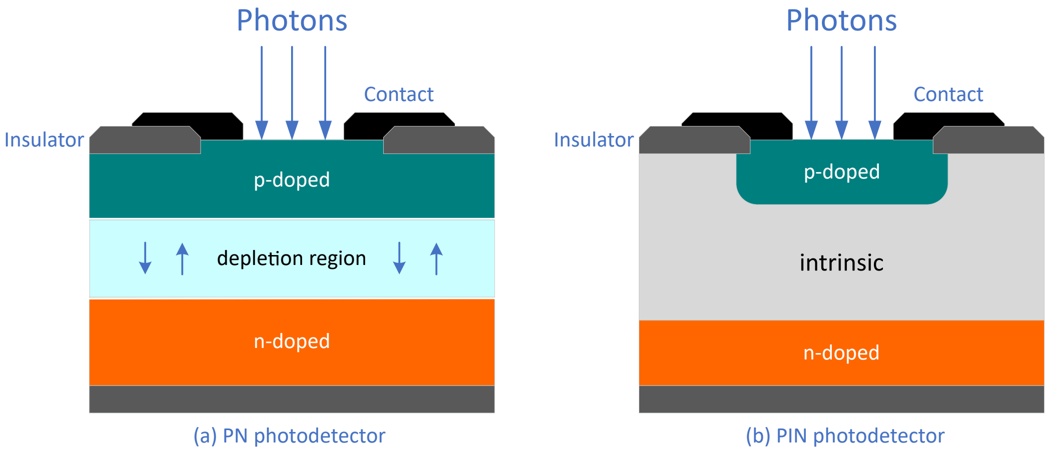

Figure 4.16: Semiconductor structure of a PN photodetector (left) and PIN photodiode (right)

photodetector, an intrinsic area is provided which allows the conversion process (Strobel, 2016, pp. 188–189).

Typically, the p layer is highly doped, while the n layer is weakly doped to improve the overall performance. The voltage is applied in reverse direction to achieve an impoverishing barrier layer, in which light can be absorbed. Light with a longer wavelength can penetrate deeper into the crystal than light with shorter wavelengths. In the area of the barrier layer, a light-induced concentration of electrons-hole pairs will form. They will move away from the pn-transition and lead to a photovoltage, which will drop over a resistance (Brückner, 2011, p. 107).

The velocity of drift within the depletion region is very high, while outside of this area, the field strength is very weak and thus, the electron-hole pairs move relatively slowly. As a result, the actual absorption of photons does not occur in the drift zone. This has a direct impact on the overall performance of the PN photodetectors, which is considerably slow. The velocity of electron-hole pairs can assume two different types of speed (Brückner, 2011, p. 120):

- Slow diffusion with diffusion speed v_{diff}
- With a certain drift speed, which is proportional to the field strength $\vec{E}$: $v_{drift} = \mu * \vec{E}$

where μ is the carrier mobility, which is in general larger than the mobility of the holes. Due to the relatively slow speed of PN photodetectors, PIN diodes are preferred for faster applications. However, bit rates of up to 40 Gb/s are possible with modern PN photodiodes (Agrawal, 2012, p. 133).

4.4.2 PIN Photodetector

PIN photodetectors utilize the inner photoelectric effect. As already mentioned and visible in figure 4.16 (b), an undoped layer, a so-called intrinsic layer, is inserted between the p- and n-layer. By doing so, the overall properties of the semiconductor structure are changed. In the middle section, a high field force will emerge. Thus, the voltage drop occurs now between the n- and p-layer and the drift is dominating. The depletion zone increases and equals the length of the absorption zone (Fasser P., 2007, p. 207).
The width of this zone depends on several factors. It should be a compromise between speed and sensitivity. A simple increment of the width can lead to a quantum efficiency η of 100%. Consequently, the response time will increase, and the overall performance will decline. There is a distinction between indirect-bandgap (IB) and direct-bandgap (DB) semiconductors. While for IB-semiconductors, the width must be in the range of 20-50 μm, the width of DB ones can be much smaller, e.g. 3-5 μm. The bandwidth is then limited by the transit times (Agrawal, 2012, p. 134). By applying a high bias voltage, the transit time decreases. At the same time, the force of the electric field and the speed of drift will be high in the depletion zone (Fasser P., 2007, p. 209). Figure 4.17 shows this behavior.

The major advantages of a PIN diode compared to a PN diode are the following (Brückner, 2011, p. 121):

- High speed and high transfer rate
- High susceptibility/sensitivity
- High linearity $\rightarrow$ large dynamic area
- Low supply voltage
- Minor noise

Another option to increase the PIN photodetector performance is by applying a double-heterostructure design. In the following table 4.5, a few characteristics of typical PIN diodes are listed (Agrawal, 2012, p. 139).

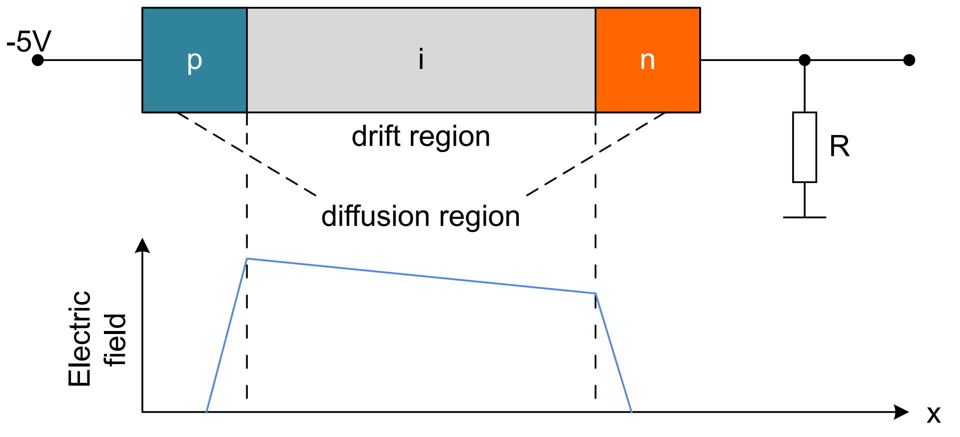

Figure 4.17: PIN Diode with the corresponding field intensity $\vec{E}$

Parameter	Symbol	Unit	Si	Ge	InGaAs
Wavelength	λ	μm	0.4-1.1	0.8-1.8	1.0-1.7
Responsivity	R	A/W	0.4-0.6	0.5-0.7	0.6-0.9
Quantum efficiency	η	%	75-90	50-55	60-70
Dark current	I_d	nA	1-10	50-500	1-20
Rise time	T_r	ns	0.5-1	0.1-0.5	0.02-0.5
Bandwidth	Δf	GHz	0.3-0.6	0.5-3	1-10
Bias voltage	V_b	V	50-100	6-10	5-6

Table 4.5: Characteristics of typical PIN diodes (Agrawal, 2012, p. 139)

Waveguide photodetectors can achieve bandwidths in the range of several hundred GHz or even THz in the 1.55 μm spectral region (Agrawal, 2012, p. 136).

4.4.3 Avalanche Photodiode (APD)

The Avalanche Photodiode (APD) is the third important type of semiconductor photodetector, which will be mentioned. They do exhibit a much larger responsivity R than the PN and PIN diodes. If the responsivity R is high, less optical power is required. It is best to use an APD if the optical power is limited. APDs are operated very close to their breakdown voltage to achieve further amplification of the photocurrent. By the incident light, an electron-hole pair will be created. The electron is accelerated and can create another electron-hole pair. This process is generally known as *impact ionization*. For each electron generation, the kinetic energy decreases by about 1 eV.

The process can repeat itself several times and is also known as *avalanche effect*, hence the name APD. This effect only stops if the barrier of the pn-layer is reached. As a result, one photon can generate several electrons. Consequently, the sensitivity of the photodiodes is very high. Other electron-hole pairs will be formed in the intrinsic conduction layer. Not only the electrons are accelerated but also the holes, which move to the pn-junction and will also induce an avalanche effect. This effect occurs with a time shift to the electron avalanche. Therefore, the speed of a PIN diode is not achievable (Fasser P., 2007, pp. 209–211). The principle of an APD is visible in figure 4.18. The $p+$ indicates a highly doped zone.

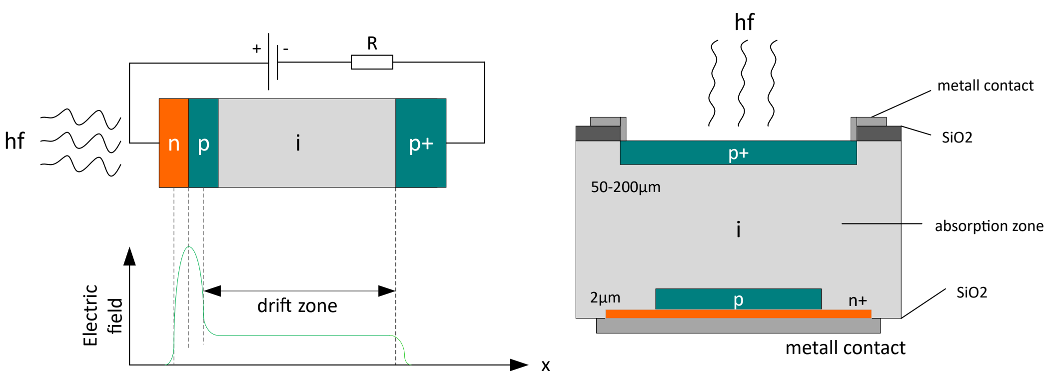

Figure 4.18: Principle concept of a semiconductor APD. Adapted from (Fasser P., 2007, p. 209)

Due to the high supply voltage, there will be noise, which affects the performance of APDs. Additionally, the temperature might pose a problem. With higher temperature, the cut-off voltage must be higher to maintain the multiplication factor. Then, the impact ionization is affected and the gain decreases.

The gain M_f of an APD can be estimated with following equation (Strobel, 2016, p. 192):

$$M_f = \frac{M_0}{\sqrt{\left(1 + (\frac{f}{f_c})^2\right)}} \tag{4.22}$$

M_0 ... gain for non-modulated light f_c ... cut-off frequency diode

$$f_c = \frac{1}{2\pi M_0 t_M} \tag{4.23}$$

t_M ... delay in gain zone

In table 4.6, various types of APDs are mentioned and compared. For some APDs, 60-300 GHz bandwidth can be achieved (Strobel, 2016, p. 192).

Parameter	Symbol	Unit	Si	Ge	InGaAs
Wavelength	λ	μm	0.4-1.1	0.8-1.8	1.0-1.7
Responsivity	R_{APD}	A/W	80-130	3-30	5-20
APD gain	M	—	100-500	50-200	10-40
k-factor	k_A	—	0.02-0.05	0.7-1.0	0.5-0.7
Dark current	I_d	nA	0.1-1	50-500	1-5
Rise time	T_r	ns	0.1-2	0.5-0.8	0.1-0.5
Bandwidth	Δf	GHz	0.2-1	0.4-0.7	1-10
Bias voltage	V_b	V	200-250	20-40	20-30

Table 4.6: Comparison of different semiconductor APDs (Agrawal, 2012, p. 140)

4.4.4 Receiver Circuit Design

The most important characteristics and requirements for an optical receiver have already been mentioned. Additionally, to obtain a full receiver structure, a preamplifier is essential to amplify the electrical signal, so that further processing of the signal is simplified and improved. Once again, a trade-off between speed and sensitivity is required when considering the receiver design. For permissible operation, a certain optical level is required where the signal-to-noise ratio is still attained. Thus, the receiver sensitivity must be a at least a defined minimum, where the SNR is still valid (Strobel, 2016, p. 199).

$$P_{min} = 10\, dBm\, log \frac{P}{P_0} \tag{4.24}$$

P_{min} ... minimal optical input power (mW) P_0 = 1 mW

For receivers, the *dynamic range* is an important design parameter. It states the range between minimum detectable signal level and maximum allowed input level (Strobel, 2016, p. 199).

Figure 4.19 depicts an optical receiver system. The whole system consists of three parts: *front-end*, *linear channel* and *data recovery*.
The *front-end* with the mentioned preamplifier and photodiode. The *linear channel* consists of a high-gain amplifier and a low-pass (LP) filter. The gain of the amplifier can be controlled to limit the average output voltage. The voltage pulse is shaped with the low-pass filter. With such a LP filter, noise can be reduced without generating intersymbol interference (ISI). As a final structure, there is *data recovery*, which includes a decision circuit and clock recovery. With those components, a spectral component, where the bandwidth equals the bitrate, can be isolated of the received signal (Agrawal, 2012, pp. 145–147).

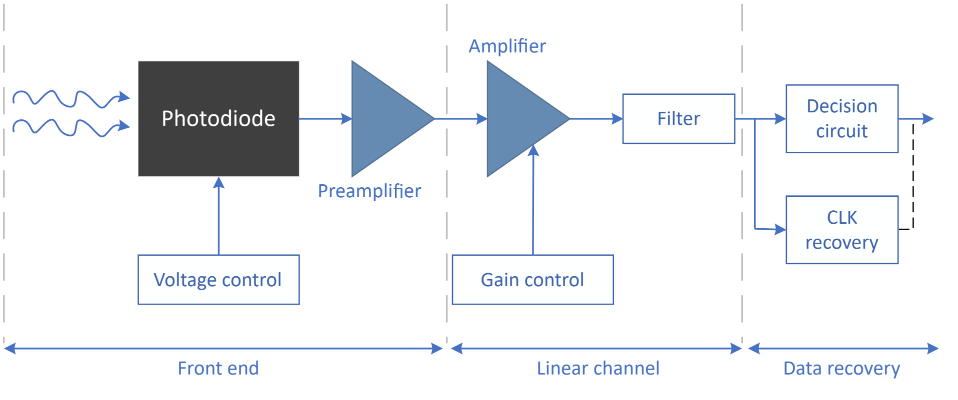

Figure 4.19: Schematic of an optical receiver system. Adapted from (Agrawal, 2012, p. 145)

The voltage drop at the input of the preamplifier is determined by following equation:

$$U_E = R_{eff} * I_P \tag{4.25}$$

I_P	photocurrent
R_{eff}	parallel connection of the load resistance and input resistance of preamplifier

When choosing a high load resistance R_L, the thermal noise in the system can be reduced significantly while increasing the sensitivity. Furthermore, the input voltage to the preamplifier will be increased when using a high R_L. However, there is naturally also a major drawback when choosing such characteristics. Since the bandwidth is directly dependent on the resistance (high-impedance) used, it will be obviously smaller. The dependency is shown with following statement (Agrawal, 2012, p. 145):

$$\Delta f = \frac{1}{2\pi R_L C_T} \tag{4.26}$$

That means that if the bandwidth is significantly smaller than the bit rate, it is not possible to employ a high-impedance front-end. To counter this effect, an equalizer can be used to attenuate low-frequency components, and hence increase the bandwidth.
The actual effective resistance can also be estimated:

$$R_{eff} \approx R_L \leq \frac{1}{2\pi f C_{eff}} \tag{4.27}$$

4.4.5 Noise

Optical receivers often exhibit noise, in most cases the so-called shot noise, which is basically quantum noise. This type of noise occurs at transitions of semiconductors. Thermal noise and amplifier noise are further sources of disturbance. Noise can be described with statistically functions and parameters. Shot noise arises, if direct current (DC) must overcome a potential barrier. In the case of semiconductors, it is a pn-transition, which is reversely polarized.

The emergence of a DC flow can have various reasons, since it is a composition of charge carrier movement (Brückner, 2011, pp. 112–113).

- The photon flux is not continuous. Furthermore, the quantum noise has to be considered due to statistical distribution of the electron-hole pairs in the receiver.
- Recombination processes also need to be observed, as electrons, which have been generated by light, might fall back from the conduction into the valence band. Thus, holes may disappear.
- Electron-hole pairs can also be generated without any excitation of light. This effect is also known as dark current noise.

The shot noise is estimated with (Grau, 2013):

$$\overline{I_{Nsh}^2} = 2eI_P B \tag{4.28}$$

Nyquist noise describes the temperature dependent noise which occurs due to the movement of electrons within resistances. The resulting heat generation is responsible for a non-uniform distribution of the electrons. Hence, a varying voltage will appear between the depletion regions. Those changes are responsible for thermal noise.

With following equation 4.29, the Nyquist noise (RMS noise current), can be described (Tietze and Schenk, 1993):

$$\overline{I_{Nth}^2} = \frac{4kTB}{R} \tag{4.29}$$

k ... Boltzmann constant (= $1.38 * 10^{-23} \frac{J}{K}$) T ... Temperature
B ... Bandwidth

The higher the bandwidth, the greater the noise current. However, a large resistance can be chosen, if the bandwidth is comparatively small.

Another type of noise is the so-called *intensity noise*. This kind occurs at the spontaneous and stimulated emission processes of laser light. LEDs are not as affected as semiconductor materials. However, intensity noise is very complex to calculate and is often simplified or even ignored (Brückner, 2011, pp. 112–113).

Considering all types of different noises, the following generalized equation for a photodiode can be established (Strobel, 2016, pp. 207):

$$\overline{I_{NPh}^2} = 2e[(I_P + I_{DV})M^2F + I_{DS}]B \tag{4.30}$$

I_{DV}	Dark current of space charge
I_{DS}	Surface leakage flow
F	Excess noise factor

In contrast to photon current, dark current can also emerge even if there is no incident light.

4.5 Optical Communication Channel

There are various types of communication channels for transmitting light. A very simple example of optical communication are beacon fires, which were already used thousands of years ago. Certain pre-defined messages, such as "danger" could be easily transmitted over large distances. However, when using this type of visible communication, certain atmospheric effects, e.g. heavy rain, fog, dust etc. influenced the effectiveness and sometimes rendered it useless. Such effects are still the bottleneck of optical communication, when using optical transmitters like lasers. Any particles, raindrops etc. with a similar size as the signal wavelength, influence the transmission and dampen the signal – meaning that only very short distances can be covered when such effects occur.
These effects are a primary research concern of *Free-Space Optics*. It is possible to improve the transmission range by using stronger lasers – those might then not comply with safety regulations and only the military might be allowed to use such powerful devices. Signals can be also transmitted through a vacuum, space or other materials/gases, where the signal can travel freely without any major impediments. However, every channel except vacuum, has various effects and inconsistencies, which can complicate the transmission (Fasser P., 2007).

Those effects will be not considered in the scope of this work, as they can be disregarded when using a different medium like optical fibers.

Optical fibers provide a controlled environment that allows signals to travel long distances. Fibers are almost impervious against electromagnetic interferences and the signal attenuation can be as small as 0.2 dB/km when using high-quality materials. Furthermore, crosstalk between the fibers is, in most of the cases, not a problem. The material of the communication channel is either glass or polymer and is in most cases homogeneous. To achieve transmission within a glass/polymer fiber, the effect of total internal reflection is applied.

The *signal-to-noise ratio* (SNR) is the most important quality indicator for analog optical links. By considering formula 4.31, non-linear distortion products can be suppressed. The absolute minimum of the signal power can be estimated (Strobel, 2016, pp. 217–218):

$$\frac{S}{N} = \frac{S}{N_P + N_V} \tag{4.31}$$

S	electrical signal power; includes the effective resistance R_{eff} (see formula 4.27), the gain M and the photocurrent I_P
N_P	noise power; includes all influences of the photodiode
N_V	includes thermal noise parameters of both resistance and preamplifier

In a digital system, the *bit error rate* (BER) is the equivalent quality indicator. BER occurs in the signal detection part, when the bit numbers are not matched correctly. With a bit pattern transceiver system, the bits can be compared, and the quality of the optical link can be evaluated. There is a direct correlation between the BER and S/N in direct transmission systems. A typical value for the BER of such a system is about 10^{-9} (Strobel, 2016, p. 225):

$$BER = \frac{1}{2} erfc \sqrt{\frac{1}{8}\left(\frac{S}{N}\right)} = \sqrt{\frac{2}{\pi}} * \frac{1}{\sqrt{\frac{S}{N}}} * e^{-\frac{1}{8}*\left(\frac{S}{N}\right)} \tag{4.32}$$

According to the Nyquist Theorem, the bit rate can be twice the bandwidth. In reality, the bit rate is lower (e.g. 4/3 of the bandwidth). The system can be limited by either attenuation or dispersion. At some point, the limit of the receiver sensitivity will be reached, and no further communication is possible.

4.5.1 Fiber Layout

An optical waveguide consists in general of a core, a cladding and a coating. The core is the part where the signal is transmitted. The cladding causes, due to the lower optical refractive index, a total reflection at the boundary layer to the core. Thus, the light is guided along the whole length of the fiber core in a controlled manner. The purpose of the coating is to protect the fiber from mechanical damages, as well as other external influences like moisture or dust autocitewestermo.

Optical fibers have many advantages, such as the high bandwidth and immunity to electromagnetic interferences. However, there are some issues with fiber loss, bending losses, coupling and so on, which will be discussed later in this chapter.

To transmit information with an optical fiber, the physical properties of the glass/polymer are utilized. The principle used in this context is the previously mentioned total reflection. If a light beam hits the boundary layer between an optical dense medium (core) with a refractive index n_1 and an optical thin medium (cladding) with a refractive index n_2, then this beam is refracted according to its angle of incidence or totally reflected. For the desired functionality, the statement $n_1 > n_2$ must be true (Fasser P., 2007).

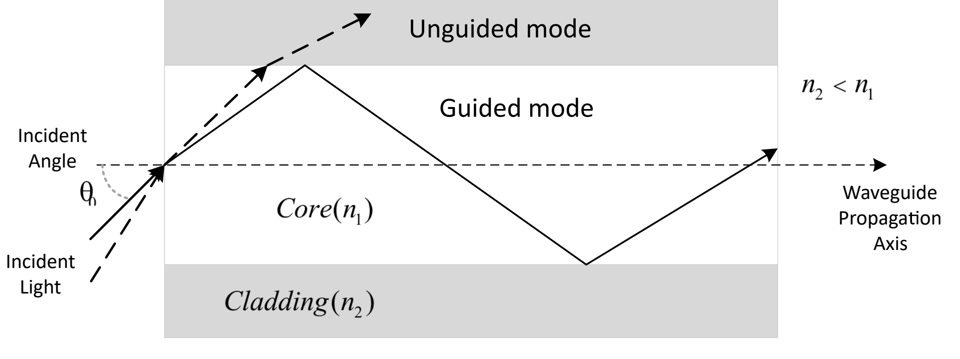

Figure 4.20: Wave propagation in an optical fiber (Sova, 2005, p. 49)

Hence, there is a correlation between the angles and refraction indices which is described by Snell's law (Hering, Stohrer, and Martin, 2007, p. 579):

$$n_1 \, sin \, \alpha_1 = n_2 \, sin \, \alpha_2 \tag{4.33}$$

The angle of incidence labels the angle between the perpendicular of the boundary layer and the incident ray. For a refraction, the refracted ray can reach a maximum 90° angle. The ray stays within the core and no energy is lost. If this value is exceeded, then the refraction transitions into a total reflection. It must be mentioned that even with a total reflection, parts of the ray are lost due to absorption. When using e.g. high-quality silica, however, this fraction is neglectable. Following equations (Strobel, 2016, pp. 48–49) show the coherence of total reflection, Snell's law and the numerical aperture A_N.

$$n \, sin \, \delta = n_1 \, cos \, \alpha_C \tag{4.34}$$

α_C	Cut-off angle at total internal reflection
δ	Angle of acceptance
n	Refraction index outside of the fiber
n_1	Core refraction index
n_2	Cladding refraction index

$$n \, sin \, \delta = n_1 \sqrt{1 - sin^2 \alpha_C} = n_1 \sqrt{1 - \left(\frac{n_2}{n_1} \right)^2} \tag{4.35}$$

A large numerical aperture is an indicator for a high coupling efficiency.

$$A_N = n \, sin \, \delta = \sqrt{n_1^2 - n_2^2} \tag{4.36}$$

Then, the normalized *refraction index difference* Δ must be determined.

$$\Delta = \frac{n_1^2 - n_2^2}{2n_1^2} \tag{4.37}$$

It is possible to approximate Δ, if the difference of $n_1 - n_2$ is rather small.

$$\Delta = \frac{n_1 - n_2}{n_1} \tag{4.38}$$

$$A_N = n_1 \sqrt{2\Delta} \tag{4.39}$$

It can be observed in figure 4.21 that the numerical aperture varies as a function of the radial coordinate r. Mathematically, this relation can be described as follows:

$$A_N = \sqrt{n^2(r) - n_2^2} \tag{4.40}$$

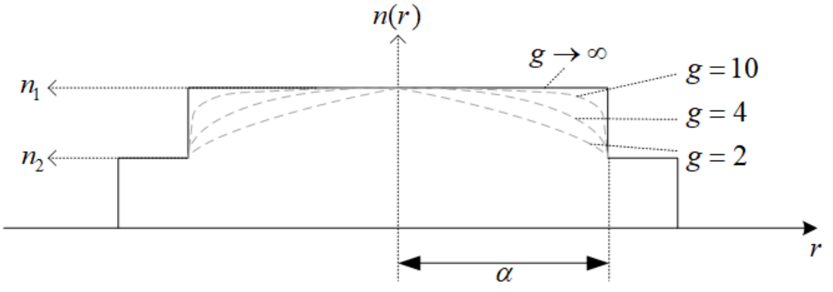

Figure 4.21: Refractive profile showing the influence of the profile parameter g (Strobel, 2016, p. 49)

The light waveforms propagating within the core are also called modes. The modes should not drop below the critical angle of the total reflection to still spread as expected. In the coating itself, mode propagation is also possible. Thus, the refraction index of the coating is higher to prevent this effect. An optical mode is in general just the solution to the wave equation. This solution must fulfill the boundary conditions and the spatial distribution of the wave should not change over the covered distance (Agrawal, 2012, pp. 31–32). There are two types of fibers, which are used for different communication scenarios:

- Single-mode fibers
- Multi-mode fibers

In a *single-mode* fiber only one mode can exist and propagate. The mode is denoted as the fundamental mode LP_{01}. There is a condition that for a normalized frequency $V < 2.405$, only the mode LP_{01} exists (Strobel, 2016, pp. 42). This circumstance is visible in figure 4.22.

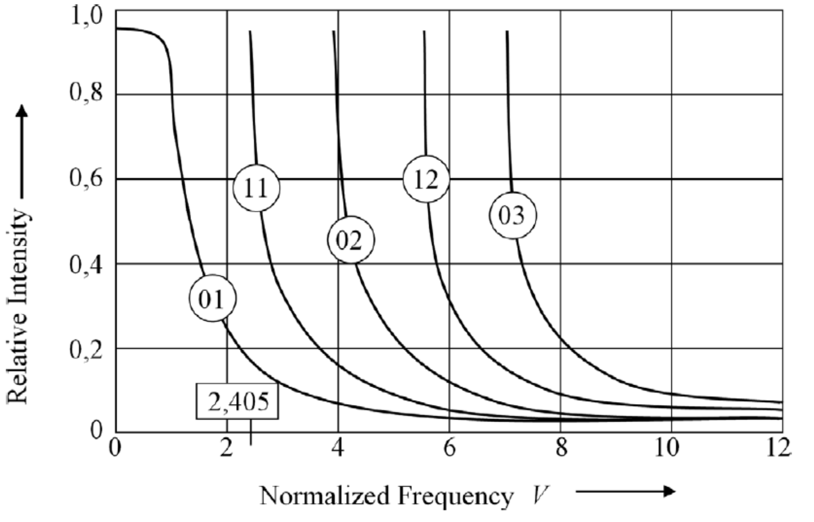

Figure 4.22: Power distribution in relation to the V-parameter (Strobel, 2016, pp. 42)

The core of a single-mode or mono-mode fiber is significantly smaller (3-10 microns) than for multi-mode fibers. The light is directed on a single linear path through the fiber. Therefore, there are no reflections at the boundaries and there is only one mode. Those fibers are useful if very long distances have to be covered. Additionally, the obtainable bandwidth is notably higher than in multi-mode fibers. Effects like mode dispersion are not occurring for this type of fiber. The structure and the beamline are visible in figure 4.23.

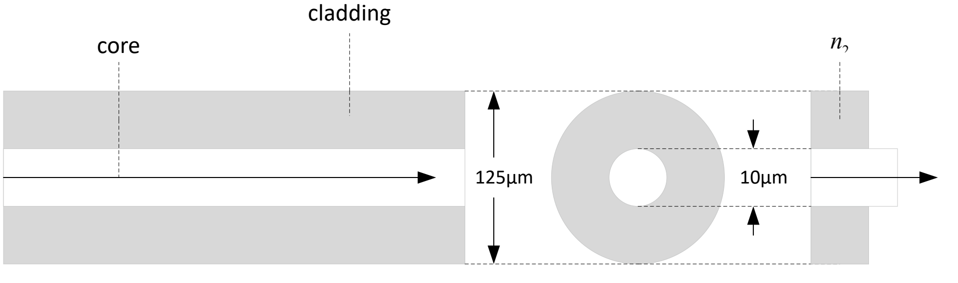

Figure 4.23: Single-mode fiber structure with a 10 μm core. Adapted from (Fasser P., 2007, p. 140)

For higher values of the V-parameter, more modes will emerge. Those type of fibers with more modes are known as multi-mode fibers. The number of modes can be easily determined with the following formula:

$$N = \frac{V^2}{2} * \frac{g}{g+2} \tag{4.41}$$

The core of a multi-mode fiber is in general with 50-400 microns quite large. The used wavelength is in the range of 850 up to 1300 nm, which is the near Infrared domain. There are two types of single-mode and multi-mode fibers: step-index (SI) and graded-index (GI).

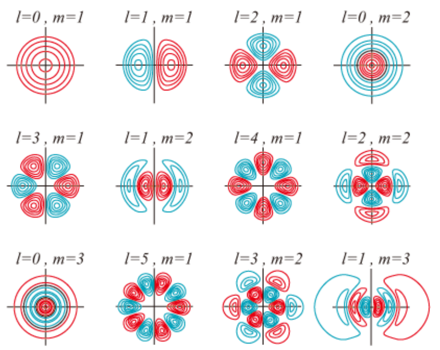

Figure 4.24: Example for various LP_{lm} modes (Kokyo, 2017)

Step-Index Fibers

The core of a step-index fiber is uniform, thus the refraction index over the whole material is the same. This also applies for the cladding which also consists of a uniform material with a smaller index of refraction than used for the core. When looking at the refraction profile of the fiber, the structure becomes quite clear (figure 4.25).

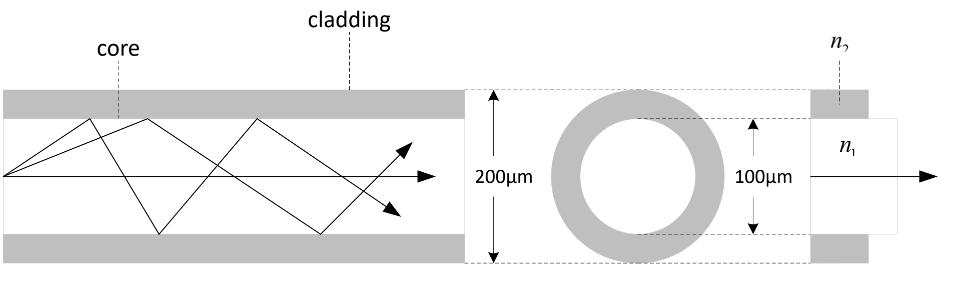

Figure 4.25: Step-index fiber. Adapted from (Fasser P., 2007, p. 130)

Graded-Index Fibers
In contrast to the step-index fibers there is not a clear step between the core and the cladding. The transition is more fluent due to a continuous variation of the refraction index. In other words, the refractive index of the fiber core is lower at the edges than at the center of the core. Consequently, all the rays in a graded-index fiber travel at a similar velocity and the resulting modal dispersion is reduced. A profile parameter g is introduced to achieve different refractive indices. The effect is visible in figures 4.21 and 4.26.

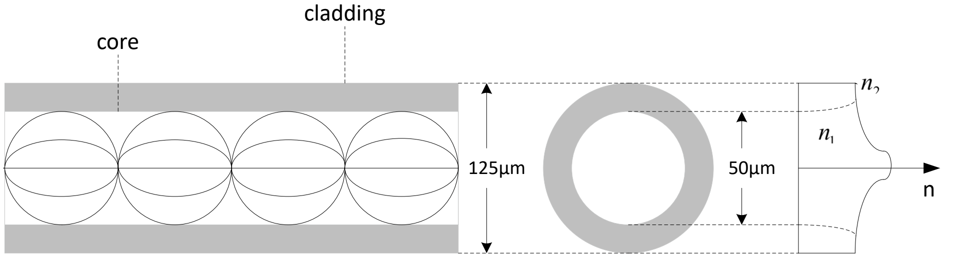

Figure 4.26: Graded-index fiber. Adapted from (Fasser P., 2007, p. 141)

4.5.2 Polymer Optical Fibers (POF)

In chapter 3.6, Polymer Optical Fibers (POFs) have been mentioned. The materials used for this type of fiber is mainly affordable plastic. The attenuation is considerably higher, for short distances however, not an issue. Those types of fibers usually have a step-index profile. POFs work most efficiently in the visible light wavelength range between 520 nm and 650 nm, where the attenuation is the least. Since the gaps between various systems and control units within a vehicle amount to a few meters, adequate data rates are achievable with modern POFs. For this kind of distance, there might be only an attenuation of approximately a few dBs, not yet considering other effects such as bending.

The most commonly used material for POFs is Polymethylmethacrylate (PMMA) with a refractive index of 1.492 and a core diameter of approximately 1 mm. Taking all these characteristics into account, the 1 mm PMMA SI-POF is the standard in almost all conventional applications.

Due to advancements in research and production, such a POF exhibits following physical attributes (Strobel, 2016, pp. 306–307):

- numerical aperture 0.5
- attenuation factor (@650 nm) in the range of 0.11-0.25 dB/m

The achievable 40 MHz x 100m bandwidth of a step-index profile fiber is restrained, and thus limited by modal dispersion. Considering the spectral efficiency, the attainable data rate can be quite low. Hence, it is beneficial to use graded-index profile fibers to gain a bandwidth-distance, which can be 100 times higher. Using different materials can improve the attenuation behavior significantly. In laboratory tests, perfluorinated polymers showed only 0.02 dB/m, as well as a wider transmission window resulting in a bandwidth-distance product of almost 2 GHz x 100m. However, modal dispersion due to the intense mode coupling, which is caused by scattering, is still a major problem for POFs.
Attenuation in fibers has been mentioned several times already. The overall sum of the losses can be represented by the following equation 4.42 (Koike, 2015, p. 22):

$$dB = -10\, log_{10} \left(\frac{P_{out}}{P_{in}} \right) \tag{4.42}$$

Below, the losses will be listed. They are the same for POFs and glass optical fibers (GOFs). Only the relative magnitudes vary with different materials. The main advantages of POF match the requirements of a modern automotive environment. Optical fibers are resistant to electromagnetic interferences (EMIs) which may interrupt the operation of various components and transmission lines. By substituting the lines, potential bottlenecks can be resolved. At the same time, when using high-quality POFs, the bandwidth can be increased considerably. The diameter of POFs is in general much larger (1 mm) compared to silica or glass fibers ($5 - 200\ \mu m$). One alternative to POFs in this kind of environment seem to be Polymer-Cladded Silica (PCS) fibers, which consist of a silica glass core while the cladding is realized with a polymer (PMMA). The core diameter is considerably smaller compared to a POF, and due to the physical properties of the glass, the bandwidth is larger than when using POFs. Additionally, the attenuation can be as low as 0.08 dB/m. If the silica core is flexible enough, this fiber might also be a viable solution in automotive applications. Compared to high quality silica fibers, which attain 0.2 dB/km attenuation, the losses seem severe. However, once again it is very important to clarify that the distances in a vehicle are very short and in most cases a length of few meters is sufficient (Strobel, 2016, pp. 46, 306–307).

The recently ratified 1000BASE-H standard seems to be the solution to achieve high transmission rates over short distances. An automotive wired connection will be in most cases less than twice the vehicle length – considering that the fiber has to be installed along the chassis. The average length of a car is about 4.5 meters, meaning that a cable will probably never be longer than 10 meters. For such minimal distances, it is easily possible to transmit data with more than 1 Gbps using POFs.

4.5.3 Attenuation in Fibers

The transmission with an optical fiber is confined in terms of attenuation and dispersion. But there are quite a few effects such as scattering, absorption and the mentioned dispersion, which all influence the optical data transmission. Those effects will be discussed in the following section. An overview over various intrinsic and extrinsic losses in fibers is depicted in figure 4.27.

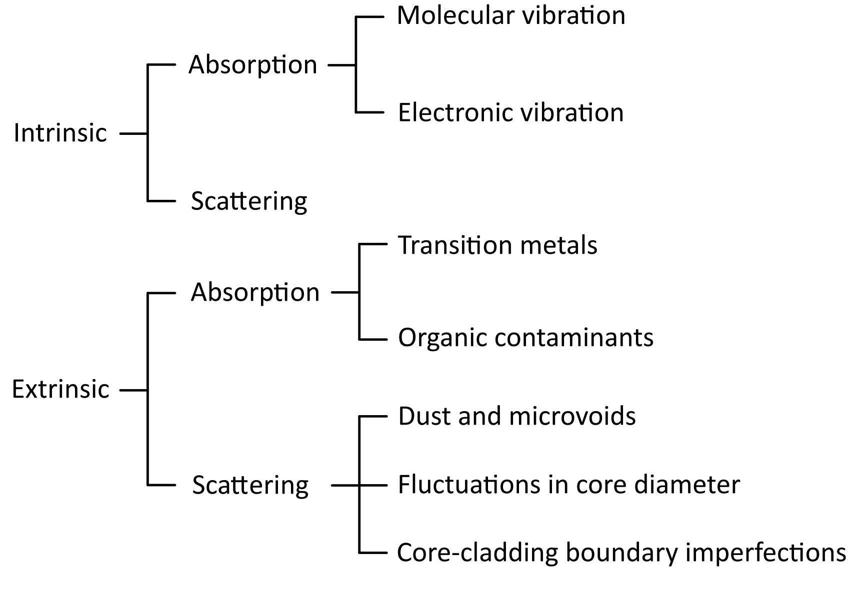

Figure 4.27: Overview of various attenuation effects in optical fibers (Koike, 2015, pp. 23).

As expected, the material does influence the level of attenuation. The absorption of light is directly dependent on the used wavelength of the light due to the different energy levels.

Scattering

Due to the specific properties of the material, intrinsic losses like scattering or absorption occur. Linear scattering, also known as Rayleigh scattering, are statistical refraction index fluctuations which are due to the stochastic molecular structure of the used waveguides. The scattered power distribution can be expressed with the following formula (Strobel, 2016, p. 48):

$$P_S = P_0 \, cos^2 \, \delta \tag{4.43}$$

P_S Scattered power
P_0 Power of the incident light wave
δ Angle with respect to the wave propagation direction

The scattered power can be easily calculated due to the strong dependency on the wavelength:

$$P_S \sim \frac{1}{\lambda^4} \tag{4.44}$$

It can be observed that scattering occurs in both the forward and reverse direction of the propagating wave (Strobel, 2016, p. 49). Considering this effect, the losses of those inaccuracies during manufacturing can be in the range of 0.12 – 0.16 dB/km for a wavelength of 1550 nm, which means that scattering is the major reason for attenuation in high-quality silica fiber. The calculation of the intrinsic loss of silica can be done by using following expression and exhibits the same wavelength dependency as the scattered power:

$$\alpha_R = \frac{C}{\lambda^4} \tag{4.45}$$

In this context, C is a material constant in the range of 0.7 – 0.9 dB/km μm^4. For a wavelength of 1550 nm, the attenuation amounts to the 0.12 - 0.16 dB/km mentioned above. It is obvious that the Rayleigh scattering is directly dependent on the wavelength. In theory, a different wavelength

of e.g. more than 3 μm would yield an attenuation less than 0.01 dB/km. However, silica fibers with this wavelength are useless due to the infrared absorption starting at 1.6 μm. Considering this information, the maximum of 0.16 dB/km is a good trade-off in terms of losses since all the other effects are a minimum at the viewed 1550 nm wavelength (Agrawal, 2012, p. 58).
Further types of scattering are the Raman scattering and Brillouin scattering. Both are regarded as inelastic, which means that the frequency of the scattered light is shifted downward (to red or blue) and the energy will decrease with the propagation distance. However, they only have to be considered in the calculations, if the power levels are sufficiently high. If a certain threshold value is exceeded, both types of scattering grow exponentially (Agrawal, 2012, pp. 59).

Mie scattering is another type of scattering which emerges due to imperfections of the waveguide itself. Such imperfections can be, e.g. core-cladding refractive index variations over the length, bubbles or particles in the fiber or diameter fluctuations (Fosco Connect, 2010).
Due to the high standards in fiber production, however, Mie scattering is rarely a problem and can be ignored in most of the cases. The reason for that is that the impurities do not exhibit the same size as the used wavelengths. For free-space communications though, Mie scattering is one of the most important attenuation parameters.

Absorption

There are different types of absorption depending on characteristics of the material in the ultra-violet and infrared spectrum. Absorption occurs at electron transitions, molecule transitions, metal ions or OH ions. This is due to the complex band structure and the resulting disparities in the structure of the glass/silica. Naturally, impurities of the raw material result in the highest losses (Fasser P., 2007, p. 146).

For example, undesired OH ions have quite a grave effect in certain absorption areas at 950 nm, 1250 nm and 1390 nm. A single extrinsic particle in a million already causes an attenuation as high as 50 dB/km at a wavelength of 1390 nm. At other wavelengths, such as 1550 nm, these OH ions do not have the same effect. Other impurities, like metal ions, are negligible compared to the OH ions at the mentioned wavelengths (Strobel, 2016, p. 60).

Absorption will occur in any material used. In the case of silica molecules, there are two interesting resonance effects, where the absorption will be rather high. Electronic resonances will appear in the ultraviolet region for wavelengths smaller than 400 nm, while vibrational resonances occur in the infrared region and above for wavelengths larger than 7000 nm. In this context it is helpful to list a few values for the attenuation caused by absorption. The intrinsic material absorption for the commonly used wavelength range of 0.8-1.6 μm is in most cases below 0.1 dB/km. For higher wavelengths, it is in fact even lower with about 0.03 dB/km. The extrinsic absorption, however, is significantly higher as mentioned before. The impurities should be less than 1 part per billion particles to achieve an acceptable value of 1 dB/km (Agrawal, 2012, pp. 57–58).

For short distances, the intrinsic absorption can be often neglected in the calculations. The extrinsic absorption has to be considered in any case and impurities can lead to a very high attenuation even for very short distances. With dry fibers, the OH ion concentration can be reduced even further, so when using such a type of fiber, the loss due to extrinsic absorption is in most cases very low and lies below 1 dB/km. In POFs, the absorption is very specific and can be best described by applying Urbach's rule 4.46 (Koike, 2015, p. 23):

$$\alpha_e = A\,exp\frac{B}{\lambda} \tag{4.46}$$

This formula characterizes the electronic transition absorption loss. A and B are the material specific constants. When using POFs with the typical PMMA material, A equals $1.58 * 10^{-12}$ while B equals $1.15 * 10^{4}$. Consequently, for a wavelength $\lambda = 650\,nm$, α_e will be considerably small and less than 1 dB/km. For different materials the attenuation at this wavelength might be distinctly larger.

Another effect that has not been mentioned yet is the *Fluorination*. Perfluorinated (PF) POFs have the advantage that the vibrational absorption is minimized. If plastic fibers are infused with such perfluorinated materials, the overall material attenuation is significantly decreased. Additionally, the costs for such POFs are then still comparably low. However, by fluorinating the fiber, the peak wavelength and consequently the optical window, is shifted. As a result, attenuation might be higher due this effect. In general, light scattering and electronic transition absorption due to perfluorination is negligibly small and will only influence certain wavelengths (Koike, 2015, pp. 28).

Dispersion

In optics, dispersion is the phenomenon in which the phase velocity of a wave depends on its frequency (Born and Wolf, 1999, pp. 14–24).
There are two different forms of dispersion – chromatic and non-chromatic. All changes in the group-velocity over the frequency are part of the chromatic dispersion. Thus, all light pulses which move inside the fiber spread over the length. This means that a narrow pulse might end up as a broad pulse at the end of the transmission medium. This effect is also known as *pulse broadening*, where t_1 stands for the full-width-at-half-maximum (FWHM) at the beginning of the link and t_2 for the FWHM at the end of the link.

$$\Delta\tau = \sqrt{t_2^2 - t_1^2} \tag{4.47}$$

Pulse broadening can be a major problem, if several pulses are transmitted in short intervals. Then adjacent pulses might overlap, and single pulses are no longer distinguishable by the detector at the end of the link. To counter this problem, the pulse intervals need to be increased to prevent the pulses overlapping. However, by doing so, the amount of information that can be transmitted, decreases considerably. Another possible action to counter pulse broadening is to shorten the transmission link. An example of such pulse broadening is depicted in figure 4.28.

All other types of dispersion are considered as non-chromatic. Multipath dispersion occurs in multi-modes fibers, where several light rays can travel along paths of different length. At the end of the fiber, rays do not arrive simultaneously due to the divergent path lengths. An input with a small spectrum would then have a quite different and considerably broadened form. This type of dispersion does not exist when using single-mode fibers, since the whole energy of induced light is transported by a single mode.

Mode Dispersion (non-chromatic dispersion): It can be observed that mode dispersion is a problem in multimode fibers with step-index profile. If light is coupled into such a medium, the light divides evenly between

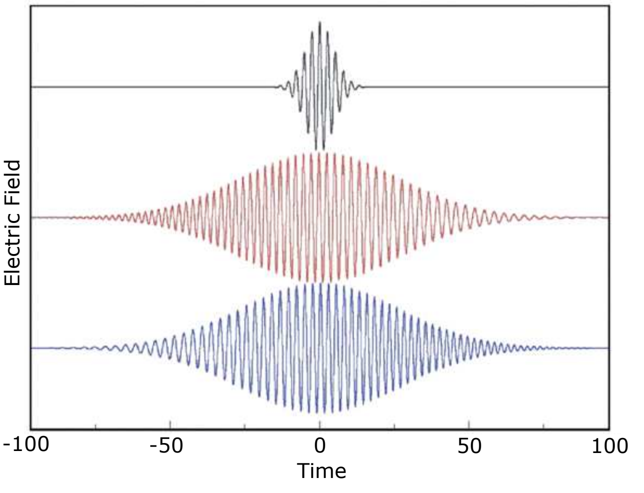

Figure 4.28: Effect of group delay dispersion on a pulse with 100 nm bandwidth (Newport Corporation, 2018)

all transmission capable modes. Even when considering monochromatic light, different values for the effective refractive index are yielded and thus various effective runtimes arise as a result. Light is not reflected parallel to the core axis, but among the silica of the core and the cladding. Therefore, the light spreads in another form than expected and requires much more time to reach the other end of the waveguide than the light, which travels along the optical axis (Fasser P., 2007, pp. 36–37). As a result, the different waves arrive with a delay and are interpreted as a single broadened pulse by the receiver. The propagation delay can be mathematically described with following equation 4.48:

$$\Delta t_{mod} = \frac{n_{1g} L}{2cn_1^2} A_N^2 = \frac{n_{1g} L}{c} \Delta \qquad (4.48)$$

L	fiber length
A_N	Numerical aperture; considers the refraction indices of both core and cladding

Material Dispersion (chromatic dispersion): Can be a desired effect in optical applications, in most cases however, it is unwished-for. Optical waveguides show different refractive indices and thus influence the propagation velocity. The propagation speed itself is limited by the physical and chemical composition of the silica and generates a material dispersion which is dependent on the wavelength. Furthermore, this chromatic dispersion is affected by the emission of the light source. When using a laser diode, which exhibits a very narrow spectral width, the material dispersion is usually very low (ITWissen.info, 2009).

Profile Dispersion: Producing high-quality optical waveguides is quite a demanding process and the silica cannot be perfectly pure to achieve optimum propagation properties. There are inaccuracies and deviations in the production process leading to additional refractions, and thus different signal travel times. As a result, it is difficult to achieve a homogenous refraction profile over the cross-section for graded-index fibers. By using a parabolic profile, the travel times between different modes can be reduced (Fasser P., 2007, p. 35).

Waveguide Dispersion: This type of dispersion is once again dependent on the properties of the optical waveguide, as well as the optical source. In contrast to the profile dispersion, the waveguide dispersion only occurs in single-mode fibers. It emerges due to a wavelength dependence in the distribution of the optical power in the core and in the cladding of the waveguide. As a result, there is pulse broadening, similar to material dispersion.

Polarization Dispersion: Like mode dispersion, this type of dispersion is non-chromatic. Dependent on the polarization, the light can travel at different speeds through the waveguide. A polarization occurs, e.g., if there is a bend in the waveguide. The material might become anisotropic and then the propagation constants differ from the expected. When considering an automotive application, the EMC is certainly a major advantage. Using high-quality fibers in this environment is not reasonable due to the high costs and the necessity of a very flexible and bendable physical medium. This requirement can mostly be met by using polymer fibers. They are far more versatile and bendable than hard glass fibers, which can break at excessive bending. Using cheaper polymer fibers with higher attenuation causes no issues since the distances within a vehicle are limited to a few meters (Damask, 2004).

Radiation

Radiation losses can emerge when converting guided modes to non-guided modes. The *V-number* is a very important parameter of the normalized optical frequency, which determines the number of modes of a step-index fiber. The modes propagate in the z-direction of the fiber with a certain wavelength λ and are dependent on the fiber parameters diameter a and numerical aperture A_N (Strobel, 2016, p. 50). Those dependencies can be encapsulated in following formula

$$V = \frac{2\pi a A_N}{\lambda} \tag{4.49}$$

Regarding the radiation losses, variations in the diameter a and the profile parameter g during production can lead to fluctuations of the V-parameter. It is also possible that such fluctuations are generated by coating or wiring of the fiber. The higher the V-parameter values, the higher the number of modes that are guided in the fiber. For a specific value of V of approximately 2.405, only a single mode can propagate within the fiber. Thus, this type of fiber with a value V < 2.405 is considered as a single-mode fiber while for higher V-parameters V > 2.405, more modes are guided resulting in a multimode fiber. The number of modes can be calculated using equation 4.41. The profile parameter g indicates the different refractive indices. While g can be neglected for step-index fibers and $N = \frac{V^2}{2}$ remains, N will be $\frac{V^2}{4}$ if a graded fiber ($g = 2$) is used. Hence, with same conditions, twice as many modes can be guided through a step-index fiber as a graded-index fiber. In general, a few hundred or thousand modes can be guided with common fibers. To give an example of typical fibers: A step-index fiber (core radius 50 μm) and a numerical aperture of 0.5 guides approximately 17000 modes at a wavelength of 850 nm. A graded-index fiber (core radius 25 μm) and numerical aperture of 0.25 guides only about 500 modes (Strobel, 2016, p. 52).

Bending

Fiber optic cables are quite flexible, so a bending might occur at any point. Silica fibers should not be bent excessively, as this could damage or even destroy them. Bending has to be considered in a vehicle, where space is very limited and only certain areas can be used for wiring. It is of utmost importance to prevent macro bending, which occurs at a certain radius R. For each fiber there is a critical angle, where the rays are irradiated and cannot be further transported within the fiber - resulting in losses of over 100 up to 1000 dB/km which equals an utter attenuation of the signal. Therefore, it is required to calculate the maximum permissible radius of bending, where the rays will still stay within the core: at a certain bend the refractive index of the cladding might be higher than the effective refractive index. The light will exit the core and be completely lost.

The bending loss can be expressed with the $\exp(-\frac{R}{R_c})$, where R is the radius of the curvature of the fiber bend. R_c can be calculated with equation 4.50. A typical value for R_c for single-mode fibers lies between 0.2 - 0.4 μm (Agrawal, 2012, pp. 58–59).

$$V = \frac{2\pi a A_N}{\lambda} \tag{4.50}$$

There are two types of bending, see figure 4.29, which might pose a serious problem in tight environments, where bends are inevitable: *micro bending* and *macro bending*.

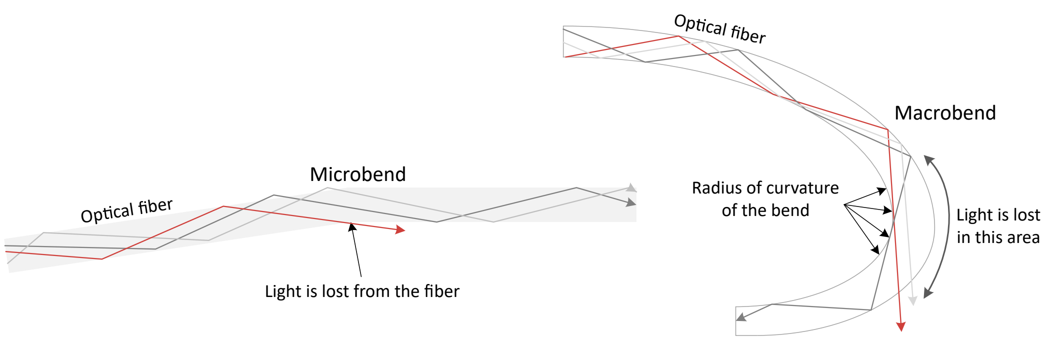

Figure 4.29: Microbending und macrobending. Adapted from (Fosco Connect, 2009)

Microbending: Describes the random axial distortions that might occur when pressure is applied to the fiber by other objects or uneven surfaces. Those bends are in most cases not preventable and the resulting losses have to be considered in any case. In worst case, the micro bending losses can amount up to 100 dB/km. Hence, it is reasonable to use wiring ducts to minimize such influences.

Macro bending: For a bend radius R bigger than 5 mm, the bending loss can be ignored. In practice, this means that most of the macro bending losses are not an issue. The bending radius for macro bending for the whole fiber should exceed 25 mm to reduce bending losses to a minimum (Strobel, 2016, p. 100). The tighter the bend the more light will be refracted out of the waveguide. It is possible to calculate the refractive index n_c for the position where the bend occurs. In following equation 4.51 the radius of the bend is considered to determine n_c.

$$n_c^2(r,\theta) = n^2(r) + \frac{2n_1^2}{R} r \cos\theta \tag{4.51}$$

The attenuation will increase further with the number of bends, the radius of the bend as well as the wavelength of the signal. There is one interesting fact about bending. Even if there are several bends, the same modes will propagate through all bends if they still exist after the most severe bend.

Coupling Losses

In general, fibers are attached to the devices via a plug-in connector. There are losses at those connectors, as well as at the coupling points. If there are differences in the core diameter or in the diameter of the mode field, there is attenuation when transmitting from a larger fiber to a smaller one. The coupling losses can be approximated with 0.36 dB. Some of the power will be lost in the cladding of the second fiber. In the other direction, from a small fiber to a larger one, no coupling losses occur. There are losses however, if there is a coupling between a step-index fiber to a graded-index fiber. These losses are in general 3 dB, which means that only half of the existing modes can propagate after coupling. The best solution, in terms of losses, is to establish a connection between two fibers by splicing them. Then, the resulting attenuation is only about 0.1 dB. Nevertheless, by doing so, it is almost impossible to split this connection again without destroying both fibers (Fasser P., 2007, pp. 149–150).

The efficiency of coupling is dependent on several factor such as the light source, the waveguide (type of fiber), and of course a very small coupling attenuation, which can be determined with equation 4.52 (Strobel, 2016, p. 120):

$$A_C = -10\,dB\,lg\,\frac{P_F}{P_L} \tag{4.52}$$

P_F Power coupled into the fiber
P_L Light source output power

A cheap LED will naturally yield a very high attenuation due to the wide radial and not very directed light emissions. In figure 4.30, various types of couplers are depicted, and their losses are listed accordingly.

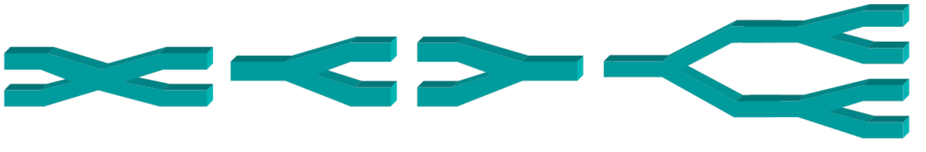

Figure 4.30: Different types of couplers and their loss. (Ziemann et al., 2008, p. 60)

Considering these coupling losses, the minimum loss in a bi-directional optical communication channel, where the signals will be both split and coupled, will amount to $2 * 3\,dB = 6\,dB$. When using single-mode fibers, there is the option to reduce the losses to a minimum by using appropriate WDM systems to support numerous channels. However, to support many channels, the overall complexity and cost will increase.

Connectors

Connectors are defined by three important parameters: Insertion loss, return loss and reflection. In general, insertion loss and reflection should be a minimum, while the return loss should be a maximum. Insertion loss and return loss often correlate – a high return loss leads to a low insertion loss (Goldstein, 2017):

$$\text{Insertion loss} \qquad I\,L_{dB} = 10\,log\frac{P_T}{P_R} \tag{4.53a}$$

$$\text{Return loss} \qquad R\,L_{dB} = 10\,log\frac{P_i}{P_r} \tag{4.53b}$$

$$\text{Reflection} \qquad R_{dB} = -10\,log\frac{P_r}{P_i} \tag{4.53c}$$

where

P_T ... Transmitted Power	P_R ... Received Power
P_i ... Incident Power	P_r ... Reflected Power

Return loss and reflection are used to describe the properties of the connectors. While the return loss is positive, the reflection is assumed as negative. There are various types of connectors which exhibit different properties. When considering the area of application, which should be vehicles, then the connectors must be resiliant against a series of influences. These include strong vibrations, dirt and minor impacts, during which the connectors must not be affected.

4.5.4 Optical Multiplexing

Optical multiplexing offers the possibility to increase the capacity and speed of an optical communication system. The channel capacity of modern standard fiber cables is in the range of 100 Gbps up to 1 Tbps. Thus, the overall capacity of such a system can be more than 100 Tbps, depending on the number of cores, channels and propagation modes, as well as the modulation used. Systems with specialized fibers can even achieve an overall capacity of several Petabits (Miles, 2018).

In most cases, the capacity is limited by components and speed of the signal conversion process. Additionally, optical amplifiers exhibit a limited bandwidth. By increasing the spectral efficiency, this problem can be countered. Furthermore, the symbol rate and spectral width will be

decreased resulting in smaller channel spacing in WDM systems (Strobel, 2016, p. 227).
The best method to increase the overall transmission capacity is to allow the propagation of several modes within a fiber. However, this requires newer types of fibers.

In this context, the intention is to use only single fibers for each independent system. As explained previously, an optical point-to-point connection is unidirectional. An easy solution is to use a second fiber for the backchannel. However, it is possible to use only one fiber for various transmitters and receivers. This structure is then called bidirectional multiplex system. There are different types of multiplexing which will be discussed.

- Optical Space Division Multiplexing (OSDM)
- Optical Time Division Multiplexing (OTDM)
- Optical Code Division Multiplexing (OCDM)
- Optical Orthogonal Frequency Division Multiplexing (OOFDM)
- Optical Wavelength Division Multiplexing (OWDM)

However, when using multiplexers, each coupler adds 3 dB to the overall attenuation of the signal. Other effects, like cross-talk, can also influence the signal quality. When using different wavelengths for the transmission via the same fiber, as it is the case in OWDM, then it is possible to transmit at the same time without losing any information.

Optical Space Division Multiplexing (OSDM)

In the first OSDM specification, several individual fibers were used. Each sender and receiver is attached to a distinct fiber. Through cross-bar-switching, fibers can be connected to all senders and receivers. By using switches, it is possible to interconnect the sender with the desired receiver, and thus establish a successful connection.

In OSDM, the bandwidth of the fibers is not utilized optimally. In addition, crosstalk might occur between channels. However, by using coherent detection systems and digital compensation, this crosstalk can be removed electronically at the receiver. To some extent, SDM fibers can support WDM and advanced modulation formats in each channel (Richardson, Fini, and Nelson, 2013, p. 354).

Nowadays, OSDM is more specific and describes a spatial division of multiple data paths through a single fiber, not a distribution to several individual, parallel fibers. In multicore fibers, there is still a physical separation of the various fibers. With an appropriate separation, the mentioned crosstalk as well as cross-coupling can be limited. The level of crosstalk needs to be less than -25 dB to achieve satisfying results for the transmission quality. 40 μm as a core spacing is in most cases sufficient.

When using multimode fibers for mode-division multiplexing (MDM), the data paths display spatial overlaps. Consequently, there will be effects such as mode coupling, which affect the propagation of the signals. Such mode propagation impacts are also known as differential mode group delay (DMGD) and differential modal loss (gain). When mode coupling occurs, information symbols will spread out and appear in other time slots. As a result, the transmission will be biased and considerably less successful, and inter-symbol interference (ISI) might also occur.
Therefore, when using multimode fibers, multiple-input multiple-output (MIMO) techniques must be applied at the receiver side to diminish those interferences. Such MIMO signal processing techniques are commonly applied in polarization-division multiplexing (PDM). With PDM and finite impulse response (FIR) filters, the polarization mode dispersion can be compensated. The mentioned DMGD and mode crosstalk can also be eliminated if the equalization filter length is greater than the impulse response spread (Richardson, Fini, and Nelson, 2013, pp. 355–356).

Certain key elements, as connectors and other components, e.g. the MIMO signal processing and spatial multiplexing density, need to be improved to enhance the overall quality of an SDM system. Only then the crosstalk can be limited to a range, where it is not an issue. Scalability is the most important parameter for future SDM systems. Coupling, modulators, demodulators etc. should be as scalable as possible to increase the overall capacity if required. The flexibility can also be increased when using passive multiplexers. Ultimately, the goal is to achieve an SDM system with high efficiency and low differential gain for a high number of modes. The spatial requirements should be minimal and interferences such as crosstalk should be kept to a minimum. For a flexible design, certain components as reconfigurable add-drop multiplexers (ROADMs) are required for both SDM, as well as WDM systems. With such a multiplexer, carriers can establish light paths and switch between the different paths (Richardson,

Fini, and Nelson, 2013, pp. 356–357).
Further details on SDM and SDM ROADM will be discussed in section 6.2.2.
In figure 4.31, the different fiber designs that are used for OSDM are shown.

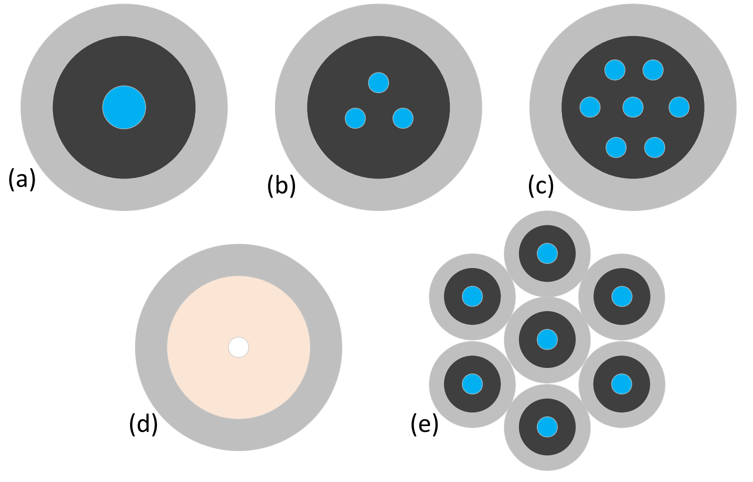

Figure 4.31: Approaches to realize optical fibers for SDM. Adapted from (Richardson, Fini, and Nelson, 2013, p. 356)

(a): A so-called few-mode fiber is used. Only a certain amount of modes can spread in this type of fiber (e.g. 6-12 distinct modes).
(b): In this type of fiber, supermodes can propagate through the fiber. Those modes have a far higher spatial mode density compared to e.g. (c).
(c): In this approach, several cores are guided in the same fiber. Here, there must be adequate gaps between the cores to prevent or minimize crosstalk. However, MIMO processing must be applied to minimize mode coupling.
(d): This fiber uses an experimental approach, where the core consists of air. By using air, some of the effects which appear in the core material can be eliminated. However, it is much more difficult to realize and to produce than the standard fibers with a silica core.
(e): This is the simplest form of a SDM realiziation. Each single-mode fiber is independently guided. Due to the coating, there is no crosstalk (Richardson, Fini, and Nelson, 2013, p. 356).

Optical Time Division Multiplexing (OTDM)

OTDM uses only one wavelength of light for all the transmissions. A single fiber is sufficient for a working transmission channel. The bitstreams of the input signals are nested inside each other and send one at a time. Each input is assigned a fixed length time slot on a communication channel. The bit rate is $N * B$, where N is the number of channels which are multiplexed and demultiplexed at the other end of the optical fiber. The goal of TDM is to send data of different senders over a channel within a certain time frame. The benefits of TDM is the increased data rate and bandwidth. Additionally, the data packets of two different transmitters will never arrive simultaneously at the receiver (Agrawal, 2012, p. 264).

The first requirement is a laser source which can generate a periodic pulse train. This sequence should match the rate of the single-channel bit rate B. The structure of an OTDM transmitter is visible in figure 4.32.

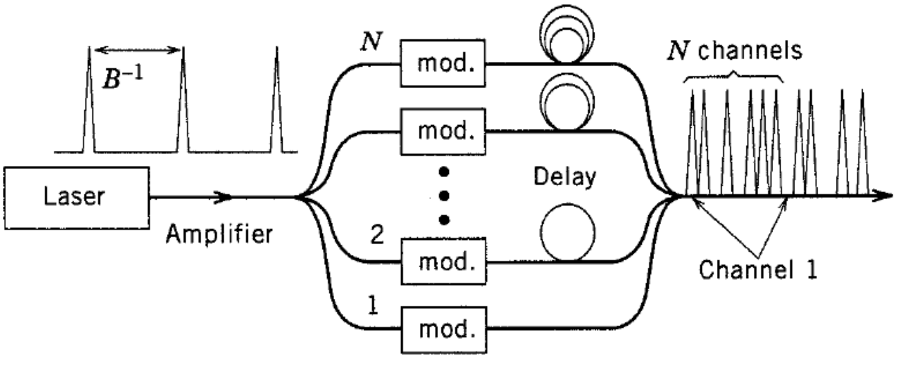

Figure 4.32: OTDM transmitter. Adapted from (Agrawal, 2012, p. 265)

The pulse width requires the following condition: $T_p < T_B = (NB)^{-1}$
Only then, each pulse can fit in the allocated time slot T_B.
The modulators depicted in figure 4.32 have the task of blocking the paths and create N independent bit stream with bit rate B. Furthermore, the paths can be individually delayed with a quite simple technique. The delay can be calculated quite simple with following statement: $\frac{n-1}{NB}$ for n = 1, . . . , N.
At some point the delay lines will be merged again and form a mixed

signal, where no overlap should occur. The splitting of the original fiber can be achieved using a splitter or fiber couplers. The delay lines are realized with single-mode fibers, where the length of the additional fiber segment is crucial and must be matched perfectly to achieve the precise delay. With a 1-mm segment, a delay of 5 ps can be achieved. This approach is very simple and in general, it is difficult to realize a high precision with such short delay speeds (Agrawal, 2012, p. 265).

OTDM uses the RZ format (see section 4.1). The optical pulses must be transmitted with a very high repetition rate of > 100 GHz (< 1 ps), so high quality semiconductor laser sources are required (Agrawal, 2012, p. 264). The goal of OTDM is to transmit data of various different senders in distinct time frames over one channel. As a result, the achieved data rates and bandwidth are significantly larger. The time frames are then demultiplexed to recover the information. There are two different approaches - synchronous and asynchronous - to utilize the communication channel the best way possible.
The *synchronous* procedure uses a fixed time frame for the data transmission. Each connection obtains a constant data transmission rate and each sender is clearly recognizable. The major drawback emerges as soon as no node is sending data. Then the time frame is unused and there is no optimal utilization of the transmission channel.
The *asynchronous* time multiplexing eradicates this drawback by allowing access only to senders that actually will send data. However, by permitting this time flexibility, the unambiguous identifiability of the messages gets lost in the process. Hence, each data packet requires an identifier in the header to attain a proper assignability when reconstructing the data at the demultiplexer. As a result, the bandwidth of the channel is used with higher efficiency, even though the size of the packets increases with the additional information in the header.

Optical Code Division Multiplexing (OCDM)

Code Division Multiplexing uses the spread-spectrum technique and is very similar to code-division multiple access (CDMA). After coding each channel, the spectrum of a channel spreads over a wider region than the original signal. Both encoder, as well as decoder are required for this kind of multiplexing. This means that the same bandwidth is available for all users

at random time slots and thus providing excellent flexibility in a dense environment. However, the channel bandwidth is utilized quite inefficiently. Still, this technique is very popular for microwave communications as it provides the best flexibility in a multiuser environment. The encoder does the actual spreading of the signal spectrum. A unique code will be used by both encoder and decoder for the spectral spreading/de-spreading of the signal (Agrawal, 2012, pp. 277–278).
This procedure gives access to each channel at a random point in time. Thus, the overall security of CDM is very high. By means of coding, the signal sequences can be detected and matched at the receiver. Consequently, the overall procedure looks like time multiplexing without any time frames. For the coding, several methods such as direct sequence, time hopping, and frequency hopping can be applied (Fasser P., 2007, pp. 182–183).

In OCDM an optical short pulse is used, which exhibits a significantly higher frequency spectrum than data bandwidth. This pulse is spread over one-bit duration T by the mentioned encoder. The decoder carries out the decoding of the signal and reconstructs the original pulse. With matched filters, the signal will be de-spreaded and as a result, the SNR of the received signal will be maximized. The impulse response $h_d(t)$ of a matched filter and the Fourier spectrum $H_d(\omega)$ will look as follows (Kitayama, Sotobayashi, and Wada, 1999, p. 2618):

$$\text{Impulse response} \qquad h_d(t) = h_e(t_0 - t) \tag{4.54a}$$

$$\text{Fourier spectrum} \qquad H_d(\omega) = H_e(\omega) * \epsilon^{-j\omega t_0} \tag{4.54b}$$

The output can then be determined by convolution of impulse responses and the matched filter. Ultimately, it can be observed that the detector output is dependent on the degree of coherence of the light source. Compared to the incoherent encoding, the coherent scheme performs twice as well. However, when using a coherent encoding scheme, interferences such as the interferometric noise have to be considered. Furthermore, certain effects like wavelength dispersion need to be observed when using OCDM with pulse code sequence for long distance transmissions (Kitayama, Sotobayashi, and Wada, 1999, p. 2620).

Optical Orthogonal Frequency Division Multiplexing (OOFDM)

In optics, the Orthogonal Frequency Division Multiplexing modulates several signals onto one separate carrier frequency resulting in narrow frequency bands. Those bands are then combined and form a broadband signal, which are transmitted independently at the same time over a single channel. During the modulation process, two identical bands emerge, and the carrier frequencies must be suppressed. Hence, the carrier frequencies are supplemented at the receiver to recreate the original signal. With additional filters, the signals can be separated and by demodulating them, they are transferred back into their original frequency position. In contrast to normal frequency division multiplexing (FDM), the subcarriers of the OFDM system are spectrally overlapping, which makes the filtering more complex. Between subcarriers, the spectral spacing can be estimated with (Strobel, 2016, p. 229)

$$\Delta f = \frac{1}{T_S} \tag{4.55}$$

where T_S denotes the OFDM symbol duration. To achieve demodulation at the receiver, the following steps are required: The subcarriers are shifted to the baseband and integrated over T_S. A matched filter is applied and as a result, an optimal subcarrier separation is attained. Another positive effect is the maximization of the SNR. For this process, the discrete Fourier transform (DFT) can be used, which executes the described operations. Another possibility is to use an efficient IFFT-based implementation.

There is quite an interesting approach proposed by (C. Li and Yang, 2016). There, the OFDM is based on the Offset Quadrature Amplitude Modulation (OQAM) and offers the advantage that the side lobe suppression rate is significantly higher than with standard OFDM. In figure 4.33, the structure of this proposed optical OFDM/OQAM is shown.

The OFDM/OQAM baseband signal can be expressed by following equation 4.56 in (C. Li and Yang, 2016, pp. 100):

$$y(t) = \sum_{k=0}^{N-1} \sum_{n=0}^{\infty} [S_k^I(n) * h(t - nT) + jS_k^Q(n) * h(t - nT + \frac{T}{2})] * e^{jk\phi_t} \tag{4.56}$$

where $\phi_t = \frac{2\pi t}{T} + \frac{\pi}{2}$

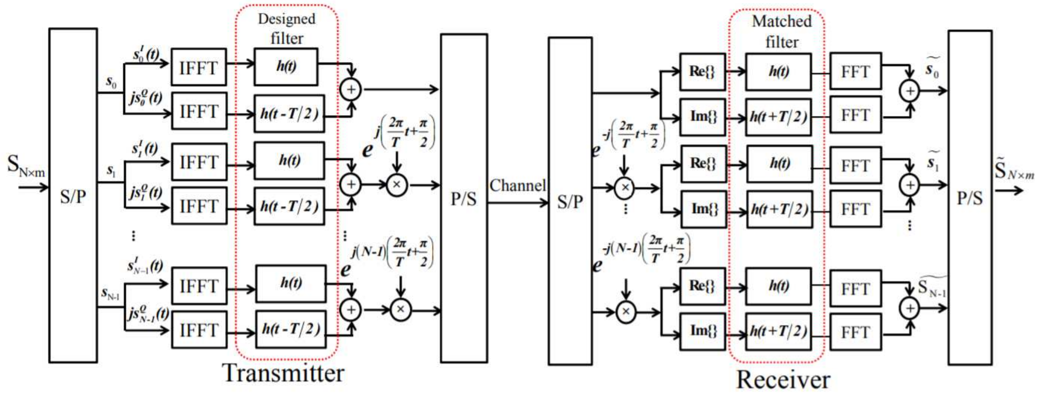

Figure 4.33: Principle structure of OFDM/OQAM (C. Li and Yang, 2016, p. 100)

The baseband signal can be converted into an optical passband signal by using an optical IQ modulator. As visible in figure 4.33, the OFDM/OQAM signal is converted at the receiver side and matched filters are applied. With the FFT, the demodulation is conducted, and the baseband signal is reconstructed. To prevent interferences, so called guard bands are introduced between the various frequency bands. By doing so, the bands should not overlap during this process.

Optical Wavelength Division Multiplexing (OWDM)

The purpose of wavelength division multiplexing is to transmit several signals over the same optical fiber at the same time. Optical signals are bundled in a multiplexer and coupled into a fiber. As a result, narrow-band wavelength areas are created and all of them represent a transmission channel, on which all the data of a sender can be modulated. At the other end of the fiber the channels are uncoupled again by a demultiplexer (optical filter) and the detector will perform a signal conversion (Brückner, 2011, p. 183).
With this procedure, several channels per window can be transmitted over the same fiber. The available bandwidth is used very effectively by this technique. It is possible to use refractive elements, e.g. a prism or diffraction grating, for the multiplexing. Furthermore, optical filters or wavelength selective couplings are suitable for this purpose (Fasser P., 2007, p. 174).

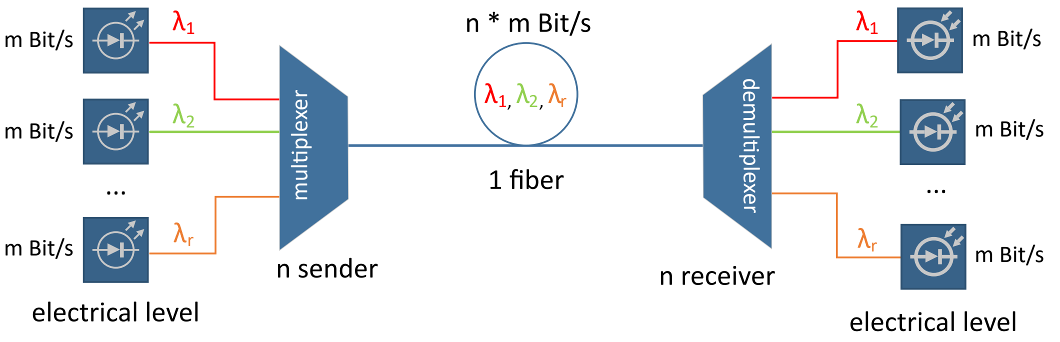

Figure 4.34: WDM system. Adapted from (Brückner, 2011, p. 183)

Using a WDM multiplexer has various advantages over splitters. The most straight forward one is the considerably lower attenuation. In a single-mode fiber it is even possible to achieve a light coupling without any additional losses. There are three different types of wavelength multiplexing, which are commonly used: DWDM, CWDM and WWDM.

Dense Wavelength Division Multiplexing (DWDM): The gap between channels (16 or 32) is rather small with only 0.4 nm up to a maximum of 1.6 nm (C- and L-band). To achieve such a small gap between the used wavelengths, it is necessary to use high-quality filters as well as specific lasers that are optimized and stabilized in terms of temperature and wavelength. Achieving those constraints comes with a massive increase in costs and complexity. With DWDM data transmission rates of 10-100 Gbps per channel (80-160 channels when combining C- and L-band) are achievable. Due to the high complexity and effort, this method is often only applied in long distance application. Every 100-200 kilometers, it is required to amplify the signal or alternatively use an electric data regeneration every 600-2000 km. An optical amplifier can reinforce all 40 channels at the same time (Brückner, 2011, p. 183–184).

Coarse Wavelength Division Multiplexing (CWDM): In contrast to DWDM this technique is less extensive and complicated, and suitable for shorter distances. The channel spacing is 20 nm for a wavelength area from 1271 nm up to 1611 nm. This is achievable by using much cheaper components than used in the DWDM, and the most important property – transmitting signal with different wavelengths over a single fiber – is preserved. Signals with CWDM can be transmitted for 70 km without any amplification and are commonly used for passive optical networks (PONs). It is obvious that the obtainable distances are only of minor interest for the automotive area, since point-to-point distances often are in the range of several meters (Brückner, 2011, p. 183–184).

The third type of wavelength multiplexing is the *Wide Wavelength Division Multiplexing* (WWDM). Only signals of the wavelength ranges 1310 nm and 1550 nm, which exhibit a low attenuation, are transmitted over a fiber.

4.6 Optical Technologies for Autonomous Vehicles

On the following pages, a few optical technologies useful for automotive applications are discussed.

4.6.1 Light Detection and Ranging (LiDAR)

In highly automated vehicles, sensors must detect, interpret and solve all kinds of different traffic situations on their own. Therefore, there is a requirement for high connectivity between all the vehicles sensors and the environment. There are quite a few different sensor systems available in modern automotive system (Leitgeb et al., 2017):

- Radio detection and ranging (RADAR), used for distance measuring between vehicles or relative speed measuring for cruise control
- Ultrasonic sensors, which are used for close distance measurements e.g. parking
- Mono/stereo cameras support the detection of obstacles and other potential perils like persons or vehicles
- Infrared cameras, such as night vision systems, to detect persons or animals on the road

The communication between the different sensor systems must be reliable, accurate and secure. Since the environment, e.g. buildings, other vehicles, traffic signs and lights, are in most cases not yet able to communicate with vehicles, a self-sufficient system is required to fulfill those requirements as best as possible. Currently, *Light detection and ranging*, short LiDAR, seems to be the most promising technology to detect any obstacles or potentially dangerous situations on and directly next to the road. LiDAR is an optical measurement procedure to detect objects and measure the distance to the optical transceiver.

The LiDAR transmitter emits laser rays, which are reflected by the environment. LiDAR sensors detect and receive the laser rays with multispectral cameras. The cameras can detect light with different wavelengths and consequently a 3D model of the surroundings of the vehicle is created. In other words, the reflected or backscattered intensity of a pulsed laser beam in relation to the preceding time of the initial emission is measured. Considering the speed of light, distance profiles of the reflection properties of objects can be derived. It is possible to draw conclusion on the speed and gap of the objects in relation to the vehicle from the different spectral colors of the reflected laser light. To achieve an acceptable accuracy of the environment, more than two million measurements per second are recorded. With this amount of data, LiDAR is by far the most accurate detection system for vehicles (Leitgeb et al., 2017).

However, it is necessary to evaluate all this data gathered by the LiDAR. Consequently, there has to be a very powerful computer on board of the vehicle to execute the required data analysis and calculations – otherwise an evaluation in real-time is not achievable. Still, the measurement rate provides only up to 10-20 frames per second. The achievable resolution lies in the range of 1-5 centimeters. Thus, this system is already precise enough for almost all common traffic situations. Since LiDAR systems are constantly being improved, the mentioned benchmarks will certainly be replaced in the foreseeable future (Leitgeb et al., 2017).

Measuring the time between sending and receiving the light is also known as the *time of flight* measurement. The duration starting with the emission of the light impulses and ending with the reception of the backscattered rays is proportional to the radial distance between the measurement system and the detected object. Light travels with a constant speed of c = 299792458 m/s through a vacuum. The speed in the medium air is about 0.28% reduced, resulting in approximately 299710 km/s.

With the following equation, the distance of an object in relation to the moving vehicle can be calculated (Winner et al., 2015, p. 318):

$$d = \frac{c * t}{2} \tag{4.57}$$

where

d ... distance in meters c ... speed of light t ... time in seconds

The light pulse has to travel to the object and the reflected light back the same distance again. Thus, the time t represents twice the distance to the object. A sophisticated LiDAR system can measure several objects in a measurement channel. However, there must be a certain distance between the objects to allow a clear classification. One serious problem can be posed by the communication channel, which is free space (air). Since the range is relatively short (up to 200 m), atmospheric effects are not necessarily a problem. If there is dense fog however, various pulses can be reflected by the water droplets in the air. Depending on the size of those droplets and wavelength, this could influence the range quite heavily. In case the light wavelength is similar to the size of the droplets, the range might be constrained, and no valid measurements of the environment would be possible – resulting in a failure of the system. The system is capable to distinguish between the different objects because not only the runtime but also the time curve is measured. When evaluated, there is a clear distinction between different objects, materials, and atmospheric effects like rain or fog. The signal curve offers valuable information about the degree of absorption and it is possible to extract information about the visual range from the temporal decline (Winner et al., 2015, p. 319).

Illustration 4.35 shows what objects look like for the LiDAR system. The emitted light waves are reflected at some point and impinged back to the LiDAR.

Almost all autonomous vehicles utilize such a system, except the Tesla models, to function on a high safe and reliable level. The range of LiDAR is up to 200 meters, the angle of detection is in most cases 360°. Currently, LiDAR systems are not very appealing to a broader public, since they are mounted on the rooftop and are quite voluminous. Additionally, they influence the aerodynamics and handling of a vehicle.

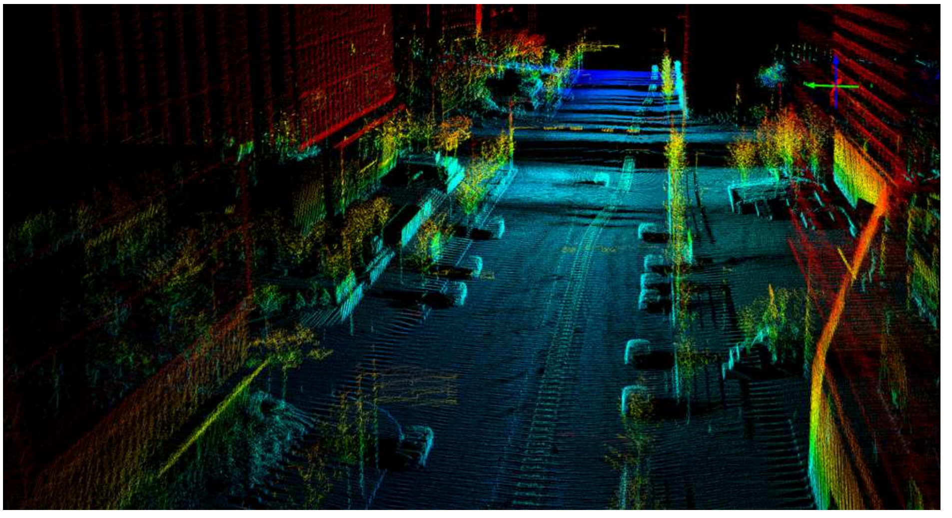

Figure 4.35: Illustration of environment detected by LiDAR (Hampstead, 2018) (Image-source: QUANERGY)

Sender

For a detailed description of optical senders see section 4.3. The wavelength used for the optical sources is typically in the range of 850 nm up to 1 μm. To name an example, Velodyne Ultra Puck™ uses a wavelength of 903 nm. The stated accuracy for a range of 200 meters is about +- 3cm and the system records either 600000 or 1.2 mio points per second. Each sensor has 16 to 64 lasers, while the rotation rate can be adjusted from 5Hz to 20Hz. The operating temperature range is $-20°C$ to $+60°C$ (Velodyne LiDAR, Inc., 2018).
To achieve the best possible distinction of objects and the resulting echoes, the measurement pulse of the sources should be as short as possible. When considering high-performance diodes in the range of 905 nm, the achievable power can be up to a few hundred watts. The pulse length is somewhere between 1 ns and 100 ns. The source size is also often quite different and the laser power can vary in a large range e.g. 3W - 650W (Laser Components, 2018).
Since there are often pedestrians in the range of LiDAR systems, the lasers must comply with certain regulations to ensure eye safety. As a result, each laser pulses with an average power of 2 mW. To put this number into perspective, this corresponds to 0.02% of the power output of a 10-watt

LED headlamp. Thus, the output power of such a laser is considerably smaller than that compared to a laser pointer, and also the time in which such a laser beam sweeps across an eye is much shorter – approximately one millisecond (Bezemek, 2017). The emitting area of the used lasers lie often in the μm. A typical value of e.g. a SPL PL 90 diode is $200\,x\,2\,\mu m^2$.

Receiver

Section 4.4 covers the basics of optical receivers. Both, PIN diodes and avalanche photodiodes (APDs) can be used for LiDAR systems. To comply with the requirements of high precision in the centimeters range, a high measurement speed is essential. As mentioned earlier, the range of measurements is starting from 10 cm up to 200 m – resulting in a maximum runtime of the light of approximately $t = \frac{c}{2*s}$ = 1,33 μs. (Total pathlength = 2 * 200 m).

Other effects such as noise of ambient light are also problematic in the reception process of photodetectors. Most interferences can be suppressed by using daylight filters. Those filters remove any radiation of wavelength less than 760 nm (Boucouvalas, 1996).
There are several effects which are important when talking about the receiver. The main influences are mentioned in section 4.4. The reflectance and absorptance indicate the losses while the transmittance is the emission which actually can pass through the channel. The weakening of the signal can be described by absorption, scattering, diffraction and reflection and is dependent on the wavelength (Winner et al., 2015, p. 324).

There are several different approaches to LiDAR systems. Velodyne sticks to their 360° models, which have to be placed on top of the vehicle. However, the newer versions such as the puck are already considerably smaller than the first versions and do still offer the same advantages as the much larger devices.
Continental and Quanergy are currently working on solid-state LiDAR systems, which are more compact in size and dynamic in the positioning. They could be hidden in the chassis of the vehicle and thus reduce any effects on the driving behavior.

In theory, it is possible to develop a functional LiDAR on a single chip, which costs about 10$ (Ackerman, 2016). The range of such chips is limited to a few meters, which is too little for an application in vehicles. However, the proof of concept shows that there might be alternative technologies available in the coming years.

4.6.2 Visible Light Communication (VLC)

As the name suggests, visible light in the frequency spectrum 430 THz (380 nm) up to 790 THz (750 nm) is used for this type of communication. All frequencies in this range are not yet regulated and still freely available for public usage.
LEDs are widely used for vehicle headlights. Thus, interesting opportunities using these lights for additional applications are emerging. By applying modulators and transmitters to the LED headlights, it is possible to transmit information. Another, not yet applied use case is using the headlights for car-to-X communication. The available LEDs provide the basic requirement for a functional VLC system. If modulators and transmitters are connected to the LEDs, it is theoretically possible to transmit information. For a complete communication channel, detectors must be installed to perceive the emitted light. If infrastructure is also equipped with the necessary equipment, the vehicles could also communicate with their environment and all kinds of data could be transmitted. One interesting fact is that not only photodiodes or similar semi-conductors can act as a detector: it is also possible to use cameras to measure the image for light signals (Leitgeb et al., 2017).

4.6.3 Power Over Fiber (PoF)

PoF is an exciting technology to power devices and sensor with low power requirements. Figure 4.36 shows what such a PoF system could look like.

Two fibers are used for a bidirectional connection. The HPOS powers the remote unit, which then can transmit the sensor data back to the Control Unit. A PoF system can only provide a limited amount of power, which is determined by the components used, such as laser, fiber, and photovoltaic cells at the receiving device. The photovoltaic converters are often designed as arrays to maximize the output. A photocurrent is

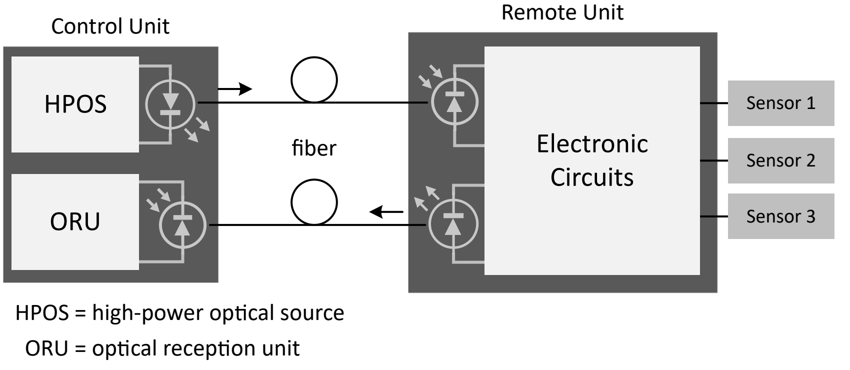

Figure 4.36: Generic PoF system. Adapted from (Rosolem, 2017, p. 260)

generated as soon as light hits the elements of the converters. The resulting output power depends on the conversion efficiency of the photovoltaic converter. Different circuits can be applied to achieve an output voltage. The voltage varies in the range of 2 to 4.8 V (Rosolem, 2017). This means that there is definitely potential to power simple sensors with this PoF technology in the near future.

5 Analysis

Considering the previously mentioned challenges the automotive sector is faced with, it seems inevitable to tackle these challenges with optical data transmission. Sensors, cameras and actuators of low-level automated vehicles already produce more than 25 GB/hour of data (Hitachi Data Systems, 2015) and there are no means of communication available to transport this increasing data volume. On the contrary, the generated data will further increase, as shown in the following table, where data of Lucid Motors (Heinrich, 2017) for semi-autonomous vehicles are summarized:

Sensor	**Number of sensors**	**Data rate / sensor**
RADAR	4-6	0.1 - 15 Mbps
LiDAR	1-5	20 - 100 Mbps
Camera	6-12	500 - 3500 Mbps
Ultrasonic	8-16	$<$ 0.1 Mbps
Motion, GNSS, IMU		$<$ 0.1 Mbps

Table 5.1: Estimated data rate for various types of sensors

Consequently, the overall required bandwidth is somewhere in the range of 3 Gbps ($\sim$ 1.4 TB/h) to 40 Gbps ($\sim$ 19 TB/h) (Heinrich, 2017). According to (J. Stewart, 2018), semi-autonomous vehicles generate six gigabytes per 30 seconds and up to 40 terabytes in eight hours.

These simple examples show how the required bandwidth increases with the number of sensors. It is difficult to estimate how the bandwidth will change for fully autonomous vehicles if further sensor-based systems are installed. One thing is certain: there must be a powerful computer on board to process all this data accordingly, and a transmission medium which can handle these large amounts of data. Currently, only optical technologies can achieve the bandwidths required for autonomous driving.

In this chapter, the previously reviewed technologies like CAN will be analyzed and potential problems will be shown. Furthermore, a test setup is constructed to demonstrate the problems discussed.

5.1 Vehicle Network

The network in the vehicle is the most important part to connect all electronic devices with each other. In chapter 2, many parts of a vehicle network have been named and described. It is quite important to remember that most of the vehicles on the road are several years old. In general, the vehicle network in most of them will be quite simple. The following figure 5.1 shows a basic car network.

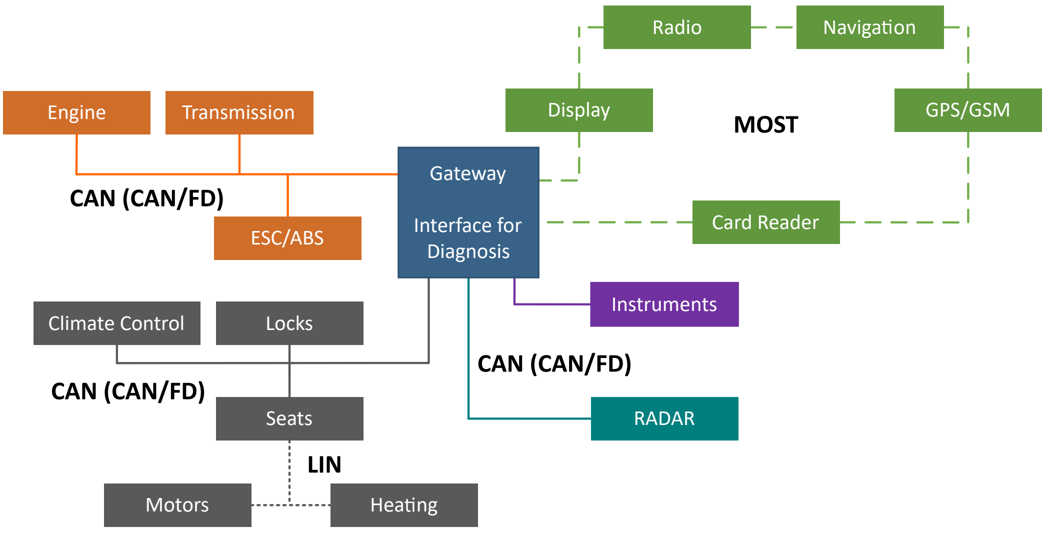

Figure 5.1: Bus systems in a common vehicle. Adapted from (Wiesinger, 2005)

The network consists mostly of CAN bus connections. Some multimedia components are connected with a MOST bus structure, to provide sufficient bandwidth for these applications. LIN is only used for rudimentary functions, where single signals are transmitted to control motors.

A network structure of modern vehicles has been considered in section 3.8. Following figure 5.2 is adapted from (Holt, 2018) and shows what an Automotive Ethernet in a vehicle could look like.

Usually, there are even more subnetworks with other bus systems, e.g. LIN (Body & Comfort). To improve clarity of the illustration, they have been left out.

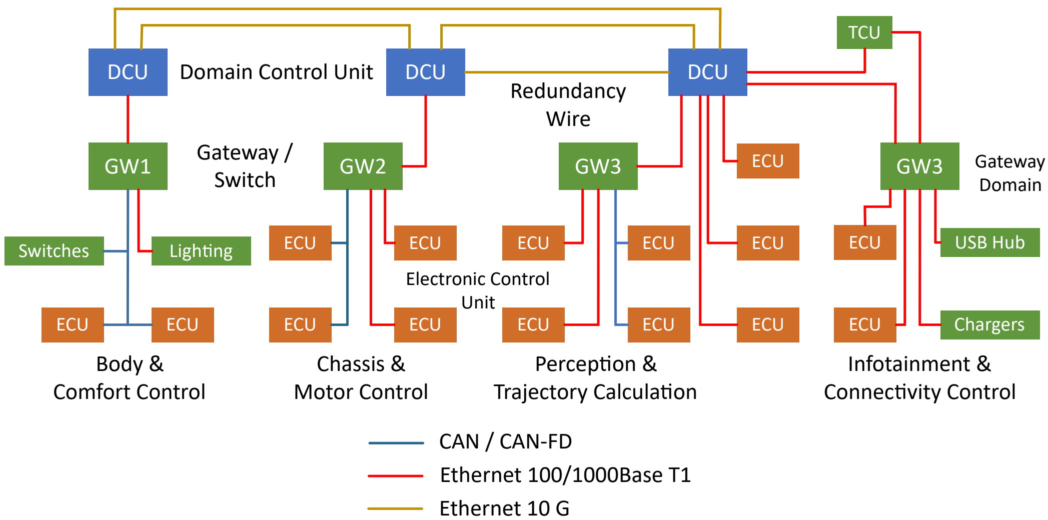

Figure 5.2: Ethernet in automotive systems. Adapted from (Holt, 2018)

The ECUs are directly connected to the gateways with an Ethernet connection. Each subdomain has its own CU, which controls the specified area of application, e.g. Motor Control. It must be noted that the network in an autonomous vehicle must look differently to structure in figure 5.2. For example, a powerful computing unit for real-time path and obstacle calculations is required as well as additional sensor systems such as LiDAR.

Many new systems have been introduced in the past decade. The number of cameras has increased and new technologies such as LiDAR are now the norm for autonomous systems. The amount of data produced by an autonomous vehicle is, as suggested in section 5, enormous.
There are more than hundred electronic control units (ECUs) present, when ADAS are built-in. The data rate requirements are directly relational to the number of sensor- and camera-based systems.

It is planned to use various wireless protocols to allow communication of vehicles with each other and their environment (V2V). Some examples will be named in the next sections.
Currently, communication with the environment is very limited. Only basic information for navigation systems, parking, and so on, is provided.

In 2019, the Cooperative Intelligent Transport Systems (C-ITS) will be available in vehicles. This system operates in the 5.9 GHz band, which is reserved for safety-relevant applications. When equipped, the vehicle can communicate with so-called road-side stations, which also have such a system installed. Following information is transmitted periodically with a Cooperative Awareness Message (CAM): position, speed, and direction. Some messages can even be transmitted car-to-car, e.g. in case of an emergency braking ahead. Consequently, safety on the roads can be improved by warning the drivers of all kinds of problems, such as congestion, road works, weather reports, accidents etc. All the mentioned technologies exhibit problems, which will be discussed in the following section (Leitgeb et al., 2017).

5.2 General Problems of Current Systems

Interferences & Safety
Electronics within a vehicle are increasing and so is the effort to protect the systems and wires from interfering signals, which can lead to a system failure in the worst case. External interferences and especially electromagnetic impulses can pose a serious threat to the electronics (Vieweg, 2014). The issues with interferences and EMC have been discussed in detail in section 2.6 and 2.7. These problems are very difficult to resolve by car mechanics, because such errors are hard to determine, and wires, as well as electronics, are hard to reach and repair.
Sophisticated assistance systems require high data rates for the transmission to cope with the high and ever-increasing amount of data signals. It is vital that those signals are transmitted immediately, as reliably and securely as possible. Otherwise, the functionality of those systems is not guaranteed. In the worst case, a failure could lead to a crash of the vehicle and thus endanger the passenger's life.

Materials & Weight
The wire harness in a modern vehicle consists of at least 80 ECUs, is a few kilometers long and weighs about 150 kg. In an autonomous car, these numbers are 2-4 times higher. Nevertheless, the number of sensors and other actuators will increase and lead to a very complex cabling effort and, of course, to more weight and material consumption. This means higher assembly and material costs as well as additional fuel consumption for the

vehicle. The more cables, the more difficult it is to protect all the electronics with proper shielding.
Using metal-based wires, especially copper, might also be a cost factor since it is a limited resource and the price has tripled since the early 2000s[1].
There are many other ideas how to reduce the weight within a vehicle. Since it is not always possible to reduce connections and assistance systems, new materials like carbon fiber are used more often.

WLAN
Modern vehicles are already connected to infrastructure to transmit or receive important information. The interface is based on WLAN technology and operates in the 2.4 GHz and 5 GHz spectrum. The 802.11ax standard seems to be the most promising technology to cope with the increasing amount of traffic due to the efficient spectrum utilization in the 1 - 7 GHz range. In this approach, the Orthogonal Frequency-Division Multiple Access (OFDMA) modulation technique is applied, where the communication has to be bidirectional. The received signal quality can then be measured during the process and the sender can adapt to this data to optimize the spectral efficiency. In total, the data throughput might be four times higher with this approach. However, other bands must be available before they can be utilized by this standard and the achievable distance is significantly lower with the 1024-QAM modulation scheme. The overall packet latency will increase, but so will the efficiency and more users get their required bandwidth (J. Li, 2017).

WLAN Safety/Security
This WLAN approach, however, is currently not very secure, since such systems cannot fulfil the requirements of an automotive application. Inferences still can disturb such systems to such an extent that communication could fail. In addition, directed cyber-attacks are much easier executed on WLAN systems. That circumstance might restrain the implementation of WLAN systems in vehicles. There have been incidents in the past, where mobile communication interfaces of various vehicle manufacturers could easily be hacked. Consequently, there must be measures in place to protect the important communication lines like engine management, before a commercial deployment is feasible.

[1]KNOEMA, 2018.

C-ITS
The mentioned Cooperative Intelligent Transport Systems (C-ITS) also exhibits several problems: the high-frequency range is very limited. Weather influences attenuate the signal further, so that the range is only a few hundred meters. This circumstance shows the limitations of this approach. Once again, a very dense infrastructure along the roads is required for a fully functional service. Installing stations along the motorway is realistic in the next years, but rural roads cannot be connected to this system in the foreseeable future. There is neither the infrastructure (fiber optics), nor the budget available to achieve full coverage.
Even though systems like C-ITS are now available, it would take decades until all cars on the road could be connected - regardless of the technology. All vehicles, which are already on the road, would require an upgrade to such a communication system. In most cases, such upgrades will not even be possible, because it would require completely new electronics and wires (Leitgeb et al., 2017).

HD Live Maps
There are many services planned regarding autonomous driving, which have to communicate directly with vehicles to achieve satisfying results. One such service is *HD live maps*, which requires live data for a navigation system. The amount of data collected in such a context can easily reach a few gigabytes per day. Once the whole road network is recorded, only minor data must be transmitted. However, the service must be available in real-time, so that any accidents, mismatches in traffic signs, roadworks etc. can be declared to the HD live map network with absolute certainty.
There are many problems with such a service, because it heavily relies on the data of other vehicles. Falsified data (e.g. 'accident ahead') could easily immobilize autonomous vehicles if they only rely on the provided information (Leitgeb et al., 2017).

Current bus systems display many problems for future advancements in the automotive sector. The low data rate, as well as insufficient real-time capabilities have been discussed in detail in section 3.1.1 and 2.4. They form a bottleneck, particularly in automated and autonomous vehicles, where the number of additional assistance systems is a multiple. One example is naturally CAN, which will be discussed in the next section.

5.3 CAN-Specific Problems

Data Rates & Bandwidth
Achievable data rates of CAN are simply not enough to support most applications in modern vehicular networks. And yet existing CAN bus systems are still expanded, or further CAN bus systems are installed within vehicles to realize, for example, ADAS.
The low transmission speed of CAN is limiting for future applications and systems. Modern ADAS with camera or LiDAR as sensors require bandwidths, which are far higher than the maximum achievable data rates of CAN. With a data rate of 125 kbps (CAN-Low-Speed-Physical-Layer) up to a maximum of 1 Mbps (CAN-High-Speed-Physical-Layer), only the most important data can be transmitted. In section 3.1.4, calculations have shown that the recommended busload for CAN is a maximum of approximately 50%. The overhead, when sending CAN messages, can exceed 50%. This means that at most half of the bus can be used for actual data transmission. With such a low bandwidth, systems are limited to a certain amount of control units, which can be part of such a bus. Considering that the number of elements, such as sensors and other actuators will further increase, this is a major bottleneck.

With CAN-FD (see section 3.3), the data rate can be increased up to 4 Mbps. However, it does not solve the problem that sensors with higher data rates (cameras, LiDAR...) cannot be supported by CAN or CAN-FD, since the generated data output could not be transported with such a limited bandwidth. Other means are then required and the overall complexity of the network increases.

Message Format
Yet another problem of CAN are the short message lengths, which limit the transmission to a maximum of 130 bit (standard format). With this message length, the transmission data rate of up to 1 Mbps is sufficient. However, if longer messages without any collisions or other issues should be sent, the data transmission rate is not adequate. If traffic on the bus is increasing, the data transmission will take considerably longer, and the bus system will no longer fulfil the defined requirements of automated driving & real-time capabilty.

Real-time Capability
As discussed in section 3.1.1, CAN does not operate in real-time. On an empty bus, the time delay is, depending on the bus length, in the range of 1 ms - 10 ms. If the traffic on the bus is higher, the delay will increase proportionally to the amount of data on the bus. For more information regarding the latency, see section 3.1.5. More sophisticated applications are limited by the CAN bus and cannot function in real-time. One example is the advanced driver assistance system Lane Keeping Assistance, for which real-time and safety, as well as a high data transmission rate, is of utmost importance. The CAN protocol can only handle minor traffic without collisions and is therefore unfeasible for the described future automotive system with such automotive applications.

Redundancy
Systems and applications have often very different requirements of redundancy. In this case, CAN is not able to offer a solution. That is also the reason why other bus systems such as FlexRay emerged to fill this gap. Systems which use FlexRay cannot be implemented with CAN.

Priorities
There is also the problem when assigning priorities to the messages, which are transported over the bus. In most cases, no issue will occur for those messages with a low identifier. Messages with a low identifier will most certainly be transmitted. Messages with a high identifier however might be delayed or suppressed completely.

Cyclic Redundancy Check (CRC)
Another well-known problem of CAN concerns the Cyclic Redundancy Check (CRC). Nodes can sometimes accept a frame and acknowledge it, even tough there are two bit flips in the frame. In CAN-FD there is also an issue with CRC. By using the dynamic stuff bits in CRC calculations, it is possible to prevent the same problem with the bit flips. However, by adding the dynamic stuff bits, the CRC calculation is more vulnerable to another fault type called *shortening* or *lengthening of the bit sequence*. Then, it is possible that a single error can corrupt the packet reception. The issue with CAN-FD is resolved by now (Mutter, 2015).

Security
Security is one of the major issues of CAN when talking about autonomous vehicles and communication of cars with the environment. CAN was never

developed with the intention of providing remote access to this network. It was designed as a closed loop with physical restrictions. However, when connecting vehicles to their environment, there is basically no protection in place. Simple interfaces, such as Bluetooth, diagnostic tools etc., already offer the possibility to infiltrate the network. In CAN, authentication as well as data encryption are completely missing. Thus, unauthorized devices can be connected to the network and used for attacks. Furthermore, there is no network segmentation in CAN, so all areas are vulnerable as soon as access has been established. CAN does not offer any data encryption and can be spoofed with high priority messages, resulting in flooding (denial of service attack) (Buttigieg, Farrugia, and Meli, 2017).

Considering all these problems, it is obvious to search for new solutions to cope with those future challenges rather sooner than later.

5.4 Challenges of Future Systems

Autonomous or automated driving is already ubiquitous. In Europe, it is still on a much smaller scale compared to the US or China. However, big players like BMW, VW etc. are quite keen on developing a safe and secure system. The development process is steady but rather slow and there are many factors, which decelerate the overall progress of such autonomous systems. It is vital to distinguish between the different levels of automation to really understand how fast and realistic a fully autonomous system is and when such a system will be available and permitted for operation. Six levels have been defined, starting with level 0, where no automation is available. Level 5 is considered as full automation. In the past few years, partial automation (level 3) was attained. An overview of the levels is given in following table 5.4:

Level of automation	Description
Level 0	*No Automation*: most of the vehicles on the road fall under this category. The driver handles everything and there are no assistance systems available in the car.
Level 1	*Driver Assistance*: there are a few assistance systems, which can support the driver at steering, braking, and throttle. These systems are often quite rudimentary and, in most cases, standard equipment in newer vehicles.
Level 2	*Partial Assistance*: additionally to the systems in Level 1, there are further systems such as object detection installed. Still, the driver has to react to all events.
Level 3	*Conditional Assistance*: the vehicles can drive autonomously in certain conditions and react to detected objects accordingly (decelerate/accelerate). However, such systems work only in simple environments such as motorways. Therefore, a driver is still required to react in certain situations.
Level 4	*High Automation*: the vehicle should be able to drive autonomously in almost all scenarios. Severe weather conditions, however, might pose a problem for the sensors. Therefore, the automatic mode will be switched off and a driver is required.
Level 5	*Full Automation*: a driver is not required anymore. The vehicle only needs an input for the destination and should drive there fully autonomously.

Table 5.2: Levels of automation, defined in SAE J3016 (*J3016_201401* 2014)

The step to high automation is a huge one, because for a fully functional level 4 system, much more data from the vehicle (sensors) and the environment are required. There are simply too many possible scenarios to consider, to attain a system which is 100% safe. Thus, it is not yet clear when the amount of data collected is sufficient to satisfy the high standards and have a system which is safe and secure enough for the public. Complexity from level 3 to 4 increases almost exponentially and there are already more than 300 million lines of code used in such systems. It is almost impossible for humans to understand what the systems do and why. Consequently, an artificial intelligence which can learn and adapt to problems (and so the code) automatically will be required. Without such a powerful tool, a fully functional level 4 system seems unrealistic in the next decade.

The long-term goal is to connect vehicles with their environment. There are a few candidates, such as WLAN and 5G to handle the upcoming traffic. However, it is not planned to add WLAN interfaces for 5G. This means that probably only one of those technologies will be used for autonomous driving and, at the moment, it looks to be 5G. Even though the mobile standard 5G is touted as the universal solution for the demand of such systems, it seems naive to think that a hybrid-solution of existing mobile technologies will be able to handle the upcoming requirements. First of all, the infrastructure for 5G is not yet available and only selected areas will have this service available in the next few years. Initially, the achievable data rates with 5G will only be about 4-10 times higher compared to 4G. Considering that there will be a lot of vehicles in densely populated areas, this gain doesn't seem to be groundbreaking. Of course, not all the data generated by a vehicle has to be transmitted.

However, when using HD live maps, which should be updated all the time, a lot of data will accumulate. Mainly LiDAR is used for that purpose, because currently it is the only sensor system with a reliable centimeter resolution rate. The LiDAR sensor output, with an assumed data rate of 50 Mbps, can amount up to 4 Terabyte for a single day. Naturally, not all the data is required to keep the maps updated. Still, a considerable amount of this information has to be transmitted in real-time to a cloud-based service. As a result, certain mobile communication cells will be very busy and will not be able to handle the data traffic.

Other problems, which have been mentioned several times before, are weight and electromagnetic compliance. Every electronic device and sensor added to the vehicle increases the weight and makes it difficult to protect the communication against interferences. However, with the proposed optical communication technologies, both factors can be improved significantly. The next chapter will discuss a vehicle network with such technologies.

It might not be possible to find different solutions that completely solve these problems. If some lightweight materials could be used for both the structure of the car as well as for transmitting data with high bandwidth, this would be such an innovative solution that might optimize all considerations. Since there have been major advancements in this direction, such an approach does not seem unlikely. Once again, the costs will decide when such a technology will be suitable for mass production.

The increased energy consumption in current semi-autonomous systems appears to be a big issue, which also has to be solved in the future. Prototypes, e.g. of Stanford University, require up to 2500 watts and produce a lot of heat. This expenditure can be reduced by modern System-on-Chip (SoC) designs, which demand far less power and are smaller in size. Computer systems used for automotive applications will have to calculate hundreds of trillion operations per second (J. Stewart, 2018), to cope with the complex nature of traffic. Until such systems are ready for mass production, a few years will pass.

5.5 Testing Setup

To create an understanding for current requirements in safety-related soft- and hardware, an analysis of common control units used in an automotive system is performed. The devices are examined, and constraints are defined, in which the system must fulfil the requirements.

The test setup consists of a single control unit, a CAN Controller and software, to monitor the communication on a common bus. The control unit is powered by an external voltage source (12 VDC). The CAN Controller, a Peak PCAN-USB FD, is the interface of the control unit and the PC. It is linked to the computer with a USB connector and powered by this connection. In figure 5.3, the schematic setup is shown.

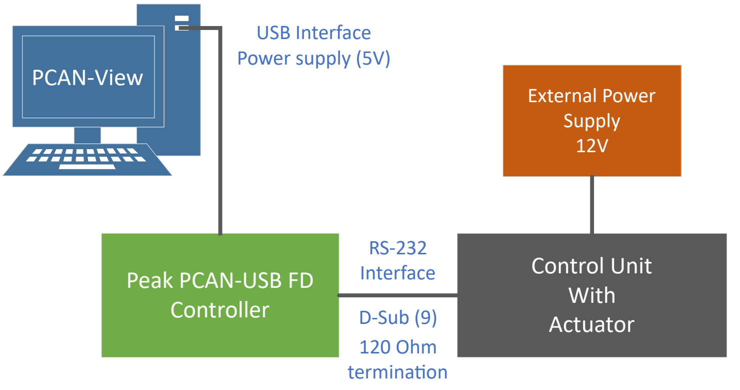

Figure 5.3: Testing setup for measuring the CAN bus load of a common control unit with actuator

When powered, the control unit automatically transmits loads of data which contain information about the state of the device. Most of the CAN messages are only for monitoring the ECU and signaling errors in a cyclic timeframe. The components of the test setup are described in the following sections.

5.5.1 Control Unit

The electronic control unit (ECU) used has an actuator, which can influence the rotating velocity of the wheels to improve the handling of a vehicle. In its standard operating mode, the ECU transmits several status messages to observe the functionality. Those status and error messages are called Diagnostic Trouble Codes (DTCs). The ECU captures such a DTC and flags it as an error code. All these signals have a certain code and can be identified based on the value (hex or decimal). Basically, all checks are done cyclically and thus quite a large amount of information is transmitted as soon as the device is powered. Most periodic cycles are somewhere between 5 ms and up to 100 ms. The frequency of checking is an indication of the importance of the different status and fault messages. There are more than a hundred different events to be validated during the operation of the system. Temperature, energy consumption and the functionality and precision of the electric engine are only a few examples of all the parameters which have to be checked constantly to ensure full functionality. Consequently, there is a considerably high amount of data on the bus only due to the status messages. Regarding the additional traffic, when actual commands are sent, the bandwidth seems limited. To handle this issue, CAN-FD and/or FlexRay are used to provide a sufficient data rate. With the higher bandwidth, more ECUs can be used in the same bus network. More general information on ECUs is available in section 2.5.

5.5.2 Peak PCAN-USB FD Controller

To access a common control unit using CAN, it is required to use a device with an appropriate interface. In this specific case, the connection to the control unit is established by using a Peak PCAN-USB FD controller. This device is an adapter for USB 2.0 (supports also 1.1 and 3.0) and acts as the high-speed CAN connection (ISO 11898-2) between the computer and the control unit. Additionally, this device supports CAN 2.0 A/B but also the advancement with Flexible Data-rate (CAN-FD). Data-rates in the range of 25 kbps up to 1 Mbps are possible. The physical CAN bus connection is realized with a 9-pin D-Sub connector. The pin assignment is visible in figure 5.4. Pin 2 and 7 are assigned as the CAN-L and CAN-H, while pin 3 and 6 are used as ground. All other pins (1,4,5,8,9) are not used. The required voltage of 5 V is supplied via the USB interface.

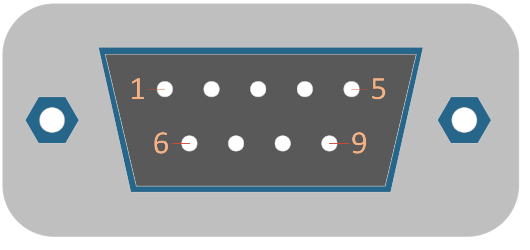

Figure 5.4: PIN assignment of RS-232 D-Sub 9 Plug

The PC is decoupled from the CAN bus via a galvanic isolation. By default, the internal CAN termination is deactivated. Thus, a 120 Ohm resistor is used at the D-Sub plug connector to supply the necessary terminating resistance as described in chapter 3.1. The task of the resistor is to prevent reflections within the wire. To exhibit the importance of this resistor, the test setup was initially done without. As a result, no incoming packages could be monitored.

5.5.3 PCAN-View

The software tool used for monitoring the traffic on the CAN bus is PCAN-View. Devices are automatically detected as soon as they are powered and connected to an active CAN bus. It is possible to transmit messages to the bus, and thus issue commands for an actuator. Transmission and data errors, as well as overflows are also indicated.
Messages are either transmitted automatically in a predefined periodically time window, or manually. Furthermore, the bit rate can be adjusted. In most common CAN systems, the bit rate will be either 250 kbps or 500 kbps. The bit rate of the control unit is set to 500 kbps. Message length in this CAN setup is up to 8 bytes long and of the format: 00 00 00 00 00 00 00 00.

In this setup, manually transmitted 8-byte CAN messages are used to control the speed of the actuator of the ECU. In the following screenshot (figure 5.5) it can be observed that the highlighted message 03 02 02 FF 00 00 00 00 with ID 0x666 is used to manually start the actuator.

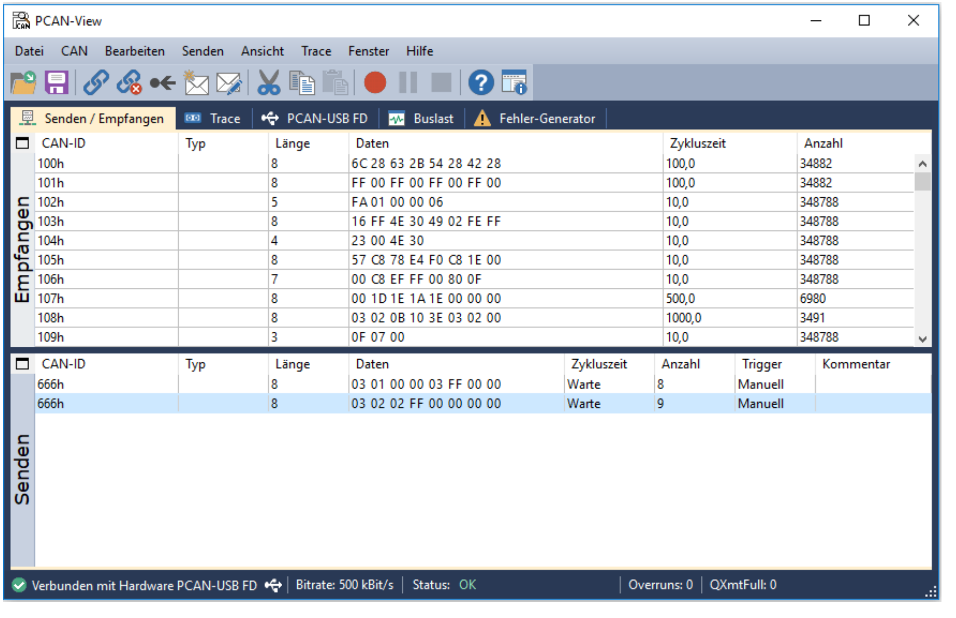

Figure 5.5: Output trace in PCAN-View of the analyzed control unit

Figure 5.6 shows the output trace of the used control unit. The trace function allows to record the traffic and analyze the data.

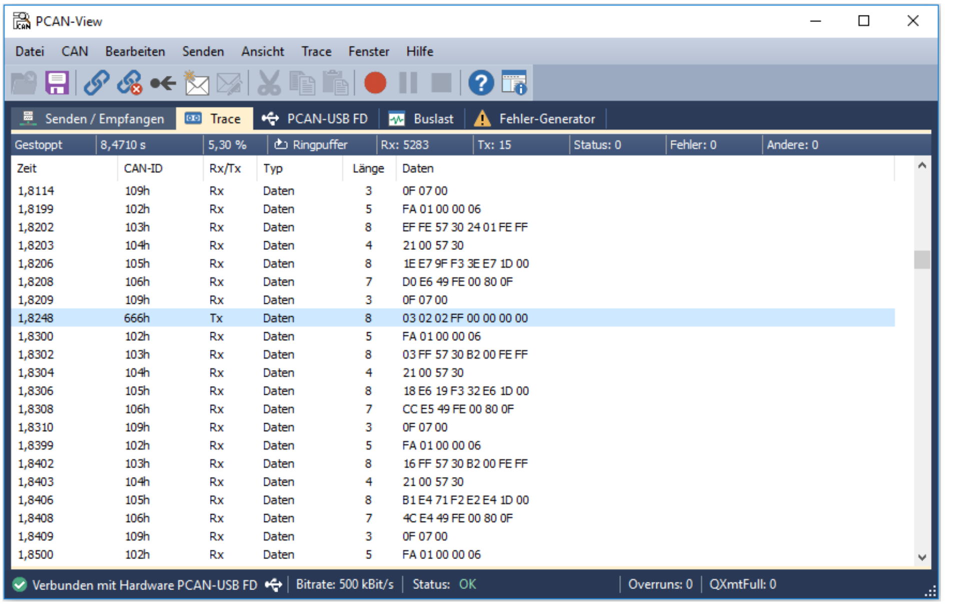

Figure 5.6: Output trace of received/transmitted messages

The CAN message sent in figure 5.5 is highlighted and can be identified by its ID (0x666), the transmitting device (TX/RX), and the actual data in the output trace. The rest of the messages are status messages, which are sent periodically by the control unit to signal the current states. As can be seen, quite a lot of messages are transmitted by the control unit itself. If there would be a continuous input stream from the transmitter side, the bus would be quite busy already.

In figure 5.7, the corresponding bus load is shown. The average bus load of 12.1% is caused only by the status messages of the control unit.

Simple status messages of a single ECU can occupy a maximum of 15.6% of the overall capacity, as indicated in figure 5.7. It is obvious that several ECUs connected to a bus will increase the load significantly, resulting in a congestion at some point. Considering a fair amount of input signals, the bus will probably be occupied with 3-4 ECUs. Furthermore, no sensors are connected in this setup. They would further increase the overall busload

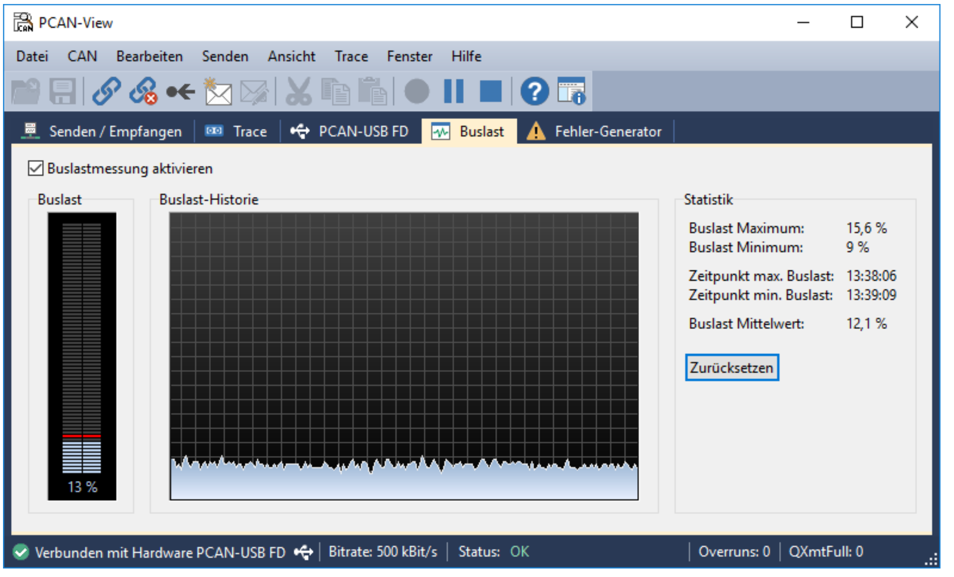

Figure 5.7: Bus load, with only status messages as traffic

significantly, especially sensors, which basically have to operate in real-time for functionality reasons. Such sensors are, e.g., rotational speed sensors.

Recalling the limitations of CAN, the recommended busload is at about 50%. If additional status queries are implemented, further sensors attached, and also input signals arriving from the transmitter side, then the bus will be fully occupied with only 2-3 ECUs in the network. This simple example shows how limiting the data rate of CAN is, even for older systems. Naturally, such control units will not be connected with a CAN bus with a data rate of 500 kbps in a vehicle. Other bus systems such as FlexRay or CAN-FD are used. They offer a bandwidth which is about 4-10 times higher. Consequently, far more devices can be connected to a bus in such a scenario. Still, this analysis shows that even such bus system can only support a limited amount of ECUs. In most cases, there will be only 4-5 such ECUs and several sensors connected to the same bus. It does make sense to separate the various systems, however, if the available bandwidth would be higher, also other systems could use the same transmission medium. This would lead to a significant reduction in wires.

Results of the Analysis

In this chapter, the problems of current and future systems were analyzed. The bus load of a control unit was evaluated, and it has been shown that the data rates and bandwidth are very limiting for vehicle applications. Furthermore, the requirements for future systems have been identified and in the following chapter 6, solutions for handling current and upcoming issues will be presented.

6 Solution and Implementation

In this chapter, the focus lies on designing a network architecture based on optical technologies, which decreases the complexity, reduces weight, and offers sufficient bandwidth for fully autonomous vehicles. Considering the problems previously discussed such as current designs, cost, performance, functionality, electromagnetic interferences, error-proneness, and weight, we have seen the necessity of a novel design for future automotive networks.
So far, no promising approach has yet been implemented in vehicles, and the access to data or testing novel designs is limited due to the secrecy of car manufacturers. A wire harness, combined with electronic components, weighs a few hundred kilos. As mentioned in the Introduction and section 5.2, weight directly affects the range and driving behavior of vehicles. A weight reduction leads to a significant boost in range and efficiency, which might give a manufacturer an edge over their competitors.

Optical technologies have been neglected in the past, because there is a major lack of know-how in the car industry to implement cost-efficient small-scale optical systems. Therefore, it is quite difficult to propose an actual working prototype to solve the problems listed above. Employing a new system based on optical technologies might have drawbacks, such as elevated power consumption and costs. However, utilization of modern ADAS will directly influence the mentioned drawbacks anyways and new ideas and solutions for powering such systems are required. This issue has also been addressed in section 5.4.
Ultimately, the concept is intended to deliver a structure for future automotive networks, where the amount of data which has to be processed during movement is substantially higher than in current networks. The requirements of the backbone of an autonomous vehicle will be comparable to these of a common core backbone. This hypothetical design can definitely provide a good foundation to help create a network for autonomous vehicles with all the intended benefits.

In the past, there have been several approaches to implement optical bus systems, such as MOST and Byteflight (see section 3.6 and 3.7) in vehicles. Except for MOST, those systems disappeared again due to high costs and missing network flexibility. Other non-optical bus systems could always offer similar properties to handle the growing traffic. With all the data requirements, which are emerging with autonomous driving, only Automotive Ethernet seems to be a viable solution. Still, there are many drawbacks of Ethernet regarding the physical layer (see section 3.8 and 5.4).

The goal of this design is to use existing technologies and combine them in the best possible way to increase reliability, safety, and at the same time reduce the complexity of the network, as well as the weight of the network, and thus, fuel consumption. The starting point will be optical technologies and multiplexing techniques, which have been discussed in detail in chapter 4. Only an optical solution will satisfy conceivable requirements. In the following pages, some of these approaches will be discussed.

6.1 KDPOF - Knowledge Development for Plastic Optical Fibers

KDPOF has been identified as the best solution for implementing Automotive Ethernet and was standardized by the European Telecommunications Standards Institute (ETSI) in 2015. This technology gives a good indication of where the automotive industry is heading. It can support both ADAS and Infotainment applications with data rates of more than 1 Gbps within the MOST stack. This means that all components used for a MOST bus can also be utilized in a KDPOF topology. These components are generally very cheap, and even with 650 nm infrared LEDs, good data rates are possible (KDPOF, 2015).
The major advantage of KDPOF is that issues with EMC are resolved. In the CISPR 25 test (see section 2.6) the setup achieves class 5. Additionally, the Japan Automotive Software Platform and Architecture (JASPAR) just announced that the conducted EMC tests on the KD1053 have successfully been passed (PresseBox, 2019). The KD1053 allows gigabit optical communication and is implemented as a 65 nm CMOS ASIC. The physical layer on this chip complies with the specifications of IEEE Std 802.3bv-2017. Over a distance of 40 meters, up to 1 Gbps can be achieved (KDPOF, 2016). The

fibers used have little weight, are reliable, and display very good bending properties. The form factor of the optical transceiver is similar to the RJ45 connector and operates with 3.3 V power supply. With POFs used, the wire harness can be approximately 23.1% cheaper and the weight of cables is considerably lower than with comparable non-optical cables (KDPOF, 2017).

KDPOF can also be applied for the Battery Management System (BMS) in electric vehicles to achieve galvanic isolation. Even though the bandwidth is increased considerably with KDPOF, current semi-automated vehicles already have a demand of at least 3-5 Gbps (KDPOF, 2017). Still, there is no other architecture on the horizon, which can achieve similar data rates and at the same time EMC. Therefore, it is likely that KDPOF will be used for semi-automated vehicles in the next decade. If this standard is refined and further developed, it might also become a solution for autonomous vehicles. This might take a few years more and there is always an uncertainty, so it is wise to look at other technologies and evaluate them for their potential. Otherwise, it will not be possible to catch up with the increasing bandwidth requirements. KDPOF will be considered as an additional technology for the subnetworks in the proposed design in section 6.3.1.

6.2 ROADM - Reconfigurable Optical Add/Drop Multiplexer

The following approaches used in this context are based on ROADMs, which consist of the following components: Wavelength Selective Switch (WSS), Optical Channel Monitoring (OCM) and Variable Optic Attenuators (VOAs). The WSS is responsible for dynamically switching the wavelengths. Consequently, any port can be connected to the network with the use of a WSS. The OCM is responsible for monitoring and calibrating optical power and the VOAs for attenuation of the wavelengths. With those elements it is possible to balance the optical power of the various wavelengths in the network (PacketLight Networks, 2016). The following figure 6.1 (PacketLight Networks, 2016) shows the structure of a two-degree ROADM.

The WSS module is the most important part in the ROADM. There are

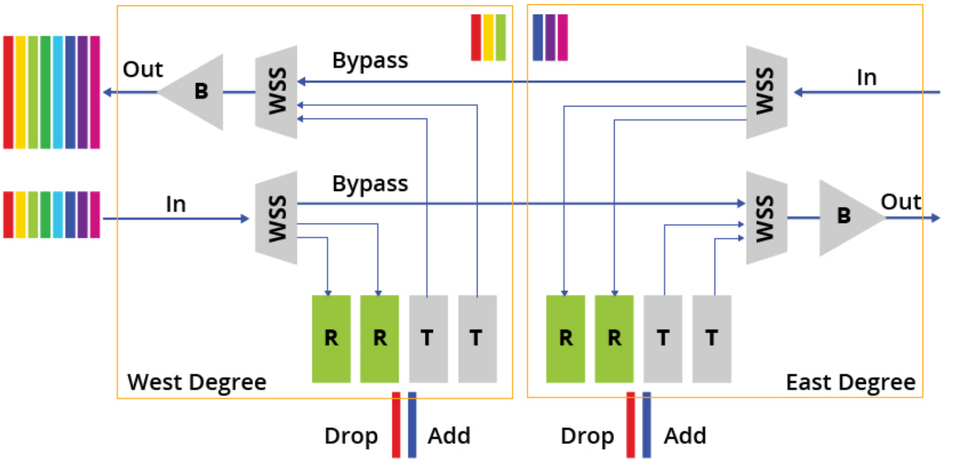

Figure 6.1: Two-degree ROADM Node (PacketLight Networks, 2016)

implementations with liquid crystal elements and micro-electro-mechanical systems (MEMS). With a WSS, each wavelength in a system can be switched to any of the output ports. In the following figure 6.2 a MEMS-based WSS is shown.

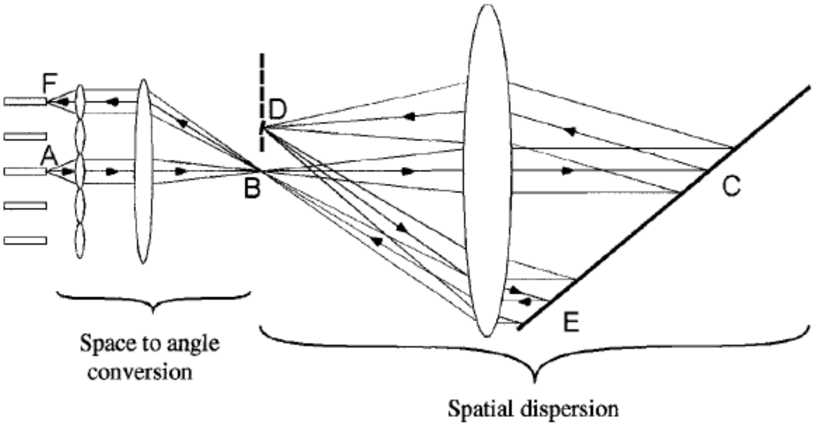

Figure 6.2: 1xN WSS design based on MEMS (Fosco Connect, 2011)

The first lens is used to achieve a space to angle conversion. Incoming optical signals are collimated by the first lens on the left. The second lens maps the rays onto a bulk diffraction grating, where the optical signal is

split into its various wavelengths. These individual rays move in different directions, with only a minimal variation in the angle. From there, the rays hit a MEMS plane and are reflected with a certain tilt angle. The tilt angle can be adjusted with electrostatic attraction, when voltage to an electrode under the movable mirrors is applied (Fosco Connect, 2011). With MEMS mirrors very fast switching (few ms) can be achieved; however, the insertion loss drift can be a problem and leads to high attenuation (Walklin, 2013, p. 2).
The beams are then focused on point B and collimated at the first lens back in the output fiber. Such a MEMS switch can toggle between 128 wavelengths with 50 GHz spacing and the total insertion loss is somewhere between 3 dB and 6 dB (PacketLight Networks, 2016).

A more recent approach is to use liquid crystal on silicon (LCoS) in WSS. It was originally designed for display technologies; however, the achievable resolution and fast response is much higher than with MEMS. A pixel array with phase-controlled pixels is used to achieve a similar beam steering as described earlier. Each pixel is used to control the phase of light. First, the light is steered through polarisation diversity optics. With some additional optics and mirrors the rays are then projected onto a grating, where the light is dispersed into the various wavelengths. The light is reflected once more and ends up on a different location of the LCoS processor. From there, the beam can be steered to a specific port of the fiber array (Fosco Connect, 2011). LCoS based WSS are definitely more interesting than MEMS for the proposed design due to faster response times. Ultimately, this will provide the system with a lower latency.

Using a system with ROADMs offers dynamic wavelength allocation, which is software-driven. In a modern ROADM system, Dense Wavelength Division Multiplexing (DWDM) is used to increase the number of wavelengths and consequently the number of usable channels. In autonomous systems, such a high bandwidth and number of wavelengths is not really necessary. With Coarse Wavelength Division Multiplexing (CWDM), much cheaper components (lasers, filters) can be used than with DWDM. The overall power consumption can be reduced because CWDM components work passively and do not require electrical power. Furthermore, the devices are small enough to be integrated in the network. Nevertheless, they need to be protected against temperature influences, vibrations, etc.

(Nooruzzaman, Koyama, et al., 2013) present an interesting approach with a single-fiber CDWM ring network. This approach seems most promising for small-scale optical networks with high bandwidth requirements. This is the case for autonomous vehicles and will be used as a starting point for the proposed concept. Details on this approach will follow in section 6.3.1. Furthermore, some of the measured data of this paper will be used for the link budget calculations in section 6.3.2.

In a CWDM-based ROADM system, up to 16 wavelengths with a 20 nm spacing can be utilized. When using cheap CWDM optical modules, the data rates for such devices can be up to 100 Gbps (DPSK, DQPSK, DP-QPSK) (Telecom Engineering, Inc., 2018). They accept any data rate and protocol (e.g. 40 GigE) on any port. In the proposed design, a maximum of eight wavelengths will suffice to satisfy the requirements and keep the complexity low.

The major advantage of ROADM systems is that such a network can dynamically adapt to the traffic. Due to the reconfigurable characteristic of ROADMs, each wavelength can travel along every possible path in the network, making the network flexible if additional devices are connected at a later date. When colorless, non-directional add/drop ports are used, it is possible to re-route the wavelengths (Woodward, Feuer, and Palacharla, 2013, p. 683).
This offers high redundancy, if other fibers can be used in case of a failure of another connection. The following list contains some of ROADM features named in (Woodward, Feuer, and Palacharla, 2013, pp. 687–689):

- *Connectivity*: All nodes are connected with each other. With add/drop (de)multiplexing, any combination of wavelengths can be supported by the system. For cost optimization, also a partial ROADM can be implemented, with a limited access to wavelengths.
- *Hitless operation*: Any changes in the network should not introduce errors. The overall flexibility should also be kept.
- *Directional separability*: The add/drop service is robust against errors and will not fail in such an event. Thus, a circuit will still work, and the protection paths will not fail simultaneously. Errors should be possible to resolve.
- *High degree for span relief*: Multiple fiber pairs between nodes can be used to increase capacity.

- *Cascadeability*: Wavelength-selective (WS) elements are used for wavelength separation. However, when a cascade of ROADMs is passed, the passband decreases, and inter-symbol interference limits the number of ROADMs.
- *Channel conditioning*: With the WS element, channel equalization can be achieved to improve the systems range.
- *Scaleability*: Initially, the size of the network must not be known. The network can grow dynamically.
- *100% add/drop capability*: A node is add/drop capable, if all wavelengths in the network can be added/removed at the node.
- *Colorless and non-directional add/drop ports*: A requirement for a dynamic network is the colorless ROADM. Any add/drop port can handle any wavelength. Only then, all transponders can be shared within the network.
- *Spectral flexibility*: The overall capacity can be further increased by using a flex-grid.
- *Flexible transponders*: With software-defined transponders, the protocols, modulation format and symbol rate can be adjusted.

ROADMs do offer many advantages; however, the high costs, size and insertion loss are still some major downsides, which have to be considered. For the proposed design, not all of those features are of importance. All nodes should be connected to each other, regardless of the topology (ring or mesh). They can also be connected via a central node, which forwards the information in the network. Another important feature is the non-directionality to allow a dynamic communication within the network. Furthermore, non-directionality increases the reliability of the network because in case of a failure, it is still possible to transmit messages over a ring in the other direction. Properties such as scaleability and spectral flexibility are only required, if a plug-and-play functionality is desired. For autonomous test vehicles, this might be very interesting since components are frequently added/removed or completely new systems are introduced into the network. Then, all of the mentioned properties are important. In the following pages, a few ROADM architectures will be considered for automotive application.

6.2.1 Wavelength-Division Multiplexing (WDM) ROADM

In general, there are two types of ROADMs: 2-degree and multidegree. The number of degrees indicates how many transmission lines are entering and exiting a ROADM node. The architectures will now be analyzed for their applicability in a vehicle.

2-degree Ring ROADM

A 2-degree ROADM node supports two CWDM/DWDM interfaces and two add/drop branches (tutorialspoint.com, 2010). This architecture exhibits limited scalability, flexibility, expandability and connectivity (Zhao, Hu, and Zhang, 2017, p. 1) compared to meshed networks. At a node, local traffic can be added to the network, and wavelengths can be blocked, dropped or simply passed through the node. If the number of nodes is fixed and all other requirements are known, this type of architecture is the cheapest to achieve high bandwidths with a minimal number of transmission lines. A simple 2-degree ring architecture can be seen in figure 6.3 and either one or two fibers can be used for communication.

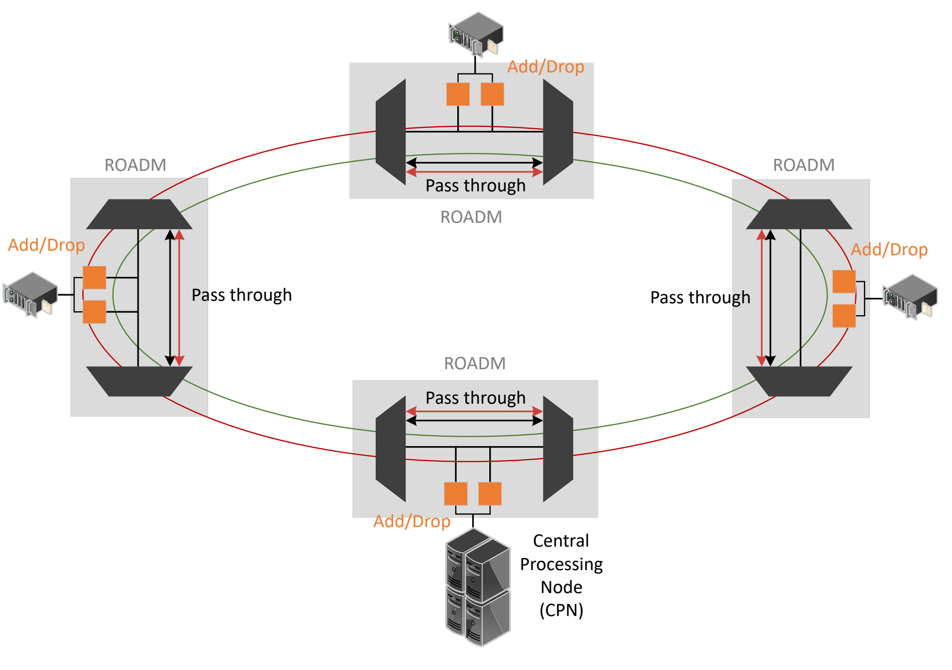

Figure 6.3: Ring architecture of a 2-degree ROADM Network

Because of the simple complexity and the properties of a 2-degree ROADM, where signals enter either from the east or west, this seems to be the most promising topology to achieve a small and low-cost system. With fewer modules in the ROADM nodes, it is also easier to fit such devices in certain positions of the vehicle (not the trunk).

N-degree Mesh ROADM

If a more sophisticated structure is required, a multi-degree mesh architecture can be used. In figure 6.4, a 3-degree ROADM network is illustrated.

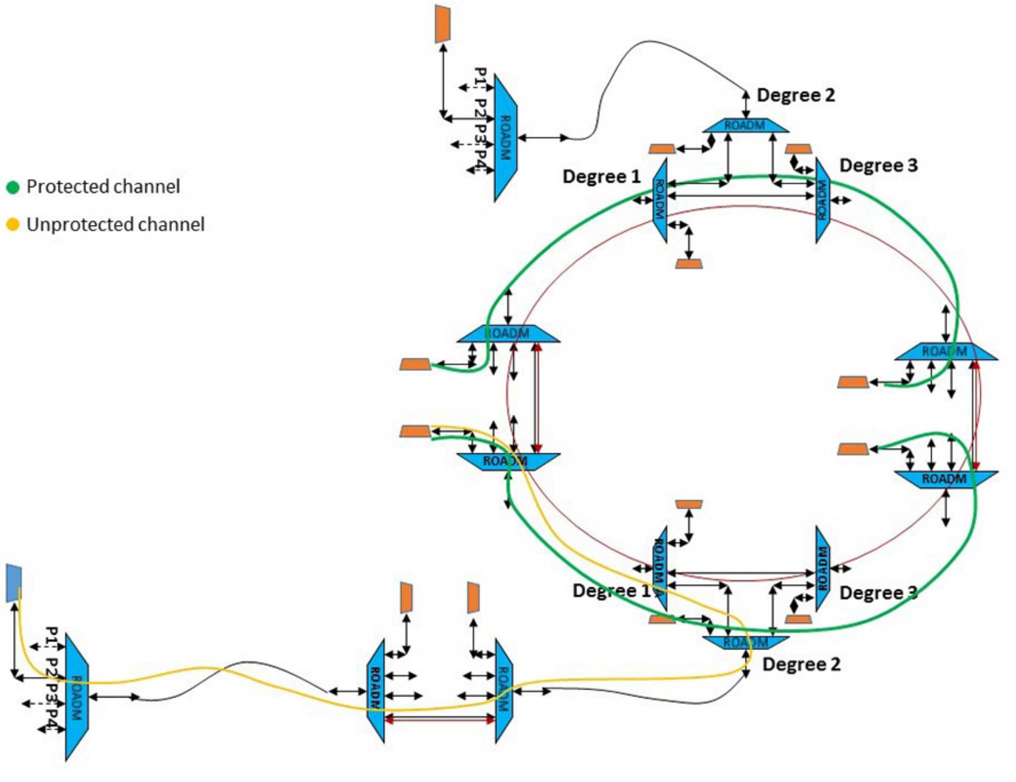

Figure 6.4: Mesh network architecture of ROADM (PacketLight Networks, 2016)

With additional NxM WSSs at the add/drop ports, it is possible to achieve a colorless, directionless and contentionless (CDC) structure. If too many WSSs are used, the cost and size of the system might be a problem and also the narrowing filtering effect will limit the maximum number of ROADMs (Zhao, Hu, and Zhang, 2017, p. 2). Another option is to use a broadcast-and-select module with a tunable filter array. The filtering with such a filter array can then be done electronically. When using photonic cross-connect switches at the ports, any ROADM structure can be upgraded to a CDC ROADM, shown in figure 6.5 (Walklin, 2013, pp. 6–8).

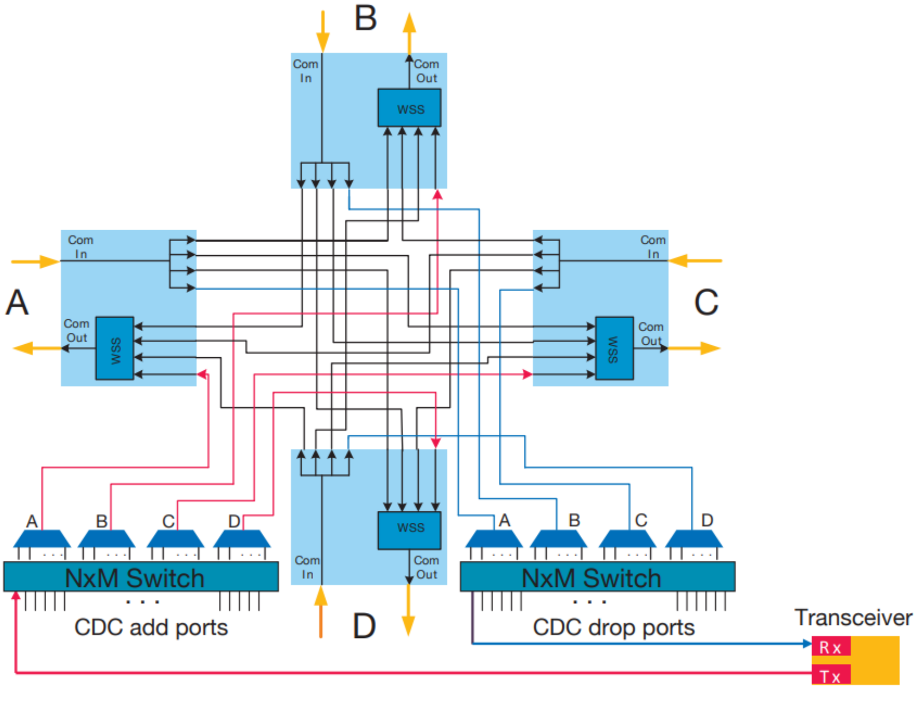

Figure 6.5: 4-degree CDC ROADM structure (Walklin, 2013, p. 8)

Naturally, it would be an optimal solution if only one CDC ROADM module could take over the functionality of the WSSs. This would reduce the complexity, size and cost of such a structure. Regardless of the ROADM network architecture used, it should be able to adapt to any changes. Consequently, it should be possible that optical circuits are added/removed with an automatic mesh restoration in place. Another important property is an automated optical layer. Then, the optical power levels (automatic power balancing) can be dynamically adjusted to the requirements (Walklin, 2013). Because of the cost and size of a meshed architecture, it seems not possible to implement such a structure in vehicles in the near future. Therefore, it makes more sense to stick to a ring architecture.

6.2.2 Space-Division Multiplexing (SDM) ROADM

Even though SDM will not be considered for the actual design, it must be mentioned to show alternative approaches for future concepts. Using SDM offers new possibilities compared to the previously introduced WDM approach. Capacity can be further increased when utilizing multiple modes and cores in multimode fibers as shown in (Feuer et al., 2013) and (Y. Li et al., 2017).
In SDM, the WSS switches not between wavelengths but between the cores or modes of a multicore fiber (MCF). With integrated components such as a silicon photonic integrated circuit (PIC), the insertion loss can be decreased to approximately 4.5 dB instead of 6 dB (Ding et al., 2016). To minimize coupling losses the transceiver modules can be directly integrated into the control unit plug connector. This also makes the whole design cheaper and the connection more accurate.

6.3 Novel Network Architecture for Autonomous Vehicles

The next step is to hypothesize what the complete network architecture of an autonomous vehicle might look like. Certain properties have already been defined in previous sections, such as real-time capabilities, high data rates, security and so on. The mentioned ROADM architectures (section 6.2) shall now be incorporated in the design.

Figure 6.6 shows an example architecture with Automotive Ethernet. This structure is quite easy to achieve and is very similar to the one discussed in section 5.1 (figure 5.2). The backbone structure is substituted with optical fibers, but also some of the other control units in the subnetworks can be connected to Ethernet fibers. All the parts which require higher bandwidth have to be defined and a KDPOF interface with the KD1053 has to be installed.

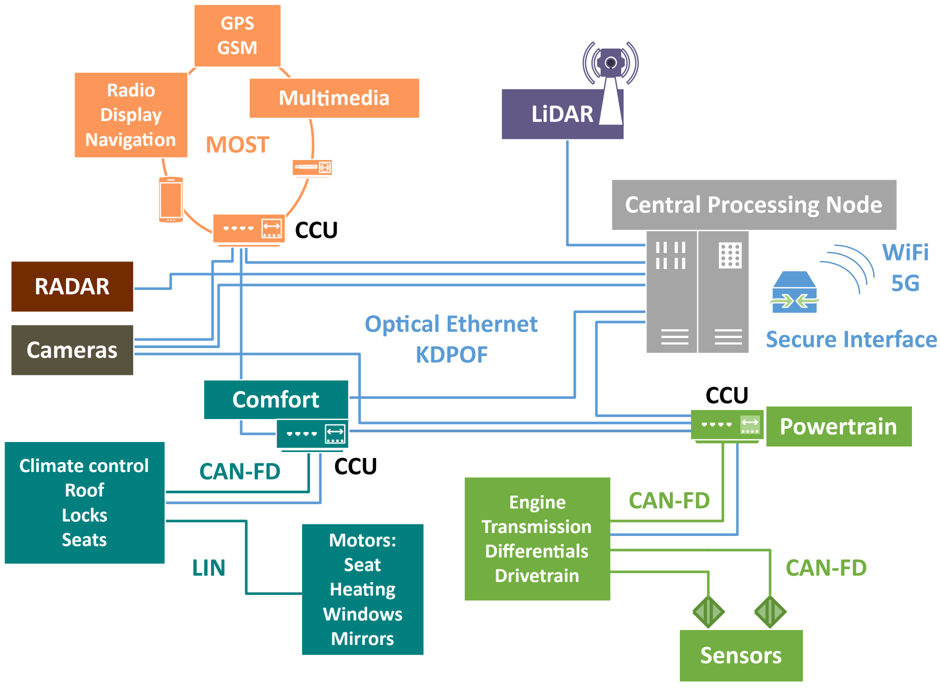

Figure 6.6: Automotive Ethernet with KDPOF implementation

In this consideration, a central processing node (CPN) handles the data streams of devices such as cameras, LiDAR, RADAR etc., which produce lots of data. This data must be processed in the CPN, and calculations have to be made to produce useable data. This data can then be forwarded to any ADAS in the vehicle. With total connectivity, the produced data should be used as effectively as possible. Ultimately, several systems could use the data of a single sensor to optimize performance and accuracy.
With KDPOF there are no issues with interferences because of the EMC of optical fibers. Furthermore, the weight of the wiring harness can be reduced by roughly 20%. However, the achievable 1 Gbps data rate is still limiting for autonomous systems. Therefore, another approach will be examined.

6.3.1 Automotive ROADM CWDM Ring

In a vehicle it is not likely that the network architecture will change once it has been implemented. Properties such as upgradability and scalability are only required in testing vehicles. Therefore, it would be possible to use a simple ring structure, either with Fixed Optical Add/Drop Multiplexers (FOADMs), S-ROADMs or other types of ROADMs. A ring architecture makes sense because there will be only a limited amount of ROADM nodes and the number will stay the same. Each node will be connected to a central control unit, which handles the communication with the subnetwork. Initially, only a few wavelengths have to be reserved and the available number of wavelengths with CWDM should suffice for an autonomous network. As mentioned before, up to 16 wavelengths can be used in a CWDM system. In this approach, eight wavelengths with a 20 nm gap will be used: 1470 / 1490 / 1510 / 1530 / 1550 / 1570 / 1590 / 1610 nm. This means that eight client interfaces can be transmitted over the same fiber. Another benefit is that with fewer channels, the insertion loss is also lower.

Depending on how the routing is handled, it is possible to use an older approach and assign wavelengths to nodes. Then, the color assignment indicates where a color will be added or dropped. This would make the structure simple and OADMs instead of ROADMs could be used. In such a topology, all traffic would go through the CPN. If only a limited number of nodes is used, passive CWDM devices would suffice to provide the wavelengths.

The goal, however, is to design a flexible network architecture, where nodes can be added over time without redesigning the structure and reassigning network ressources. Therefore, a ROADM CWDM ring needs to be considered. For automotive applications, CWDM has been identified as more useful because of the following reasons (Nooruzzaman and Halima, 2016, p. 153):

- *Components*: Components such as lasers, filters etc. are much cheaper. The precision requirements for channel spacing are much lower.
- *Cooling*: For CWDM components, no additional cooling is required. Temperature variations are not an issue due to the large channel spacing.

- *Insertion Loss*: Filters in CWDM cause smaller insertion loss than the additional components required for DWDM.
- *Power Consumption*: No channel stabilization is necessary. This leads to less power consumption.

By applying the approach by (Nooruzzaman, Koyama, et al., 2013), the most cost-effective structure with ROADMs can be achieved. A single-fiber bidirectional ring with stackable ROADMs (S-ROADMs) forms this setup. The transmission is purely optical when passing through intermediate nodes. A module consists of four three-port ROADMs and 2x2 add/drop switches, has two ports and both of them can be used as either input or output simultaneously. Each module uses two different wavelengths and can reconfigure both. Consequently, a S-ROADM node can create 2N links in such a network.

Figure 6.7 shows a ROADM CWDM ring network architecture. The distances between the various nodes are very short. Consequently, the cheapest components could be used and still a high bandwidth can be achieved.

By implementing a ring architecture with directionless communication, redundancy can be achieved. It is possible to use a single fiber, as described before, then the overall complexity and cost is reduced by at least 50% (Nooruzzaman, Koyama, et al., 2013). With a single fiber, the weight of the harness will also be reduced significantly. A second fiber can be used to increase redundancy, and thus, safety.

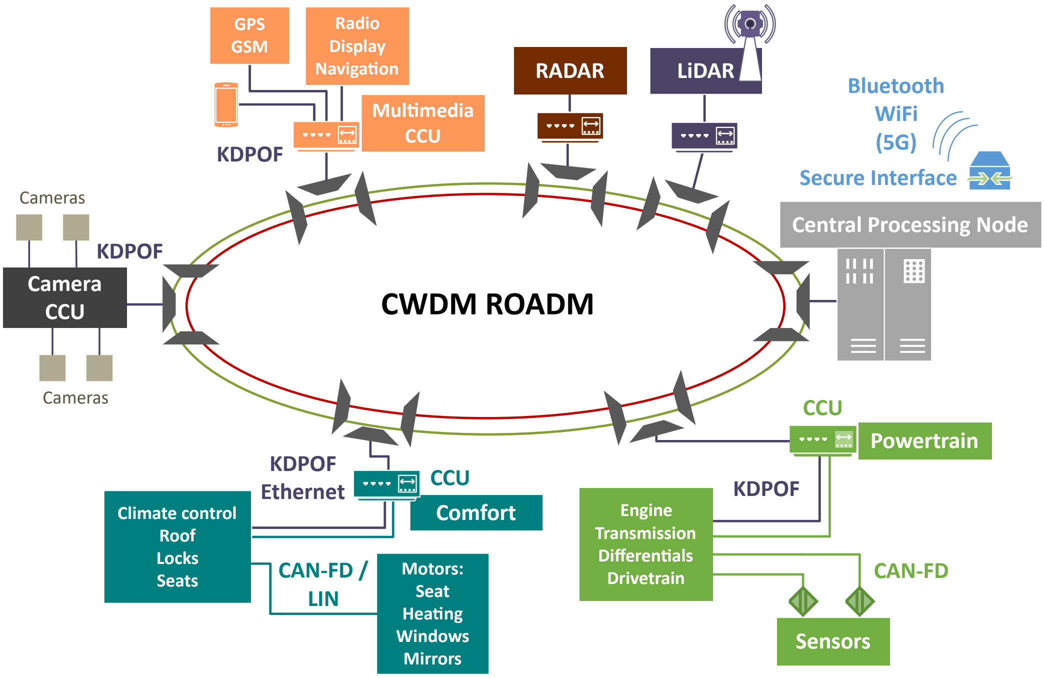

Figure 6.7: Concept of a ROADM CWDM ring network. KDPOF can be used in the subnetworks.

Naturally, some adaptions are required, because such a system must be optimized in space, cost, weight, and power consumption. An approach with a ROADM CWDM ring seems to be the most promising to achieve high bandwidth in an environment where space is limited and the cost of the network is of utmost importance.

In section 6.3.2, some calculations are performed to estimate the achievable data rates in an automotive setup. One major problem is definitely the size of common off-the-shelf devices, because they are designed to fit in server racks. However, considering the required number of wavelengths, it should be possible to make the devices much smaller (size of a common control unit) and there are already some implementations available which might fit the purpose.

If a maximum number of nodes is permitted, it is necessary to think about the network structure. Existing subsystems, as shown in figure 6.7, should only have one access to the core network ring. LiDAR, RADAR and camera systems must be connected and the data should be merged in some kind of CCU, before the data is transmitted over the backbone. Certainly, this is a simplified contemplation, and in reality, the overall structure might be more complex, or a different connection to the CPN would offer advantages. For example, if only one LiDAR unit is used it might be better, if it is directly connected to the CPN instead of connecting it to the core network ring. The information can be transmitted from the CPN anyways and an additional ROADM node might only increase the overall loss. If numerous LiDAR sensors are used, e.g. Solid-State LiDARs, then it would make sense to connect them to CCUs in their proximity or a central LiDAR unit, from where the data is forwarded to the CPN.

Since KDPOF seems to be quite an interesting solution for the upcoming years, it makes sense to consider this technology for this design. It would be possible to create a hybrid network with a CWDM ROADM core ring and some of the subnetworks could use KDPOF for communication. This would further increase bandwidth for systems (cameras, RADARs, drive-by-wire) and optical transmission lines reduce the overall weight and problems with interferences.

A meshed ROADM will not be considered in this approach. At the moment, the complexity and costs are still too high to offer a real solution in the automotive context.

There are some conditions that have to be met to optimize the presented architecture:

- *Number of nodes*: The number of nodes should be limited to a maximum of eight nodes. As shown in figure 6.7, only devices with high bandwidth requirements such as LiDAR, RADAR, cameras etc. should be directly connected to the ring. All other devices are connected to a central control unit, which is responsible for a subnetwork. On this subnetwork, other means of communication can be used.
- *Positioning*: The positioning of the modules and connected CCUs has to be optimized to keep wiring of the subnetworks to a minimum. Only then, the wire harness can be reduced in number of cables and weight.
- *Single-fiber/Dual-fiber*: With a single-fiber ring design the weight can be minimized and the complexity is low. A dual-fiber ring increases

complexity, but also reliability (redundancy).

- *Centralization*: All modules and devices are connected to the network. A central processing node (CPN) is required to do all the important calculations and forwarding of messages to the nodes, which can also use the data of other subnetworks.
- *Connectivity*: With the centralization, sensor data of a subnetwork are available for all other systems. Not all data will be important but certain data can be used to improve the overall reliability of the various systems. Example: The camera stream can be used to calculate if a braking maneuver might be necessary. This information is processed in the CPN and forwarded to the powertrain subnetwork, where the car will be decelerated automatically based on this information. The more sensor data are available, the better the overall system performance will be.
- *Fast switching*: The devices used must be able to handle fast switching to allow a low latency, and thus, real-time.

In the following sections, a few calculations with optical transmissions will be performed to give an idea of the potential benefits.

6.3.2 Optical Link Budget Calculation

The calculations in this section are done by reference to (DeCusatis, 2014). The analysis and calculation of an optical link can be elaborate and complicated. In most cases, a rough estimation is sufficient. In this context, however, the estimation should be as accurate as possible to emphasize the advantages in terms of achievable bandwidth and bit error rate over short distance optical communication. In the link budget both active and passive component losses, as well as any other effects must be considered. Examples for losses (DeCusatis, 2014, p. 56) are listed in the table below:

In general, all the specific values for calculation are provided in a data sheet. However, most of them should be verified by measurements. Furthermore, a margin has to be defined if the values are not accurate. This margin is typically in the range of 0.5 - 1 dB.

Transmission loss is the most important type for long transmission distances. It can be estimated by considering length, fiber attenuation, etc. when certain components such as repeaters are required to regenerate the

Active loss	Passive loss
Optical wavelength	Optical fiber attenuation
Transmitter power	Connectors
Receiver sensitivity	Splices
Receiver dynamic range	Splitters
System gain	

Table 6.1: Typical losses in an optical link

signal. The distances in a vehicle are rather short; thus, the transmission loss will be very small when using high quality fibers. For several meters of a single-mode fiber the loss will be in most cases below 0.1 dB. Multi-mode fibers will exhibit marginally higher transmission loss. The fiber length of a ring in a vehicle will usually be about 10-20 meters. Connector losses are significantly higher than the loss of a fiber. The maximum connector loss (ISO/IEC 11801) is defined at 0.75 dB. High quality connectors can achieve losses lower than 0.3 dB; single-mode fiber connectors exhibit losses of only 0.1 - 0.2 dB (FS.COM, 2015).

Optical Fiber Loss Calculation

To calculate the overall link loss of an optic fiber system, there are many different types of losses that have to be taken into account. In chapter 4, most of them have been explained in detail. Typical loss parameters are: Cable length loss, coupling loss at the transmitter and receiver, further coupling losses at passive fiber couplings, loss margin, splice losses. The overall loss can be calculated with a simple addition of the various individual losses, as seen in equation 6.1

$$\alpha_{total} = \alpha_{fiber} + \alpha_{splice} + \alpha_{coupling} + \alpha_{connectors} + \alpha_{margin} \tag{6.1}$$

α_{fiber} ... fiber length (km) * fiber attenuation per km
α_{splice} ... splice loss * number of splices
$\alpha_{connectors}$ ... connector loss * number of connectors
α_{margin} ... loss margin

This formula is an approximation for a straight fiber, with a few connectors and splices. The exact material properties will never be known because of the imperfections during the manufacturing process. Hence, this approximation must suffice for a first assessment. To apply this initial calculation to a real example: First it is required to define a realistic length of an optical fiber for automotive application. In most cases, the distances will not be longer than the maximum length of a vehicle. Just to be safe, double the length will be considered – due to the fact that a straight connection within a vehicle is near impossible, and many detours or bends might be required.

Worst Case (WC) Calculation
A cheap standardized Polymethyl methacrylate (PMMA) plastic optical fiber (POF) of the type A4a.2 with a wavelength of 650 nm or 850 nm can have a maximum attenuation of up to 250 dB/km (Tsukamoto, 2014). This is an overly high value and not really state-of-the-art anymore, but it fits for WC calculations.
For a distance of a few meters within the car, this still seems acceptable. The length of the fiber can only be estimated. To have a realistic approximation the length and width of a standard SUV will be used and multiplied by 2. A standard SUV such as the BMW X2 has a length of 4.3 m and width of 1.8 m. Thus, the fiber length will be assumed as 12 meters.

$$\alpha_{fiber} = 0.0120 * 250 \, \frac{dB}{km} = 3 \, dB \tag{6.2}$$

The loss can be also estimated with 0.15 – 0.2 dB per meter at 650 nm (The FOA, 2004). This would result in almost the same value as calculated in equation 6.2. Coupling and splice losses are dependent on the number of connections and devices that we assume are connected to the fiber. For this example, eight devices are in the optical link. Then there are at least as many splices and connectors. A standard mechanical connector (HFBR-4501Z/4511Z) shows a maximum connector loss of 2.8 dB (while the typical loss is at 1.5 dB and the minimum at 0.7 dB). In general, a fiber splice loss is low with 0.1 - 0.2 dB per splice (Thorlabs, Inc., 2017). As mentioned in 6.3.2, the maximum connector loss is defined at 0.75 dB.

For the WC calculation we will assume this value.

$$\alpha_{connectors} = 0.75\,dB * 8 = 6\,dB \tag{6.3}$$

$$\alpha_{splice} = 0.2\,dB * 8 = 1.6\,dB \tag{6.4}$$

At the transmitters and receivers only minor coupling losses occur that can be neglected under normal circumstances. In this case minor losses are assumed due to bad connectors. Finally, the safety margin must be added, which is defined at 3 dB. This margin is required to consider degradation of components over time which occurs because of wear and dirt. As a result, the overall link loss of a straight POF with a length of 12 meters can be estimated with:

$$\begin{aligned} \alpha_{total} &= \alpha_{fiber} + \alpha_{splice} + \alpha_{coupling} + \alpha_{connectors} + \alpha_{margin} \\ &= 3\,dB + 1.6\,dB + 0.5\,dB + 6\,dB + 3\,dB = 14.1\,dB \end{aligned} \tag{6.5}$$

Note that those calculations represent the worst case for the POF attenuation with the cheapest components. Obviously, the test results might be significantly better. In this context, 14.1 dB loss equals approximately 96% of lost power (Timbercon, 2015). Consequently, only about 4% of the original power output at the transmitter arrives at the receiver.

Average Case Calculation
Intrinsic and extrinsic losses such as Rayleigh scattering are already considered in the attenuation of the fiber. However, the power output can be increased by using different components or materials. Nowadays there is a wide range of inexpensive POFs available which achieve much better results than 250 dB/km. A graded-index POF (A4g) exhibits far less attenuation than an A4a.2. Instead of 250 dB/km, only 6 dB/km are achieved. A common fiber with very good bending properties such as a ClearCurve multimode optical fiber exhibits a maximum attenuation of 2.3 dB/km@850 nm and 0.6 dB/km@1300 nm (Corning, Inc., 2011).
As a result, the fiber attenuation does not really influence the overall loss in this case. In these considerations, 2.3 dB/km will be chosen for the calculations in equation 6.6. The greatest influence originates from the connectors in the calculation. When reducing the number of connectors or using high-quality ones, the overall attenuation can be improved by quite a margin. Thus, the number of couplings/connectors/splices should

be limited to achieve the best results. These basics are important for the fundamental considerations in the design phase.

The attenuation of a connector is defined by the insertion loss, return loss, and reflection. Details on this topic have been discussed in section 4.5.3. High-quality connectors achieve much better results for insertion and return loss than assumed in calculation 6.5.
The insertion loss of a common POF connector is in the range of 0.3 dB (Shenzhen Dys Fiber Optic Technology Co., Ltd, 2016). This means that the resulting attenuation in our calculation is considerably lower.

Since bending, scattering, and other effects will occur, these parameters will also be considered in the adjusted calculations. The bend radius can be as low as 4 mm for common plastic-clad silica (PCS) fibers, while the resulting attenuation is in the range of only 0.1 dB per bend. For POFs the bend radius should be a maximum of 9 mm to stay below 0.5 dB attenuation per bend. In this example, 0.4 dB attenuation due to bending is assumed (Clarkin, 2006). In a KDPOF test setup it has been shown that for 2-3 bends there will not be any change in the performance, hence data rate. Only if there are many tight bends, the power will be lost eventually (KDPOF, 2017).

The maximum allowed splice loss for any type of fiber is 0.3 dB. Thus, the average splicing loss is somewhere between 0.1 - 0.2 dB. Consequently, 0.15 dB are chosen. For eight fibers this means that an overall loss of 1.2 dB has to be considered.

With the adjusted values the overall loss of an automotive fiber connection with a length of 12 m can be approximated with:

$$\begin{aligned}\alpha_{total} &= \alpha_{fiber} + \alpha_{splice} + \alpha_{coupling} + \alpha_{connectors} + \alpha_{bending} + \alpha_{margin} = \\ &= 0.0276\,dB + 1.2\,dB + 0\,dB + 2.4\,dB + 0.4\,dB + 3\,dB = \\ &= 7.0276\,dB\end{aligned} \tag{6.6}$$

In the average case, there is quite an improvement and almost 20% of the signal power reaches the receiver outputs. When considering a 40 GbE system, a data rate of at least 8 Gbps should be possible. Without the margin, up to 16 Gbps should be possible.
If a simple point-to-point connection is used, the attenuation will be far

lower. In the next step, the optical link budget for the presented CWDM ROADM will be estimated.

CWDM ROADM Link Power Budget

A standard optical link has been considered in the calculations. Now the link power budget of a CWDM ROADM ring architecture will be estimated.

Each component of a ROADM module introduces losses into the system. There are losses at the switches, each add/drop port, for each pass-through (PT), and they increase with each module. In the mentioned example in section 6.3.1 by (Nooruzzaman, Koyama, et al., 2013) some measurements have been done with a single-fiber CWDM ROADM system. Those values will be taken as reference for the calculations.

Following values were obtained by measurement:

- Reflection Loss: L_r = 0.319 dB
- Passing Loss: L_p = 0.391 dB
- Loss at switches: L_{SW} = 0.441 dB

The add/drop loss and the pass-through loss for one direction can be calculated with the following equations 6.7 and 6.8 by (Nooruzzaman, Koyama, et al., 2013, p. 912):

$$L_{ad}(n) = L_{dp}(n) = 2\,(n-1)\,L_r + L_p + L_{SW} \tag{6.7}$$

$$L_{PT}(n) = 4(n-1)L_r + 2L_p + L_{SW} \tag{6.8}$$

n denotes the number of modules. Therefore, the loss increases with more modules. With 3 modules, the add/drop loss amounts to 2.1 dB. The measured pass-through losses vary between 3.8 and 4.1 dB (Nooruzzaman, Koyama, et al., 2013, p. 913). Depending on how many nodes a wavelength has to pass through, the overall insertion loss can be estimated.

$$\begin{aligned} L_{insertion} &= L_{ad} + L_{dp} + L_{PT} = \\ &= 1.79\,dB + 1.79\,dB + 3.83\,dB = 7.41\,dB \end{aligned} \tag{6.9}$$

The insertion loss is also dependent on the wavelength, and thus, it might be higher than calculated. In this context, this will not be considered to keep the example simple.

The overall Link Power Budget can be calculated by substracting the minimum receiver sensitivity from the transmitter power (Wang, 2017):

$$Link\,Power\,Budget = T_x\,Power - R_x\,Sensitivity \tag{6.10}$$

For this example, following values are assumed for transmitter power and receiver sensitivity: $T_x = 2\,dBm$ and $R_x = -30\,dBm$.
Consequently, the overall power budget is

$$P_{budget} = T_x - R_x = 2\,dBm - (-30)\,dBm = 32\,dB \tag{6.11}$$

When considering the losses calculated in 6.9, then the overall link budget is

$$P_{budget} = 32\,dB - 7.41\,dB = 24.59\,dB \tag{6.12}$$

Since the distance is not a criterion in this consideration, the maximum distance does not have to be determined. Because of the short distances, only the losses of the modules are important for the calculations. It must be noted that with newer devices and better components, much better results can be achieved. For instance, if modern CWDM ROADM are used, the insertion loss can be as low as 3.1 dB (Wang, 2017). For these considerations, however, it is quite fitting to use cheap components with a certain variance to keep the costs to a minimum.

Even though those calculations are just vague estimations, they provide a good idea of what to expect in such a system. If rather cheap components are used, the attenuation of the signal can be up to 80%. In a 100 GbE system, this would result in data rates of approximately 20 Gbps. With more modern devices it is possible to reduce the attenuation to only 3 dB, which equals 50% of lost power. The achievable data rates would definitely provide an adequate backbone for autonomous vehicles. Even if the number of sensors doubles or triples, the bandwidth would suffice to support the autonomous systems.

6.3.3 Protocol Layer

Finally, the protocol layer is considered. In previous sections it has been established that Ethernet will be the technology used for future automotive applications. Therefore, it is reasonable to think of a fitting protocol, which can handle the upcoming challenges. A standard protocol cannot be used in a vehicle, because the requirements and properties of a common protocol are often not sufficient. Message priorities, real-time and security are just a few of those challenges which have to be tackled by an automotive protocol.
Without a fitting protocol, the physical data rates cannot be achieved. The Transmission Control Protocol (TCP) would probably be the most obvious choice; however, some properties of this protocol are not suitable for the utilization in vehicles. Problems of TCP stated in the specifications of SCTP (R. Stewart et al., 2007):

- *"TCP provides both reliable data transfer and strict order-of-transmission delivery of data. Some applications need reliable transfer without sequence maintenance, while others would be satisfied with partial ordering of the data. In both of these cases the head-of-line blocking offered by TCP causes unnecessary delay."*
- *"The stream-oriented nature of TCP is often an inconvenience. Applications must add their own record marking to delineate their messages and must make explicit use of the push facility to ensure that a complete message is transferred in a reasonable time."*
- *"The limited scope of TCP sockets complicates the task of providing highly-available data transfer capability using multi-homed hosts."*
- *"TCP is relatively vulnerable to denial of service attacks, such as SYN attacks."*

In contrast, the Stream Control Transmission Protocol (SCTP) offers a combination of some of the best properties of User Datagram Protocol (UDP) and TCP – message-orientation for reliability and in-sequence transport of messages with congestion control. By adapting it for an in-vehicle usage scenario, it seems to be a good solution.

In a vehicle, the order of transmission is not of importance. However, it is crucial that certain messages are transmitted faster (with a higher priority) than others. This is possible with SCTP since this protocol assigns a sequence number to each message sent in a data stream. TCP assigns only one sequence number to a whole segment, so no real distinction between single messages can be made. Ordering messages is optional in SCTP but proves very useful for automotive applications since assigning priorities is required for accurate functionality. Another benefit of SCTP over TCP is that it provides redundant paths to increase reliability. SCTP uses heartbeats to check if a connection is still valid. If one node fails, the connection will find another way, if available. The SCTP protocol has some additional security features and adaptability, which might come in handy for Car-2-X communication in the future (Kraus et al., 2016, p. 7).

Vehicles are already partially connected to their environment. In 2018, Daimler announced that they plan to make software updates via the Cloud (Rothlaender, 2018). By providing such services, the vehicles must be protected additionally against any intrusion attacks and this is only possible with a protocol with a security stack. Therefore, SCTP satisfies many of the requirements of modern automotive networks.

7 Conclusion

In this thesis, challenges of networks in autonomous vehicles have been discussed. Currently, there are significant issues with data rates, complexity, weight, security, and interferences, which influence the reliability, safety, driving behaviour and fuel consumption. At the moment, autonomous vehicles are designed to be completely self-sufficient systems. They only rely on the on-board sensor systems and do not receive any trusted feedback from the environment. Such a system structure produces enormous amounts of data which have to be transmitted and processed within the vehicles' networks.

Chapters 1, 2 and 3 provided background knowledge for the problems defined in this thesis. Current systems were analyzed to show existing and potential bottlenecks.

In chapter 4, the relevance of optical communication technologies for improved data transmission with high data rates has been established. All the various effects which influence the transmission quality as well as attenuation of an optical signal have been discussed. LiDAR is the most important optical technology used to allow autonomous driving by measuring the environment.

In chapter 5, the properties of existing and future systems have been analyzed to estimate the requirements of fully autonomous vehicles. Furthermore, a real system with control units was observed and tested to show the significant limitations of systems that are still being used. With this analysis, the importance of optical systems was emphasized to cope with most existing and upcoming issues.

In the final chapter 6, a design based on existing optical technologies has been presented. For this design, KDPOF and ROADMs have been considered and analyzed. Since the achievable data rates of KDPOF are currently still low (max. 1 Gbps), a different approach with ROADMs has been suggested. For this new concept, the optical link budget for the proposed design has been calculated. These rough estimations show the potential of an optical communication system based on ROADMs. The achievable data rates are in the gigabits, while gaining all the benefits of optical communications such as electromagnetic compliance against

interferences and weight reduction. This proves that the proposed concept can fulfill the high bandwidth demands of future autonomous vehicles.
With the proposed single-ring architecture, the weight of the wire harness can be reduced by 20-50%. Since the CWDM ROADMs work passively, the power consumption could be reduced.
However, the proposed setup reveals a few drawbacks. CWDM ROADMs are large in size and need to be optimized for automotive application. Additionally, the devices must handle the various temperature ranges, mechanical wear, and vibrations. During manufacturing or repairs, the overall complexity might increase for the trained personnel involved.
Nevertheless, the advantages of the physical properties of optical communications and the high achievable bandwidths clearly indicate that this effort might be worthwhile.

Outlook

It is almost impossible to predict when fully autonomous vehicles will be available. There are many factors which influence the advancements in this regard. If vehicles only rely on the data produced by their on-board sensors, it might be difficult to achieve fast progress. The required hardware would exceed the space available in regular vehicles. If the data could be processed and calculated remotely, it would decrease the complexity and system size in vehicles. However, secure communication with a vehicle's environment is not yet possible. Therefore, it seems unrealistic to achieve a Cloud-based system in the next decade. The optimal solution to reduce or eliminate a wire harness completely would be to directly infuse the transmission lines into the chassis. Then, the overall complexity, weight, etc. could be reduced to almost zero.
Other scenarios for application could be airplanes and ships, where dimensions are larger and more space is available. Then, the weight savings by implementing a system with a single or dual fiber would yield even better results.

Bibliography

Abele, Rüdiger (Nov. 2017). *An electrically driven unit*. URL: https://www.daimler.com/innovation/next/an-electrically-driven-unit.html (visited on 11/28/2018) (cit. on p. 10).

Ackerman, Evan (Sept. 2016). "Cheap Lidar: The Key to Making Self-Driving Cars Affordable." In: *IEEE Spectrum*. URL: https://spectrum.ieee.org/transportation/advanced-cars/cheap-lidar-the-key-to-making-selfdriving-cars-affordable (visited on 12/11/2018) (cit. on p. 139).

Agrawal, G.P. (2012). *Fiber-Optic Communication Systems*. Wiley Series in Microwave and Optical Engineering. Wiley. ISBN: 9780470922828 (cit. on pp. 75, 76, 78, 80, 81, 92–95, 97, 98, 100–102, 108, 115, 116, 121, 128–130).

Audi AG (2002). *New data bus systems - LIN, MOST, Bluetooth*. URL: http://www.volkspage.net/technik/ssp/ssp/SSP_286_d1.pdf (visited on 11/14/2018) (cit. on p. 63).

Berwanger, Josef, Martin Peller, and Robert Griessbach (Jan. 2000). "Byte-flight a new protocol for safety critical applications." In: *Seoul 2000 FISITA World Automotive Congress* (cit. on pp. 64–66).

Bezemek, Mike (2017). *LASER Safety in a LiDAR World*. URL: http://velodynelidar.com/newsroom/laser-safety-lidar-world/ (visited on 01/07/2019) (cit. on p. 138).

Blackman, Jason and Scott Monroe (2013). "Overview of 3.3V CAN (Controller Area Network) Transceivers." In: *Texas Instruments Application Report SLLA337* (cit. on p. 36).

Bloomberg (2018). *Who's Winning the Self-Driving Car Race?* URL: http://fortune.com/2018/05/31/whos-winning-the-self-driving-car-race/ (visited on 01/22/2019) (cit. on p. 1).

BMW AG, Daimler AG (2010). *FlexRay Communications System Protocol Specification Version 3.0.1 Revision A*. en. Standard. FlexRay Consortium (cit. on p. 56).

Bogenberger, R. (2011). "BMW AG: IP & Ethernet as potential mainstream automotive technologies." In: *Product Day Hanser Automotive*, pp. 1–5 (cit. on p. 67).

Borgeest, K. (2010). *Elektronik in der Fahrzeugtechnik: Hardware, Software, Systeme und Projektmanagement*. ATZ/MTZ-Fachbuch. Vieweg+Teubner Verlag. ISBN: 9783834893376. URL: https://books.google.at/books?id=%5C_V8h6svwwXQC (cit. on pp. 54, 64).

Born, Max and Emil Wolf (1999). *Principles of Optics: Electromagnetic Theory of Propagation, Interference and Diffraction of Light (7th Edition)*. 7th. Cambridge University Press. ISBN: 0521642221 (cit. on p. 117).

Boucouvalas, A. C. (June 1996). "Ambient light noise and its effect on receiver design for indoor wireless optical links." In: *Proceedings of ICC/SUPERCOMM '96 - International Conference on Communications*. Vol. 3, pp. 1472–1476. DOI: 10.1109/ICC.1996.533654 (cit. on p. 138).

Bradley, R. (2001). *Understanding Computer Science for Advanced Level*. Nelson Thornes. ISBN: 9780748761470. URL: https://books.google.at/books?id=gnuwPpBcO-MC (cit. on pp. 14, 17).

Brückner, V. (2011). *Elemente optischer Netze: Grundlagen und Praxis der optischen Datenübertragung*. Informations- und Kommunikationstechnik. Vieweg+Teubner Verlag. ISBN: 9783834810342. URL: https://books.google.at/books?id=hRk4gXjo0e0C (cit. on pp. 86, 87, 91, 96, 97, 103, 132–134).

Buttigieg, Robert, Mario Farrugia, and Clyde Meli (2017). "Security Issues in Controller Area Networks in Automobiles." In: *CoRR* abs/1711.05824. arXiv: 1711.05824. URL: http://arxiv.org/abs/1711.05824 (cit. on p. 149).

Clarkin, James (2006). *PCS Optical Fibers for an Automobile Data Bus*. Tech. rep. Polymicro Technologies. URL: https://www.molex.com/mx_upload/superfamily/polymicro/pdfs/PCS_Optical_Fibers_for_an_Automobile_Data_Bus_Sept_2006.pdf (visited on 01/22/2019) (cit. on p. 179).

Collins, Dan (2018a). *Complete Guide to Car Suspension*. URL: https://www.carbibles.com/guide-to-car-suspension/ (visited on 01/23/2019) (cit. on p. 12).

Collins, Dan (2018b). *How Car Steering Systems Work*. URL: https://www.carbibles.com/car-steering-systems/ (visited on 01/23/2019) (cit. on p. 13).

Corning, Inc. (2011). *Corning® ClearCurve® Multimode Optical Fiber*. Corning Incorporated. URL: http://www.eng.ucy.ac.cy/ece455/docs/DataSheets/PI1468_Jan2011(MMF).pdf (visited on 01/17/2019) (cit. on p. 178).

CSS Electronics (2018). *CAN BUS EXPLAINED - A SIMPLE INTRO*. https://www.csselectronics.com/screen/page/simple-intro-to-can-bus/language/en. Accessed: 2018-11-29 (cit. on p. 40).

Damask, J.N. (2004). *Polarization Optics in Telecommunications*. Springer Series in Optical Sciences. Springer. ISBN: 9780387224930. URL: https://books.google.at/books?id=QdBeYWj4IjwC (cit. on p. 119).

Davis, Robert I. et al. (Apr. 2007). "Controller Area Network (CAN) schedulability analysis: Refuted, revisited and revised." In: *Real-Time Systems* 35.3, pp. 239–272. ISSN: 1573-1383. DOI: 10.1007/s11241-007-9012-7. URL: https://doi.org/10.1007/s11241-007-9012-7 (cit. on p. 47).

DeCusatis, Casimer (2014). *Handbook of Fiber Optic Data Communication: A Practical Guide to Optical Networking: Fourth Edition*. 4rd. Orlando, FL, USA: Academic Press, Inc. ISBN: 9780124016736 (cit. on p. 175).

Di Natale, M. et al. (2012). *Understanding and Using the Controller Area Network Communication Protocol: Theory and Practice*. SpringerLink : Bücher. Springer New York. ISBN: 9781461403135. DOI: 10.1007/978-1-4614-0314-2 (cit. on pp. 38–40, 46, 48).

Diament, P. (1990). *Wave Transmission and Fiber Optics*. Macmillan Publishing Company. ISBN: 9780029460870 (cit. on p. 77).

Ding, Yunhong et al. (2016). "Reconfigurable SDM Switching Using Novel Silicon Photonic Integrated Circuit." In: *Scientific reports 6* Article number: 39058 (2016). DOI: https://doi.org/10.1038/srep39058. URL: https://www.nature.com/articles/srep39058 (cit. on p. 169).

Dohmke, T. (2002). "Bussysteme im Automobil CAN, FlexRay und MOST." In: *Entwicklung verteilter eingebetteter Systeme* (cit. on pp. 34, 41).

Dossin J. Leimer F., Wolf A. (2007). *Lichtwellenleiter*. Tech. rep. Leipzig University of Applied Sciences, Germany (cit. on pp. 84, 86).

elektronik-kompendium.de (2013). *Lichtwellenleiter (LWL / Glasfaser)*. URL: http://www.elektronik-kompendium.de/sites/kom/0301282.htm (visited on 11/22/2018) (cit. on pp. 73, 74).

energy.gov (Nov. 2013). *Internal Combustion Engine Basics*. URL: https://www.energy.gov/eere/vehicles/articles/internal-combustion-engine-basics (visited on 11/28/2018) (cit. on p. 11).

Fasser P., Leitgeb E. (2007). *Optische Nachrichtentechnik, Skriptum*. Skriptenreferat, Hochschülerschaft der TU Graz GmbH (cit. on pp. 76, 82, 83, 87, 91, 93, 97, 99, 104, 106, 109–111, 115, 118, 119, 122, 130, 132).

Feuer, Mark D. et al. (2013). "ROADM System for Space Division Multiplexing with Spatial Superchannels." In: *Optical Fiber Communication*

Conference/National Fiber Optic Engineers Conference 2013. Optical Society of America, PDP5B.8. DOI: 10.1364/NFOEC.2013.PDP5B.8. URL: http://www.osapublishing.org/abstract.cfm?URI=NFOEC-2013-PDP5B.8 (cit. on p. 169).

Fosco Connect (2009). *Fiber Optic Bend Radius Protection*. URL: https://www.fiberoptics4sale.com/blogs/archive-posts/95051526-fiber-optic-bend-radius-protection (visited on 12/18/2018) (cit. on p. 121).

Fosco Connect (2010). *Optical Fiber Loss and Attenuation*. URL: https://www.fiberoptics4sale.com/blogs/archive-posts/95048006-optical-fiber-loss-and-attenuation (visited on 12/18/2018) (cit. on p. 115).

Fosco Connect (2011). *What is a Wavelength Selective Switch (WSS)?* URL: https://www.fiberoptics4sale.com/blogs/archive-posts/95046534-what-is-wavelength-selective-switch-wss (visited on 01/14/2019) (cit. on pp. 162, 163).

FS.COM (2015). *How to Reduce Various Types of Losses in Optical Fiber?* URL: https://community.fs.com/blog/understanding-loss-in-fiber-optic.html (visited on 01/25/2019) (cit. on p. 176).

Goldstein, Seymour (Nov. 2017). *Steckerdämpfung, Rückflussdämpfung und Reflexion – „Höhen und Tiefen"*. URL: https://de.flukenetworks.com/blog/cabling-chronicles/return-loss-and-reflectance-fine-points (visited on 12/18/2018) (cit. on p. 124).

Grau, G. (2013). *Optische Nachrichtentechnik: Eine Einführung*. Springer Berlin Heidelberg. ISBN: 9783642966576 (cit. on p. 103).

Groth, David and Toby Skandier (2005). *Network+ Study Guide, 4th Edition*. Alameda, CA, USA: SYBEX Inc. ISBN: 0782144063 (cit. on pp. 15, 17).

Hammerschmidt, Christoph (2014). "Computer auf vier Rädern." In: *PC-Welt 08/2014*, pp. 72–73 (cit. on pp. 2–4).

Hampstead, John Paul (2018). *3D point cloud data generated by a Quanergy LiDAR sensor*. URL: https://www.freightwaves.com/news/autonomous-trucking/quanergyceoripsvelodyne (visited on 01/07/2019) (cit. on p. 137).

Hecht, J. (2011). *Understanding Lasers: An Entry-Level Guide*. IEEE Press Understanding Science & Technology Series. Wiley. ISBN: 9781118210048 (cit. on pp. 90, 91).

Heinecke, H et al. (Jan. 2002). "FlexRay - Ein Kommunikationssystem für das Automobil der Zukunft." In: *Elektronik Automotive* (cit. on p. 58).

Heinrich, Stephan (2017). *Flash Memory in the emerging age of autonomy*. https://www.flashmemorysummit.com/English/Collaterals/Proceedings/2017/20170808_FT12_Heinrich.pdf (cit. on p. 141).

Hering, Ekbert, Martin Stohrer, and Rolf Martin (2007). *Physik für Ingenieure*. Berlin [u.a.]: Springer. ISBN: 9783540718550. URL: http://www.worldcat.org/search?qt=worldcat_org_all&q=3540718559 (cit. on p. 106).

Hillier, V.A.W. (1991). *Fundamentals of Motor Vehicle Technology*. Stanley Thornes. ISBN: 9780748705313 (cit. on p. 9).

Hitachi Data Systems (2015). *The Internet on Wheels and Hitachi, Ltd.* Hitachi Data Systems. URL: https://theinternetofthings.report/Resources/Whitepapers/d6a53388-6c46-4847-a72a-036bf053384a_The%20Internet%20on%20Wheels%20and%20Hitachi,%20Ltd..pdf (cit. on p. 141).

Hochmuth, M. (n.d.). *Optische Kommunikation und Optische Netze*. TU Dresden. URL: https://www.rn.inf.tu-dresden.de/lectures/optik/omk.pdf (cit. on p. 79).

Holt, Simon (2018). *High-Speed Network Solutions for the Next Generation of Connected Vehicles*. URL: http://www.newelectronics.co.uk/electronics-technology/high-speed-network-solutions-for-the-next-generation-of-connected-vehicles/176923/ (visited on 12/30/2018) (cit. on pp. 142, 143).

How the braking system works (2018). URL: https://www.howacarworks.com/basics/how-the-braking-system-works (visited on 11/28/2018) (cit. on p. 13).

IEEE Std 802.3bv-2017 (Mar. 2017). *IEEE Standard for Ethernet Amendment 9: Physical Layer Specifications and Management Parameters for 1000 Mb/s Operation Over Plastic Optical Fiber*. Standard, pp. 1–140. DOI: 10.1109/IEEESTD.2017.7875375 (cit. on p. 72).

Introduction to Transmission Systems (2018). URL: http://www.tezu.ernet.in/sae/Download/transmission.pdf (visited on 11/28/2018) (cit. on p. 12).

ISO 11898-1:2015 (2015). *Road vehicles – Controller area network (CAN) – Part 1: Data link layer and physical signalling*. en. Standard ISO 11898-1:2015. Geneva, CH: International Organization for Standardization. URL: https://www.iso.org/obp/ui/#iso:std:iso:11898:-1:ed-2:v1:en (cit. on p. 34).

ISO TC 22/SC 3 (1998). *Road vehicles – Diagnostic systems – Part 3: Verification of the communication between vehicle and OBD II scan tool*. en.

Standard ISO 9141-3:1998. Geneva, CH: International Organization for Standardization. URL: https://www.iso.org/obp/ui/#iso:std:iso:9141:-3:ed-1:v1:en (cit. on p. 52).

ITWissen.info (2009). *Materialdispersion*. URL: https://www.itwissen.info/Materialdispersion-material-dispersion.html (visited on 01/13/2019) (cit. on p. 119).

Jain, Aditya et al. (May 2015). "A comparative study of visual and auditory reaction times on the basis of gender and physical activity levels of medical first year students." In: *International Journal of Applied and Basic Medical Research* 5, p. 122. DOI: 10.4103/2229-516X.157168 (cit. on p. 24).

Jesse, Bernd (Aug. 2016). "Time Synchronization in Automotive Ethernet Networks." In: *Automobil Elektronik, issue July/August 2016*, pp. 1–5 (cit. on p. 69).

KDPOF (2015). *Automotive Applications*. URL: http://www.kdpof.com/automotive/ (visited on 01/19/2019) (cit. on p. 160).

KDPOF (2016). *KD1053 Automotive 1000BASE-H Transceiver*. Tech. rep. KDPOF. URL: http://www.kdpof.com/wp-content/uploads/2016/03/br018__KD1053_Product_Brochure__v2_0.pdf (visited on 01/20/2019) (cit. on p. 160).

KDPOF (2017). *Robust High Speed Communications Technology over POF on Airborne applications*. Tech. rep. KDPOF. URL: http://www.secpho.org/wp-content/uploads/2017/03/26-KDPOF-UAVs.pdf (visited on 01/19/2019) (cit. on pp. 161, 179).

Kitayama, Ken-ichi, Hideyuki Sotobayashi, and Naoya Wada (1999). "Optical Code Division Multiplexing (OCDM) and Its Applications to Photonic Networks." In: *IEICE Trans. Fundamentals, Vol.E82-A, No.12 Dec. 1999* (cit. on p. 130).

KNOEMA (2018). *Copper Prices Forecast: Long Term 2018 to 2030*. URL: https://knoema.de/prujshc/copper-prices-forecast-long-term-2018-to-2030-data-and-charts (visited on 12/30/2018) (cit. on p. 145).

Koike, Y. (2015). *Fundamentals of Plastic Optical Fibers*. Wiley-VCH, Berlin. ISBN: 9783527410064 (cit. on pp. 112, 113, 116, 117).

Kokyo, Inc. (2017). *Normalized propagation constant and waveguide parameter*. URL: https://en.symphotony.com/fiber-lasers/propagation-constant-waveguide-parameter/ (visited on 12/18/2018) (cit. on p. 110).

Kossel, Axel (2014). "Sind wir schon da? Roboter Autos mischen sich in den Verkehr." In: *C't Magazin für Computer Technik Ausgabe 9, 2014*, pp. 132–135 (cit. on pp. 4, 5).

Kraus, D. et al. (July 2016). "Replacement of the Controller Area Network (CAN) protocol for future automotive bus system solutions by substitution via optical networks." In: *2016 18th International Conference on Transparent Optical Networks (ICTON)*, pp. 1–8. doi: 10.1109/ICTON.2016.7550335 (cit. on p. 183).

ksi.at (2013). *Lichtwellenleiter (LWL)*. url: https://www.ksi.at/online-kataloge/show_rechts.asp?l=1&katnr=9A (visited on 12/12/2018) (cit. on p. 74).

Laser Components (2018). *Impulslaserdioden*. url: https://www.lasercomponents.com/de/produkt/impulslaserdioden-bei-905-nm/ (visited on 01/07/2019) (cit. on p. 137).

Lawrenz, W. (1997). *Can System Engineering: From Theory to Practical Applications*. Rethinking ageing series. Springer New York. isbn: 9780387949390 (cit. on p. 47).

Leitgeb, Erich et al. (2017). "Optische Technologien für automatisiertes Fahren." In: *Studie für Bundesministerium für Verkehr, Innovation und Technologie (BMVIT)* (cit. on pp. 134, 135, 139, 144, 146).

Li, Chao and Qi Yang (2016). "Optical OFDM/OQAM for the Future Fiber-optics Communications." In: *Procedia Engineering* 140. International Conference on Materials for Advanced Technologies (ICMAT2015) – 4th Photonics Global Conference 2015, pp. 99–106. issn: 1877-7058. doi: https://doi.org/10.1016/j.proeng.2015.09.238. url: http://www.sciencedirect.com/science/article/pii/S1877705815033160 (cit. on pp. 131, 132).

Li, Jennifer (Oct. 2017). *IEEE-News: 10-GBit-WLAN, Light Communication, Ethernet im Auto*. url: https://www.heise.de/ct/artikel/IEEE-News-10-GBit-WLAN-Light-Communication-Ethernet-im-Auto-3846599.html (visited on 01/03/2019) (cit. on p. 145).

Li, Y. et al. (Mar. 2017). "Hardware programmable SDM/WDM ROADM." In: *2017 Optical Fiber Communications Conference and Exhibition (OFC)*, pp. 1–3 (cit. on p. 169).

Mayer, E. (2006). "Serial bus systems in the automobile – Architecture, tasks and advantages." In: *Elektronik Automotive 7/2006*, pp. 70–73 (cit. on pp. 34, 35).

Miles, Dean (2018). *One Petabyte Per Second: Simply Amazing*. URL: https://www.tek.com/one-petabyte-second-simply-amazing (visited on 01/02/2019) (cit. on p. 124).

MOST Cooperation (2010). *MOST Specification*. en. Standard Rev. 3.0 E2. MOST Cooperation. URL: https://www.mostcooperation.com/publications/specifications-organizational-procedures/request-download/mostspecification-3v0e2pdf/ (cit. on pp. 59, 61).

Mutter, Arthur (2015). "CAN FD and the CRC issue." In: *CAN Newsletter 1/2015*, pp. 4–10. URL: https://can-newsletter.org/uploads/media/raw/604de101b0ecaed387518831d32b044e.pdf (cit. on pp. 52, 148).

National Instruments (2014). *Controller Area Network (CAN) Overview*. URL: http://www.ni.com/white-paper/2732/en/ (visited on 11/28/2018) (cit. on pp. 33, 39).

Newport Corporation (2018). *The Effect of Dispersion on Ultrashort Pulses*. URL: https://www.newport.com/n/the-effect-of-dispersion-on-ultrashort-pulses (visited on 12/18/2018) (cit. on p. 118).

Nooruzzaman, M. and E. Halima (Aug. 2016). "Low-cost hybrid ROADM architectures for scalable C/DWDM metro networks." In: *IEEE Communications Magazine* 54.8, pp. 153–161. ISSN: 0163-6804. DOI: 10.1109/MCOM.2016.7537190 (cit. on p. 171).

Nooruzzaman, M., O. Koyama, et al. (Aug. 2013). "Scalable single-fiber CWDM ring networks with stackable ROADMs." In: *IEEE/OSA Journal of Optical Communications and Networking* 5.8, pp. 910–920. ISSN: 1943-0620. DOI: 10.1364/JOCN.5.000910 (cit. on pp. 164, 172, 180).

PacketLight Networks (2016). *ROADM*. URL: https://www.packetlight.com/innovations/roadm (visited on 01/14/2019) (cit. on pp. 161–163, 167).

Paolo, Emilio (2018). *Automotive EMC*. https://interferencetechnology.com/automotive-emc-2/#. Blog (cit. on pp. 28, 30, 31).

PresseBox (2019). *KDPOF Automotive Optical Gigabit Ethernet Receives Compliance Approval from Premier Japanese Automotive Industry Body*. URL: https://www.pressebox.de/inaktiv/kdpof-knowledge-development-for-pof/Optisches-Automotive-Gigabit-Ethernet-von-KDPOF-erhaelt-Compliance-Zulassung-durch-fuehrendes-japanisches-Automobilindustrie-Gremium/boxid/937017 (visited on 01/21/2019) (cit. on p. 160).

Reif, K. (2010). *Batterien, Bordnetze und Vernetzung*. Bosch Fachinformation Automobil. Vieweg+Teubner Verlag. ISBN: 9783834897138. URL: https://books.google.at/books?id=8NCldt82AoQC (cit. on pp. 27, 29, 30).

Reif, K. (2011). *Bosch Autoelektrik und Autoelektronik: Bordnetze, Sensoren und elektronische Systeme*. Bosch Fachinformation Automobil. Vieweg+Teubner Verlag. ISBN: 9783834899026. URL: https://books.google.at/books?id=d00pBAAAQBAJ (cit. on pp. 20, 25, 26, 53, 55–58, 60).

Reif, K. (2014). *Automobilelektronik: Eine Einführung für Ingenieure*. ATZ/MTZ-Fachbuch. Springer Fachmedien Wiesbaden. ISBN: 9783658050481. URL: https://books.google.at/books?id=UyugBQAAQBAJ (cit. on pp. 18–20, 49, 52, 55, 57, 58).

Richardson, D.J., John Fini, and Lynn Nelson (May 2013). "Space Division Multiplexing in Optical Fibres." In: *Nature Photonics* 7, pp. 354–362. DOI: 10.1038/nphoton.2013.94 (cit. on pp. 125–127).

Rosolem, Joao Batista (2017). "Power-Over-Fiber Applications for Telecommunications and for Electric Utilities." In: *IntechOpen*. URL: https://www.intechopen.com/books/optical-fiber-and-wireless-communications/power-over-fiber-applications-for-telecommunications-and-for-electric-utilities (visited on 01/07/2019) (cit. on p. 140).

Rothlaender, Peter (2018). *Daimler embraces the cloud to innovate faster*. URL: https://customers.microsoft.com/it-it/story/daimler-manufacturing-azuredevtest (visited on 01/24/2019) (cit. on p. 183).

Santos, Max Mauro Dias et al. (2017). "On the Timing Analysis at Automotive Real-Time Embedded Systems." In: *SAE Technical Paper 2017-01-1618*. URL: https://doi.org/10.4271/2017-01-1618 (cit. on pp. 21–23).

Sauerwald, Mark (2015). "Ten tips for successful designing with automotive EMC/EMI requirements." In: *Analog Applications Journal AAJ 3Q 2015*, pp. 4–6. URL: http://www.ti.com/lit/an/slyt636/slyt636.pdf (cit. on p. 28).

Schaal, Hans-Werner (Apr. 2012). "IP and Ethernet in Motor Vehicles." In: *Automobil Elektronik, issue 4/2012*. URL: https://assets.vector.com/cms/content/know-how/_technical-articles/Ethernet_IP_ElektronikAutomotive_201204_PressArticle_EN.pdf (cit. on pp. 66, 67).

Schmid, Markus (2006). "Automotive Bus Systems." In: *Atmel Applications Journal* 6, pp. 29–32. URL: https://eng.umd.edu/~austin/enes489p/project-resources/SchmidAutoBusSystems.pdf (cit. on pp. 59–62).

Schubert, E. Fred (2006). "LED basics: Optical properties." In: *Light-Emitting Diodes*. 2nd ed. Cambridge University Press, pp. 86–100. DOI: 10.1017/CBO9780511790546.006 (cit. on p. 85).

Shah, Saurin D. (2009). "Electrification of Transport and Oil Displacement: How Plug-Ins Could Lead to a 50 Percent Reduction in U.S. Demand for Oil." In: *Plug-In Electric Vehicles: What Role for Washington?* Brookings Institution Press. Chap. 2, pp. 22–44 (cit. on p. 11).

Shenzhen Dys Fiber Optic Technology Co., Ltd (2016). *SC / APC Plastic Optical Fiber Connectors*. URL: http://www.opticalfiberpatchcord.com/china-sc_apc_plastic_optical_fiber_connectors_for_optical_distribution_frame-2820465.html (visited on 01/14/2019) (cit. on p. 179).

Sova, Ray M. (Nov. 2005). "Fundamentals of POF Data Link Design: Automotive and Home Design Examples." In: POFWorld 05 EAST. URL: https://books.google.at/books?id=mWDjB%5C_E9oVgC (cit. on p. 106).

Specks, J.W. and A Rajnäk (Jan. 2003). "LIN - Protocol, development tools, and software interfaces for local interconnect networks in vehicles." In: *9th International Conference on Electronic Systems for Vehicles*, pp. 5335–5358 (cit. on p. 54).

Stewart, Jack (2018). *Self-Driving Cars use crazy amounts of power, and it's becoming a problem*. URL: https://www.wired.com/story/self-driving-cars-power-consumption-nvidia-chip/ (visited on 01/08/2019) (cit. on pp. 141, 152).

Stewart, R. et al. (2007). *Stream Control Transmission Protocol (RFC4960)*. Network Working Group. URL: https://tools.ietf.org/html/rfc4960 (cit. on p. 182).

Strobel, Otto (2016). *Optical and microwave technologies for telecommunication networks*. First Edition. John Wiley & Sons. ISBN: 9781119971900 (cit. on pp. 78, 81, 83–85, 88–90, 93, 94, 96, 100, 101, 104, 105, 107–109, 112–114, 116, 120, 122, 123, 125, 131).

Tanenbaum, Andrew S. and David J. Wetherall (2010). *Computer Networks*. 5th. Upper Saddle River, NJ, USA: Prentice Hall Press. ISBN: 0132126958, 9780132126953 (cit. on p. 74).

J3016_201401 (Jan. 2014). *Taxonomy and Definitions for Terms Related to On-Road Motor Vehicle Automated Driving Systems*. DOI: https://doi.org/10.4271/J3016_201401 (cit. on p. 150).

Telecom Engineering, Inc. (2018). *CWDM Lite Multiplexers*. URL: http://www.telecomengineering.com/downloads/pdf/CWDM/M-ROADM%20CWDM%20Product%20Catalog.pdf (visited on 01/22/2019) (cit. on p. 164).

The FOA (2004). *Plastic Optical Fiber (POF)*. URL: http://www.thefoa.org/tech/pof.htm (visited on 01/11/2019) (cit. on p. 177).

Thorlabs, Inc. (2017). *Fiber Optics Selection Guide*. URL: https://www.thorlabs.com/images/Catalog/V19_13_FiberOpt.pdf (visited on 01/13/2019) (cit. on p. 177).

Tietze, U. and C. Schenk (1993). *Halbleiter-Schaltungstechnik*. Berlin. ISBN: 9783540561842 (cit. on p. 103).

Timbercon (2015). *dB vs. Optical Power Loss*. URL: http://www.timbercon.com/db-power-loss/ (visited on 01/23/2019) (cit. on p. 178).

Tsukamoto, Yoshihiro (2014). *Plastic optical fiber standard*. Mitsubishi Rayon Co., Ltd. URL: http://www.ieee802.org/3/GEPOFSG/public/Sep_2014/Tsukamoto_GEPOF_01b_0914.pdf (cit. on p. 177).

TTTech Computertechnik AG (2018). *Time Sensitive Networking (TSN)*. URL: https://www.tttech.com/technologies/time-sensitive-networking-tsn/ (visited on 12/30/2018) (cit. on p. 70).

tutorialspoint.com (2010). *Optical Networks - ROADM*. URL: https://www.tutorialspoint.com/optical_networks/optical_networks_roadm.htm (visited on 01/15/2019) (cit. on p. 166).

Vector Informatik GmbH (2018). *Einführung in CAN — Prinzip des Buszugriffs*. URL: https://elearning.vector.com/mod/page/view.php?id=53 (visited on 01/23/2019) (cit. on p. 19).

Velodyne LiDAR, Inc. (2018). *ULTRA Puck*. VLP-32C. 63-9378 Rev. D. Velodyne LiDAR, Inc. (cit. on p. 137).

Vieweg, S. (2014). *Bosch Automotive Electric and Automotive Electronics, Robert Bosch GmbH, 5th Ed*. Handbook. Springer Fachmedien Wiesbaden. ISBN: 9783658017842 (cit. on p. 144).

Walklin, Sheldon (2013). “ROADMs in Next-Generation Networks.” In: *Optelian - White Paper*, pp. 1–23. URL: https://www.optelian.com/wp-content/uploads/2016/10/Optelian-ROADMsNextGenNetworks-WP.pdf (cit. on pp. 163, 168).

Wang, Chloe (2017). *How to Calculate Power Budget and Link Distance in CWDM Network*. URL: http://www.fiber-optic-components.com/calculate-power-budget-link-distance-cwdm-network.html (visited on 01/23/2019) (cit. on p. 181).

Wiesinger, Johannes (2005). *Der CAN-Bus - Grundlagen von Automobil Bussystemen*. URL: https://www.kfztech.de/kfztechnik/elo/can/can_grundlagen_1.htm (visited on 01/10/2019) (cit. on p. 142).

Winner, Hermann et al., eds. (2015). *Handbuch Fahrerassistenzsysteme*. 3rd ed. ATZ/MTZ-Fachbuch. Wiesbaden: Springer Vieweg. ISBN: 978-3-658-05733-6. DOI: 10.1007/978-3-658-05734-3 (cit. on pp. 136, 138).

Woodward, Sheryl L., Mark D. Feuer, and Paparao Palacharla (2013). "Chapter 15 - ROADM-Node Architectures for Reconfigurable Photonic Networks." In: *Optical Fiber Telecommunications (Sixth Edition)*. Ed. by Ivan P. Kaminow, Tingye Li, and Alan E. Willner. Sixth Edition. Optics and Photonics. Boston: Academic Press, pp. 683–707. DOI: https://doi.org/10.1016/B978-0-12-396960-6.00015-8. URL: http://www.sciencedirect.com/science/article/pii/B9780123969606000158 (cit. on p. 164).

Zhao, Li, Weisheng Hu, and Xiaojian Zhang (2017). "Architecture and performance of grouped ROADM rings with shared optical amplifier and grouped add/drop ports for hybrid data center network." In: *Optical Switching and Networking* 23, pp. 1–4. ISSN: 1573-4277. DOI: https://doi.org/10.1016/j.osn.2016.08.002. URL: http://www.sciencedirect.com/science/article/pii/S157342771630073X (cit. on pp. 166, 168).

Ziemann, O et al. (Jan. 2008). *POF handbook: Optical short range transmission systems*, pp. 1–886. DOI: 10.1007/978-3-540-76629-2 (cit. on p. 123).

Zimmermann, W. and R. Schmidgall (2014). *Bussysteme in der Fahrzeugtechnik: Protokolle, Standards und Softwarearchitektur*. ATZ/MTZ-Fachbuch. Vieweg+Teubner Verlag. ISBN: 9783834809070. URL: https://books.google.at/books?id=muK7cQAACAAJ (cit. on pp. 35–38, 42–45, 49–52, 56, 57, 59, 61–63, 67, 68, 71, 72).

Zubia, Joseba and Jon Arrue (2001). "Plastic Optical Fibers: An Introduction to Their Technological Processes and Applications." In: *Optical Fiber Technology* 7.2, pp. 101–140. ISSN: 1068-5200. DOI: https://doi.org/10.1006/ofte.2000.0355. URL: http://www.sciencedirect.com/science/article/pii/S1068520000903559 (cit. on p. 75).